Modelling of energy requirements for thermal conditioning in the Uruguayan residential sector

Sofía Gervaz Canessa

Programa de Posgrado en Ingeniería de la Energía
Facultad de Ingeniería
Universidad de la República

Montevideo – Uruguay
Marzo de 2021

Modelling of energy requirements for thermal conditioning in the Uruguayan residential sector

Sofía Gervaz Canessa

Tesis de Maestría presentada al Programa de Posgrado en Ingeniería de la Energía, Facultad de Ingeniería de la Universidad de la República, como parte de los requisitos necesarios para la obtención del título de Magíster en Ingeniería de la Energía.

Director:
Dr. Ing. Federico Favre

Codirector:
Dr. Ing. Pedro Curto

Director académico:
Dr. Ing. Federico Favre

Montevideo – Uruguay
Marzo de 2021

Gervaz Canessa, Sofía

Modelling of energy requirements for thermal conditioning in the Uruguayan residential sector / Sofía Gervaz Canessa. - Montevideo: Universidad de la República, Facultad de Ingeniería, 2021.

IX, 146 p. 29, 7cm.

Director:

Federico Favre

Codirector:

Pedro Curto

Director académico:

Federico Favre

Tesis de Maestría – Universidad de la República, Programa en Ingeniería de la Energía, 2021.

Referencias bibliográficas: p. 127 – 132.

1. eficiencia energética, 2. sector residencial uruguayo, 3. Urban Building Energy Models, 4. automatización de modelado en EnergyPlus. I. Favre, Federico, *et al.* II. Universidad de la República, Programa de Posgrado en Ingeniería de la Energía. III. Título.

INTEGRANTES DEL TRIBUNAL DE DEFENSA DE TESIS

_____

D.Sc. Prof. Nombre del 1er Examinador Apellido

_____

Ph.D. Prof. Nombre del 2do Examinador Apellido

_____

D.Sc. Prof. Nombre del 3er Examinador Apellido

_____

Ph.D. Prof. Nombre del 4to Examinador Apellido

_____

Ph.D. Prof. Nombre del 5to Examinador Apellido

Montevideo – Uruguay
Marzo de 2021

Agradecimientos

Primero, agradecer a Federico por la paciencia y dedicación con las que me guió en este trabajo. Sus conocimientos y consejos fueron claves en todas las etapas. A Pedro, por estar siempre a disposición y por sus valiosos aportes.

A mis compañeros del curso de Transferencia de Calor por su gran apoyo, fundamental para terminar esta tesis. A Andrea, por su ayuda con las simulaciones en COMSOL y a Agustín por estar siempre dispuesto a colaborar. También a la Comisión Académica de Posgrado de la Universidad de la República por el apoyo económico a lo largo de estos dos años.

Por último, agradecer a mi familia por todo el apoyo y el esfuerzo que dedicaron a mi formación. Y un gracias especial a Guillermo, por acompañarme en este camino, apoyándome e impulsándome siempre a seguir creciendo.

RESUMEN

Los modelos de evaluación energética a escala urbana (UBEM, por sus siglas en inglés) están siendo foco de interés en varios países, ya que surgen como herramientas capaces de modelar los patrones de consumo de energía en el sector residencial. Para el caso de Uruguay, y a pesar de tratarse de un sector relevante en cuanto al consumo de energía, aun no existen desarrollos que modelen la demanda del sector residencial en detalle. Esta tesis se trata de un primer abordaje hacia un UBEM de Uruguay. Durante el trabajo se desarrolló una herramienta capaz de modelar los requerimientos de energía para acondicionamiento térmico en el parque habitacional uruguayo. La herramienta consiste en funciones desarrolladas en Python, y en particular en la librería Eppy, que se encargan de generar y simular la gran cantidad de modelos de EnergyPlus utilizados para representar el parque habitacional. Los resultados de las simulaciones se analizan tanto para el sector residencial en su totalidad así como disgregados según características relevantes de los edificios. Se identificaron los segmentos dentro del sector que tienen los mayores requerimientos de energía para acondicionamiento térmico así como las principales causas de estas altas demandas.

Palabras claves:
eficiencia energética, sector residencial uruguayo, Urban Building Energy Models, automatización de modelado en EnergyPlus.

ABSTRACT

Urban Building Energy Models (UBEM) are gaining worldwide interest as tools capable of providing deep understanding of energy patterns in the building sector. Though an important consumer, there are yet no developments that model energy demand in the Uruguayan residential sector in detail. This thesis is a first approach towards a Uruguay's UBEM. A tool capable of modelling energy requirements for space conditioning in the residential building stock was developed. Python functions and in particular its Eppy library, were used to generate and simulate a large quantity of EnergyPlus models required to represent the whole housing stock. Results are analysed for both the entire residential sector and also disaggregated according to relevant buildings characteristics. Segments with the highest demand for achieving thermal comfort within the residential sector were identified along with the major drivers for their high energy requirements.

Keywords:
energy efficiency, Uruguayan residential sector, Urban Building Energy Models, automated modelling in EnergyPlus.

Contents

Chapter 1

Introduction

In 2018, the world's residential sector consumed 21% of total final energy, constituting the third largest consumer [1]. This relevant proportion in which residential buildings contribute to the total final energy demand, combined with the intention of reducing energy intensity and greenhouse gases emissions, result in the need to effectively assess and manage energy consumption in the residential sector. There is therefore more and more interest in understanding energy patterns in buildings, which are quite complex given the high levels of interdependence they have on many sources.

Within this context, Urban Building Energy Models (UBEM) are gaining relevance as tools capable of modelling residential sector energy demand in detail at both temporal and spacial resolutions. Among the different UBEM types there are the physic-based bottom-up models, which determine residential sector energy consumption based on simulations run for buildings identified as typical within the stock. Results obtained for these typical buildings, or archetypes, are then extrapolated to represent the whole stock according to the prevalence of the modelled sample.

This type of models rely on the already well established and verified Building Energy Models (BEM). BEM are capable of modelling buildings energy performance based on their physical characteristics, local weather data and the thermodynamic principles which govern the interaction between a building and its surroundings. Among the models following this approach, EnergyPlus [2] appears as a rather mature and widely used software tool.

In Uruguay, residential sector is also a relevant one as it contributed to 19% of total final energy consumption in 2019 [3]. However, little has been done to

develop a local detailed model that allows to understand its energy patterns. Given that UBEM outcomes are highly dependant on weather data and building stock characteristics, it is not possible to utilize models implemented for other countries.

The objective of this work is thus to begin the path towards a local UBEM. Specifically, the aim is to model heating and cooling requirements for thermal comfort in the residential sector. The intention is to develop a physic-based bottom-up model which could be used to determine energy requirements for space conditioning for the country as a whole, and also disaggregated according to buildings significant characteristics and their local climate. The whole model is based on the Uruguayan housing stock characterisation performed in FSE_1_2017_1_144779 [4], in which the residential sector was divided into archetypes used to represent different buildings sharing some characteristics identified as relevant.

The methodology followed to address the goal of modelling heating and cooling requirements in the Uruguayan residential sector can be divided into three main stages. In the first, which corresponds to Chapter 2, EnergyPlus was selected as the engine in which the buildings simulations were going to rely on. The models implemented in EnergyPlus that would be used to solve the heat balance equations were also determined in this stage, as well as the results that were going to be processed after each simulation.

Secondly, given that the simulations were going to be performed upon archetypes used to represent a wide variety of buildings, it is important to determine the impact certain differences between those buildings represented by the same archetype could have on the results. This issue is approached in Chapter 3 and represents the second stage of the process. There, a study performed on an example archetype is presented, where the effect of different building orientations and surroundings was analysed.

The final stage is the model development itself, which is described in Chapter 4. This entailed the automation of the buildings models generation and simulation processes, and also of the results processing. In this regard, a tool was developed consisting of Python functions which interact with EnergyPlus input and output files through Eppy library. A simulation was then performed using this tool. The results were analysed for the country as a whole as well as disaggregated according to some relevant buildings characteristics.

Finally, Chapter 5 contains the work conclusions. A description of the thesis main outcomes can be found there and also comments regarding their limitations and the direction that future lines of work could follow.

Chapter 2

Building energy modelling using EnergyPlus

2.1 Introduction

The need to meet the growing demand for useful energy while at the same time reducing greenhouse gases (GHG) emissions is one of the major drivers towards a sustainable built environment. To achieve this goal, different tools have been developed so as to understand energy use. For buildings in particular, simulation tools appear as an option to address their complex dynamics, where heat flows can be very complicated and with high levels of interdependence on many sources. According to Spliter [5], it is since the 1960s that simulation of building thermal performance has been an active area of investigation. In the last decades, and due to the continuous development of computing capacity and computers access, these simulation tools have become more powerful and widely used.

There are different building energy models that allow to study energy consumption at building level. Among them, there are the physics-based tools which use detailed physics-based equations to model building components and systems. This technique is known as Building Energy Modelling (BEM) and it is used to model whole buildings and their sub-systems thermal behaviour in terms of energy consumption and indoor comfort [6]. According to BEM Library [7], "using BEM to compare energy-efficiency options directs design decisions prior to construction. It also guides existing building projects to optimize operation or explore retrofit opportunities". In other words, BEM

tools can be used as part of a new building design process or when considering updates to existing buildings in terms of either architecture or operation.

There are several mature software simulation tools that use this approach, among which there are Energy Plus [2], Trnsys [8] and ESP-r [9]. Both EnergyPlus and ESP-r are open-source building simulation software tools. The former was developed by the United States Department of Energy (DOE), while the latter was developed by the Energy Systems Research Unit (ESRU) of the University of Strathclyde in Glasgow. On the other hand, Trnsys is a commercial graphically based software environment used to simulate the behaviour of transient systems. All these three software simulation tools were tested with the International Energy Agency (IEA) Building Energy Simulation Test (BESTEST) [10] and have been widely used to analyse energy consumption at building level.

Lima and Olivera [11], for instance, developed a model of a Brazilian school restaurant in EnergyPlus. In order to do so, information regarding architectural design, constructions, equipments and schedules was used. Also, during the course of the study some zones temperatures were measured in order to calibrate the model. ESP-r was used by Psomas et al. [12] to analyse the impact of an automated window opening control system on a single-family house in Denmark. To achieve this goal, the ESP-r software was coupled with another tool where the openings controllers algorithms were established. Trnsys, on the other hand, was used by Liu et al. [13] to study the feasibility of the application of groundwater source heat pumps (GSHP) in residential buildings in China. In the study, a typical residential building was modelled in different climatic zones and simulations were run with and without the GSHP systems so as to analyse the impact of their application.

In this thesis, in order to quantify residential sector thermal energy requirements, a large amount of individual building simulations were executed. To this end, EnergyPlus 8.7 was selected as the simulation engine on the grounds that it is a well-established and verified building energy simulation tool. Besides, it has an open-source license and has been widely used to analyse buildings energy consumption. The tool also allows for adding new simulation capabilities by developing new modules in Fortran90/95, yet, this was not required during the course of this study.

In this chapter, the main characteristics of the software are presented along with the models used in this study for the buildings simulations. For those

cases were the model selected is not the EnergyPlus default, there is also an explanation of the reasons behind their selection. Finally, there is a description of the results processing performed in this work for each building simulation.

2.2 Program structure

According to EnergyPlus documentation [2], "EnergyPlus is a whole building simulation program that engineers, architects, and researchers use to model both energy consumption -for heating, cooling, ventilation, lighting and plug and process loads- and water use in buildings". The program works as a modular system where all the aspects of the simulation such as loads, systems and plants are integrated. The structure of EnergyPlus internal elements and the Integrated Solution Manager are summarized in Figure 2.1. The Simulation Manager controls the entire simulation process, whereas the Integrated Solution Manager manages the surface and air heat balances and acts as an interface between the heat balance and the Building System Simulation Manager. As it is an open source program, EnergyPlus source code is available to inspect and modify if required.

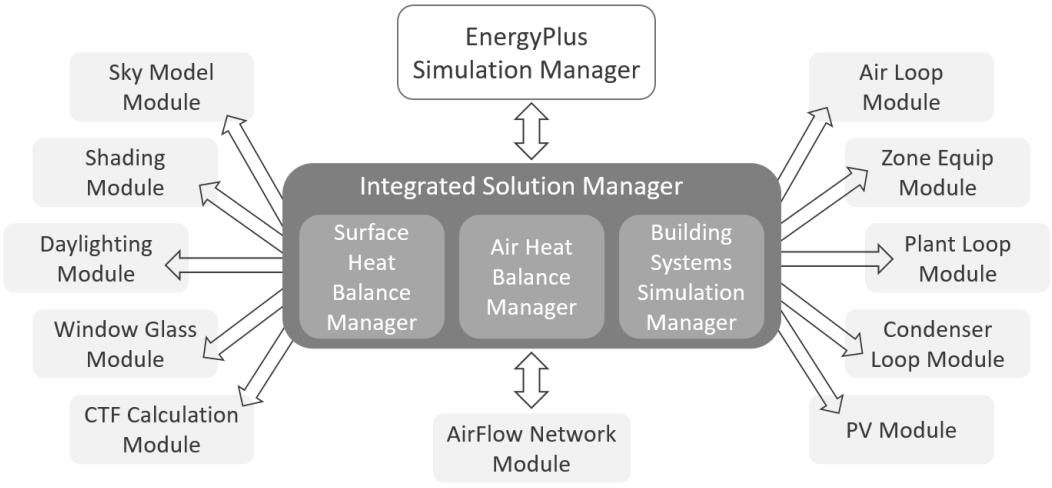

Figure 2.1: EnergyPlus internal elements. Source: "Getting Started" [14].

As most simulation packages, all the energy balances accounting for heat transfer by convection through the building surfaces, incoming or outgoing energy from infiltration and ventilation air, internal gains, long wave and solar radiation exchanges, thermal mass and inputs from Heating, Ventilating and

Air Conditioning (HVAC) systems are performed for each zone defined in the building model. An EnergyPlus zone is, therefore, a thermal and not a geometric concept. It is an air volume at a uniform temperature plus all the heat transfer and heat storage surfaces bounding or inside of that air volume [14]. Defining the building zones is, then, one of the first and most relevant steps when generating an EnergyPlus model as it determines the amount of energy balances the software needs to solve and, consequently, impacts on the simulation time and the accuracy of the results.

As it was developed as a simulation engine that end-users would typically use through a graphical interface, EnergyPlus input and output files were designed for easy maintenance and expansion rather than for user readability [15]. Inputs and outputs are thus simple ASCII text which are generally best left to a graphical user interface. However, the software is often used directly and that is how it was used in this study.

Main input files include the Input Data File (IDF) which is an ASCII file containing the data describing the simulation parameters as well as the building and the HVAC systems to be simulated. Also, there is the EnergyPlus Weather file (EPW) which is an ASCII file containing the hourly or sub-hourly weather data needed for the simulation, such as temperature, humidity, wind velocity and solar radiation. Besides, the EPW also includes basic location information and undisturbed ground temperatures, among some other information.

On the other hand, there are the output files. The most relevant include a CSV file where the results of the simulation are presented in terms of the user requested variables and time step, and an HTML file with the reports requested as a result. There are also a text file containing warnings and error messages issued by EnergyPlus during the simulation process, and an output in AutoCad DXF format which allows to graphically visualize the building geometry defined in the IDF.

2.3 Models

2.3.1 Air heat balance

For every zone defined within the model and for each time step, EnergyPlus solves the zone air heat balance. It includes the energy stored in zone air, the convective internal loads, the convective heat transfer from zone surfaces, the

heat transfer due to ventilation and infiltration of outside air and due to inter zone air mixing and the air systems output (see Equation 2.1).

$$C_z \frac{\mathrm{d}T_z}{\mathrm{d}t} = \sum_{i=1}^{N_l} \dot{Q}_i + \sum_{i=1}^{N_s} h_i A_i (T_{si} - T_z) + \dot{m}_{inf} C_p (T_\infty - T_z) + \\ + \sum_{i=1}^{N_z} \dot{m}_i C_p (T_{zi} - T_z) + \dot{Q}_{sys} \tag{2.1}$$

In Eq. 2.1 C_z and T_z are the zone air heat capacity and temperature, the $\dot{Q}_i$ are the convective gains due to internal loads, h_i, A_i and T_{si} are the zone surfaces convection coefficients, areas and temperatures; $\dot{m}_{inf}$ is the airmass flow rate entering the zone from the outside due to infiltration and ventilation, C_p is the air specific heat, T_∞ is the outside temperature, $\dot{m}_i$ are the airmass flow rates entering the zone from other zones due to inter zone air mixing, T_{zi} are those other zones temperatures and $\dot{Q}_{sys}$ is the air systems output. Besides, N_l, N_s and N_z are the total amount of internal loads, zone surfaces and zones, respectively.

The model used in this work to solve zone air heat balance equation is EnergyPlus default which is `3rdOrderBackwardDifference` that uses the third order finite difference approximation shown in Equation 2.2:

$$\left.\frac{\mathrm{d}T_z}{\mathrm{d}t}\right|_t \approx (\delta t)^{-1} \left(\frac{11}{6} T_z^t - 3T_z^{t-\delta t} + \frac{3}{2} T_z^{t-2\delta t} - \frac{1}{3} T_z^{t-3\delta t} \right) \tag{2.2}$$

where δt is the simulation time step and T_z^t is the zone temperature at time t.

The convective internal loads ($\sum_{i=1}^{N_l} \dot{Q}_i$ in Eq. 2.1) are determined based on the internal gains input information. In this work, the internal gains considered were people, lighting and electric equipment. In all three cases the input fields include the total load that ends up as heat contributing to zone loads and the fraction radiant, visible, latent or lost depending on the type of internal gain. Then, the convective heat gain is assumed to be the difference between the total load and the other type of heats (radiation, latent or lost) determined according to those fractions. Lost heat is defined only for electric equipment and represents the electric energy consumed by the equipment that does not end up as heat contributing to the zone loads. It could be energy converted to mechanical work or heat vented to the atmosphere.

Convection exchanges from interior surfaces into the zone ($\sum_{i=1}^{N_s} h_i A_i (T_{si} - T_z)$ in Eq. 2.1) are determined by solving the surfaces heat balances as described in Section 2.3.2. On the other hand, the infiltration and ventilation air mass flows either from the outside ($\dot{m}_{inf} C_p (T_\infty - T_z)$ in Eq. 2.1) or from other thermal zones ($\sum_{i=1}^{N_z} \dot{m}_i C_p (T_{zi} - T_z)$ in Eq. 2.1) are solved as described in Section 2.3.3. Finally, the term regarding the air system energy $\dot{Q}_{sys}$ in Eq. 2.1 is calculated as detailed in Section 2.3.4.

2.3.2 Surface heat balance

The surface heat balance solved by EnergyPlus for the enclosure surfaces as well as for every surface bounding each zone can be expressed as shown in Equation 2.3:

$$\dot{q}_{SWR} + \dot{q}_{LWR} + \dot{q}_{conv} - \dot{q}_k = 0 \tag{2.3}$$

where $\dot{q}_{SWR}$ is the absorbed short wave length radiation heat flow, $\dot{q}_{LWR}$ is the net long wave length radiation heat flow entering the surface, $\dot{q}_{conv}$ is the convective heat exchange from surrounding air to the surface and $\dot{q}_k$ is the conduction heat flow from the surface and into the wall, roof or floor.

The first term includes direct, reflected and diffuse sunlight or emittance from internal sources such as lights, depending on whether the surface being studied is an exterior or an interior surface. This term is influenced by location, surface facing angle and tilt, material properties and weather conditions. The second one includes the exchange with the environment (sky and ground), other zone surfaces, equipment and people. It depends on surfaces absorptivity and surfaces, ground and sky temperatures and view factors. The convection term depends on the convection coefficient and surface and air temperatures. There are several models implemented in EnergyPlus which can be used to determine convection coefficients. In this work the EnergyPlus default models were used, which are the `TARP`[1] algorithm for inside coefficients and the `DOE-2` for outside ones [17]. Finally, the conduction term can be calculated by a wide variety of formulations depending on the type of surface.

EnergyPlus distinguishes between surfaces belonging to walls or roofs, ground coupled surfaces and non-opaque surfaces like windows. Within each category there are several models which are already implemented in the soft-

[1] Based on the Thermal Analysis Research Program [16]

ware that can be used to solve surfaces heat balances and determine heat transfer through them. In this section the models selected in this study are described, along with their most relevant hypotheses. Due to its complexity, ground heat transfer model was particularly studied and compared to a multidimensional simulation implemented in another software.

Conduction through the walls and roof

EnergyPlus assumes surfaces of this kind to be at uniform temperature, diffuse emitters and reflectors, opaque and grey ($\tau = 0$, $\alpha = \epsilon$). Also, the heat flux leaving the surface is considered to be evenly distributed across the surface and the medium within the enclosure is assumed as non-participating.

Regarding the conduction term in the heat balance equation, conduction heat transfer through walls and roof is modelled as a one-dimensional, transient process with constant material properties. The resulting simplified heat diffusion equation is shown in Equation 2.4:

$$\frac{\partial^2 T}{\partial x^2}(x,t) = \frac{1}{\alpha}\frac{\partial T}{\partial t}(x,t) \tag{2.4}$$

where T, x, α and t are the temperature, coordinate in the heat flux direction, thermal diffusivity and time, respectively. In order to simplify the nomenclature, explicit reference to x and t as the variables of T function will henceforth be avoided.

Then, Fourier's law expressed in Equation 2.5 determines the conduction heat flux ($\dot{q}''$) as a function of thermal conductivity of the material (k) and temperature gradient across a differential thickness.

$$\dot{q}'' = -k\frac{\partial T}{\partial x}\hat{i} \tag{2.5}$$

Therefore, by knowing the materials properties and initial and boundary conditions, heat transfer can be determined by solving Eqs. 2.4 and 2.5. Given that Eq. 2.4 is a partial differential equation, the system is usually solved numerically, often by means of the Conduction Transfer Function (CTF) method [18]. This method results in a simple linear equation and is EnergyPlus default heat balance algorithm and the one used in this work. It expresses the current conduction heat flux at either face of the surface in terms of the current temperature and some of the previous temperatures, at both inside and

outside faces, and some of the previous flux at the given face (see Equations 2.6 and 2.7) [17].

$$\dot{q}''_{ki}(t) = -Z_0 T_{i,t} - \sum_{j=1}^{nz} Z_j T_{i,t-j\delta} + Y_0 T_{o,t} + \sum_{j=1}^{nz} Y_j T_{o,t-j\delta} + \sum_{j=1}^{nq} \phi_j \dot{q}''_{ki,t-j\delta} \quad (2.6)$$

$$\dot{q}''_{ko}(t) = -Y_0 T_{i,t} - \sum_{j=1}^{nz} Y_j T_{i,t-j\delta} + X_0 T_{o,t} + \sum_{j=1}^{nz} X_j T_{o,t-j\delta} + \sum_{j=1}^{nq} \phi_j \dot{q}''_{ko,t-j\delta} \quad (2.7)$$

In Eq. 2.6 and 2.7 $\dot{q}''_{ki}$ and $\dot{q}''_{ko}$ are the inside and outside faces heat fluxes, respectively. T_i and T_o are the inside and outside face temperatures, δ is the time step and nz and nq are the numbers of history terms for the temperatures and the heat flux, respectively. Finally, X_j, Y_j and Z_j are the outside, cross and inside CTF coefficients while ϕ_j is the flux CTF coefficient. All these CTF coefficients (CTFs) represent the materials thermal response as determined by its properties. CTFs are temperature independent and, therefore, only need to be determined once for each construction type. EnergyPlus uses the state space (SS) method in order to calculate CTFs as detailed in [17].

The CTF method does not take into account moisture storage or diffusion in the construction elements. So by choosing it as the algorithm used for calculating the performance of the building surfaces, the solutions obtained are sensible heat only solutions.

Conduction through the ground

Two main difficulties arise when it comes to determine ground heat transfer. The first one is due to the fact that conduction heat transfer calculations in EnergyPlus are one-dimensional, whereas conduction through the ground is two or three-dimensional. This triggers modelling problems regardless of the method used to determine conduction through the ground. The second difficulty is the great difference in the timescales involved in the processes. Specifically, while the thermal zone modelling is on an hourly scale, ground heat transfer is on a monthly timescale [19].

There are different approaches for simulating heat transfer with horizontal building surfaces in contact with the ground in EnergyPus. The simplest con-

sists of setting the temperatures of the surface in contact with the ground for each month. However, and despite being the simplest model and the one which requires less computational effort, this approach has two main drawbacks: that the temperatures required as inputs are usually unknown data, and that the model is not sensitive to floor and ground interface temperatures variations within the month. While this second disadvantage may not be relevant due to the ground heat transfer timescale, the first is. As a workaround for this issue there is the Slab preprocessor, an auxiliary program in the EnergyPlus package which runs previously than the actual simulation and solves the interface temperatures. Nevertheless, the Slab preprocessor requires the inside temperatures as part of the input data, which may actually be the desired results for the main simulation. Therefore, following this approach could be quite cumbersome as it could result in an iterative process in which both inside and ground interface temperatures are solved by successive executions of the preprocessor and the main simulation.

In this work, a general finite difference ground model implemented in EnergyPlus (`GroundDomain:Slab`) was used. This model uses an implicit finite difference formulation to solve for the ground temperatures. It therefore results in a stable simulation for all time steps and grid sizes, but an iteration loop must be performed to converge the temperatures in the domain for each time step [17]. The approach of this model is to create a surface of equivalent area within the ground domain as a representation of the horizontal surfaces coupled to the ground domain. This surface interacts with the ground and provides temperature boundary conditions to the coupled surfaces for their use in the one-dimensional heat equations. The coupling method is that suggested in [20] and represented in Figure 2.2.

The average surface conduction heat flux from all surfaces connected to the ground is imposed as the ground domain boundary condition at the interface cells. Heat flux at each interface cell is adjusted according to Equation 2.8:

$$q_{out,i} = q_{out,1D} \frac{T_{zone} - T_{out,i}}{T_{zone} - T_{out,average}} \tag{2.8}$$

where subindex i refers to each interface cell, subindex $zone$ refers to each EnergyPlus thermal zone and ($q_{out,1D}$) is the average surface conduction heat flux from all surfaces coupled to the ground.

At the ground domain sides and lower surfaces, undisturbed temperature profiles are imposed. Finally, heat balance is performed to the ground surface cells where long and short wave radiation, conduction, convection and evapotranspiration are considered. Then, the ground model determines the temperature profile among the interface ($T_{out,i}$), and its average ($T_{out,average}$) is imposed as the boundary condition to the coupled surfaces at the next time step.

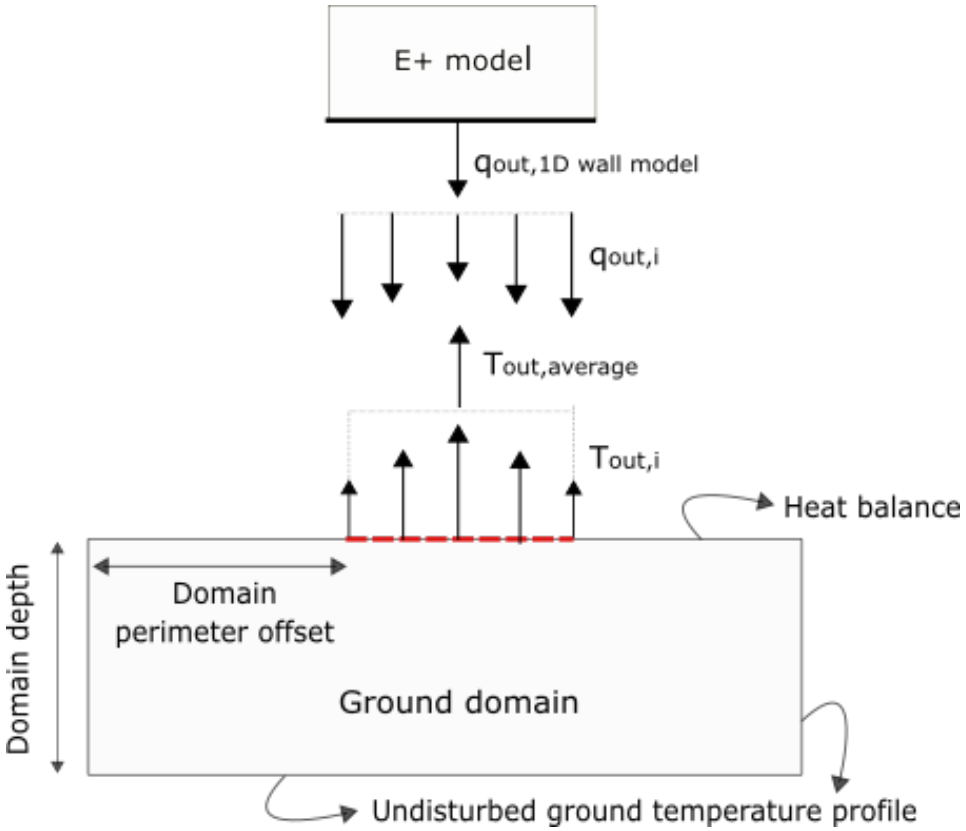

Figure 2.2: Coupling method.

The undisturbed ground temperatures which are the boundary condition at the ground domain sides and lower surfaces are based on the correlation developed by Kusuda T. and Achenbach P. [21]. This correlation uses three parameters for ground temperature at the surface to determine undisturbed ground temperature as a function of depth and time ($T(z,t)$) as shown in Equation 2.9.

$$T(z,t) = \overline{T_s} - \Delta\overline{T_s}\, e^{-z\sqrt{\frac{\pi}{\alpha\tau}}} cos\left(\frac{2\pi t}{\tau} - \theta\right) \tag{2.9}$$

Where $\overline{T_s}$ and $\Delta\overline{T_s}$ (both in °C) are the average annual soil surface temperature and the amplitude of the soil temperature change throughout the year, respectively. θ is the phase shift or day of minimum surface temperature, α is the ground thermal diffusivity and τ is the time constant, which is 365. EnergyPlus has the capability of determining $\overline{T_s}$, $\Delta\overline{T_s}$ and θ based on the typical undisturbed 0.5 m depth soil temperatures, included in the weather files.

The `GroundDomain:Slab` model has been tested and compared to other models in the IEA BESTEST for Ground Coupled Heat Transfer [22]. Yet, as part of this work, some extra tests were carried out. These tests consisted of running some models in EnergyPlus using the `GroundDomain:Slab` model for solving ground heat transfer and then using another model, the Slab preprocessor. Besides, for the case of the `GroundDomain:Slab` model, two different undisturbed ground temperatures models were tested: the one developed by Kusuda and Achenbach described before and another based on one-dimensional finite difference heat transfer model. Then, these results were compared to those obtained in COMSOL [23], a well-established general purpose simulation software which uses the finite element method to solve the heat balance equations.

Two test cases were defined based on the same construction shown in Figure 2.3. It consists of a 10 m x 10 m slab, with 3 m of height and wall thickness of 0.2 m. Thermal properties both for the soil and the walls are $k_{soil} = k_{wall} = 1.5$ W/mK and $\alpha_{soil} = \alpha_{wall} = 4.6X10^{-7}$ m^2/s. The temperature inside the zone is $T_{in} = 20$°C and the convection coefficients are $h_{in} = 6\,\mathrm{W/m^2K}$ and $h_{out} = 12\,\mathrm{W/m^2K}$. In test case 1, $T_{out} = 0$°C all throughout the year whereas in test case 2, $T_{out} = 5sin\left(\frac{\pi}{12}(t-9)\right)$ where t is the hour of the day. Moreover, three different combinations of vertical insulation depth (e) and thermal resistance (R_{ins}) were defined for each test case. In Table 2.1 the test cases are presented along with their outside temperature and vertical insulation characteristics.

For implementing these tests cases in EnergyPlus the undisturbed 0.5 m depth soil temperatures were set to 0°C for every month. Ground domain dimensions were 15 m both for the perimeter offset as well as for the domain depth. Slab location was modelled as in grade, meaning that the slab top surface is levelled with ground surface, and the slab material thermal properties were the same as for the soil. An hourly simulation time step was selected and geometric mesh coefficient and mesh density parameter were both left

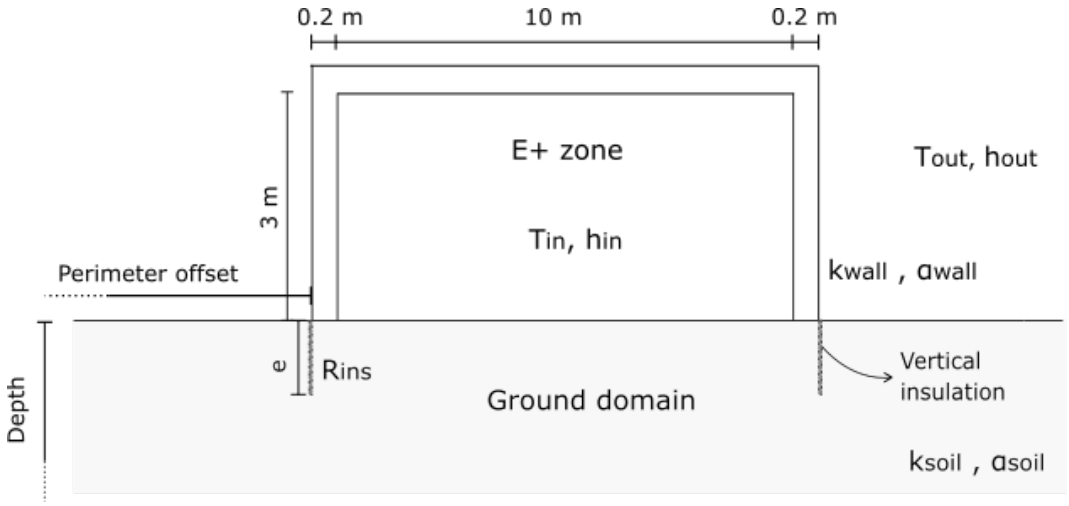

Figure 2.3: Test cases schematic view.

Table 2.1: Test cases definition.

Test Case	$\mathbf{T_{out}}(^{\circ}\mathbf{C})$	**Insulation**	
		Depth	$R_{ins}(m^2K/W)$
1a	0	0	0
1b	0	0.6	0.5
1c	0	0.6	1
2a	$5sin\left(\frac{\pi}{12}(t-9)\right)$	0	0
2b	$5sin\left(\frac{\pi}{12}(t-9)\right)$	0.6	0.5
2c	$5sin\left(\frac{\pi}{12}(t-9)\right)$	0.6	1

as suggested by EnergyPlus: 1.6 and 6, respectively. The geometric mesh coefficient represents the compression of cell distribution and values for this field are limited from 1.0 (uniform cell distribution) to 2.0 (highly skewed distribution). On the other hand, the mesh density parameter represents the number of cells to be placed between any two domain partitions (slab edges, insulation edges, etc.) during mesh development [24].

For the test cases implementation in COMSOL, the Heat Transfer in Solids module was used were stationary and time dependant analyses were performed for test cases 1 and 2, respectively. Based on the symmetry of the geometry, the domain was set to be one quarter of the model and materials were defined according to the mentioned thermal properties. Boundary conditions were adiabatic at the symmetry planes and at 50 m depth and 25 m of perimeter offset, whereas the established convection coefficients and exterior and interior temperatures were used as the boundary conditions for the domain top

surface. The mesh used is COMSOL default and its characteristics regarding `Sequence type` and `Element size` are `Physics controlled mesh` and `Finer`, respectively. This configuration implies the following parameters:

- Maximum element size: 2.86 m
- Minimum element size: 0.208 m
- Maximum element growth rate: 1.4
- Curvature factor: 0.4
- Resolution of narrow regions: 0.4

The domain defined for the test cases implementation in COMSOL is presented in Figure 2.4 with the mesh used (see Fig. 2.4a) and the obtained temperatures and heat flux lines for test case 1a (Figs 2.4b and 2.4c, respectively).

The results obtained for the heat transferred through the ground according to each model are in Tables 2.2 and 2.3. Taking into consideration that inside temperature is a fix value in both scenarios, in test case 1 the heat obtained is a constant value because the outside temperature is also constant. On the other hand, in test case 2 the outside temperature varies throughout the day with a sinusoidal behaviour and, so, the same happens to the heat transferred in this case scenario. This is the reason why in Tab. 2.2 the heat is presented as a single value whereas in Tab. 2.3 results are represented by both the mean value and the amplitude.

The first conclusion that can be drawn from Tab. 2.2 and 2.3 is that all the three EnergyPlus models could be used to represent ground heat transfer. For the case of Slab preprocessor model, it calculates a single mean value for each month for the interface temperature in the ground domain ($T_{out,i}$ in Fig. 2.2). It is therefore not capable of considering the case 2 variations in the outside temperature throughout the day, entailing amplitude values of 0 in all cases in Tab. 2.3.

In order to have an idea of which of the models implemented in EnergyPlus is the most accurate, and even though only three scenarios were considered, the Root Mean Square Deviation (RMSD) and the Mean Bias Deviation (MBD) were calculated for each example case, taking the COMSOL results as the reference. These results are shown in Tables 2.4 and 2.5 for the test case 1 and 2, respectively and are expressed relative to the mean of the COMSOL results.

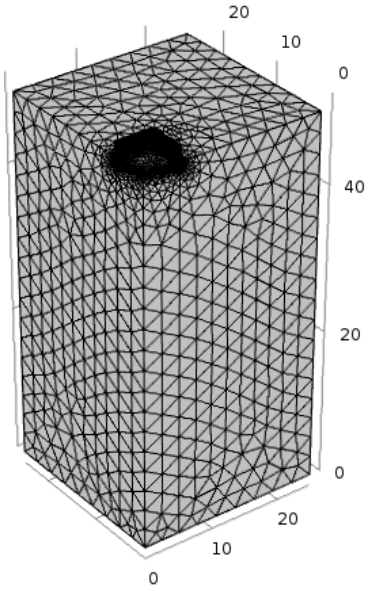

(a) Mesh.

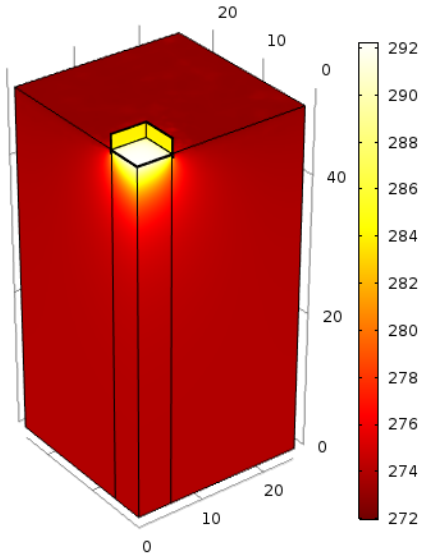

(b) Resulting temperatures.

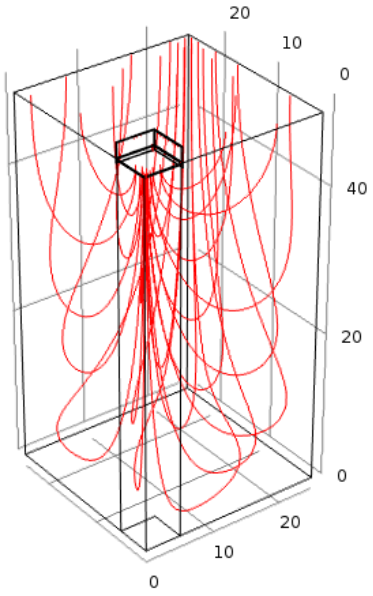

(c) Resulting heat flux lines.

Figure 2.4: COMSOL domain and results.

In test case 1, the `GroundDomain:Slab` model with Kusuda and Achenbach undisturbed ground temperatures proved to be the most accurate when taking COMSOL as the reference. In this case, Slab preprocessor underestimated the heat through the ground by far whereas `GroundDomain:Slab FD` overestimated it. On the other hand, in test case 2, Slab preprocessor and `GroundDomain:Slab KA` represent quite fairly the mean heat transfer but not its amplitude, which was underestimated by all three models. Yet, in test case

Table 2.2: Test case 1 results.

Test Case	$\mathbf{Q_{ground}(W)}$			
	COMSOL	Slab preprocessor	GroundDomain: Slab K-A †	GroundDomain: Slab FD ††
1a	1272.0	1027.9	1236.0	1380.2
1b	1125.0	966.0	1143.5	1288.8
1c	1125.0	931.0	1080.6	1225.8

† GroundDomain:Slab and Kusuda and Achenbach undisturbed ground temperatures.
† † GroundDomain:Slab and finite difference undisturbed ground temperatures.

Table 2.3: Test case 2 results.

Test Case		$\mathbf{Q_{ground}(W)}$			
		COMSOL	Slab preprocessor	GroundDomain: Slab K-A	GroundDomain: Slab FD
2a	mean amplitude	1274.7 3.2	1230.8 0.0	1234.2 2.9	1374.6 3.0
2b	mean amplitude	1125.3 2.8	1133.8 0.0	1142.4 0.1	1283.4 0.2
2c	mean amplitude	1125.1 2.8	1080.8 0.0	1079.5 0.1	1220.4 0.1

Table 2.4: Test case 1 RMSD and MBD.

Model	RMSD (%)	MBD (%)
Slab preprocessor	17.2	-17.0
GroundDomain:Slab K-A	3.0	-1.8
GroundDomain:Slab FD	10.9	10.6

Table 2.5: Test case 2 RMSD and MBD.

Model		RMSD (%)	MBD (%)
Slab preprocessor	mean amplitude	3.1 100.2	-2.3 -100.0
GroundDomain:Slab K-A	mean amplitude	3.1 75.9	-2.0 -64.8
GroundDomain:Slab FD	mean amplitude	10.3 73.9	10.0 -62.4

2 as in real applications, variations throughout a day in the heat transferred through the ground are rather small compared to its mean value (see Tab.2.3). So the accuracy of the amplitude calculation is not relevant for the building heat balance. Therefore, from test case 2 results, it could be concluded that both Slab preprocessor and `GroundDomain:Slab KA` are the best options.

All in all, the `GroundDomain:Slab` model with the undisturbed ground temperatures determined as suggested by Kusuda and Achenbach appears to be the most accurate model from the three considered. Yet, in this study only two test cases and three scenarios within each were considered. For the analysis to reach more valuable and formally correct conclusions, more cases and scenarios should be compared. Nevertheless, the `GroundDomain:Slab` model with the undisturbed ground temperatures determined as suggested by Kusuda and Achenbach has already been thoroughly tested in the IEA BESTEST for Ground Coupled Heat Transfer [22]. In consequence, this is the model selected in this work for solving ground heat transfer when running the buildings simulations.

Windows heat transfer

Windows calculations are based on the layer-by-layer approach implemented in EnergyPlus. It considers windows to be composed of different components including glazing, air or another gas gaps separating glazing layers, frame, dividers and shading devices. From all of these, the only component which is required to be present is the glazing, that should consist of at least one plane glass layer.

EnergyPlus determines the window glass face temperatures and the heat transferred through the glazing by solving the heat balance equations on each glazing surface every time step. These equations are more complex than in the case of walls given that windows consist of layers of non-opaque surfaces. As established in [17], some assumptions are made in order to solve the heat balances:

1. Heat storage in the glass can be neglected based on the assumption that glass layers are thin enough. This entails that there are no heat capacity terms in the equations.
2. Glass faces are isothermal and so heat flow is one dimensional and perpendicular to the glass faces.
3. The glass layers are opaque to infrared radiation.
4. The short wave radiation is uniformly absorbed in a glass layer and so, for the heat balance, it is apportioned equally to the two faces of the layer.

Also, for the zone heat balance calculation the inside surface temperature of the frame and divider are needed. Therefore, heat balance equations on both inside and outside surfaces of frames and dividers are solved. They are assumed to be isothermal and the frame and dividers profiles are considered to be rectangular.

Finally, there are the shading devices which can be either on the exterior or on the interior side of the window or also between glass layers. In this work only exterior shading devices were considered. Its thermal model considers the long wave radiation from the ground and sky absorbed by the device or transmitted by the device and absorbed by the adjacent glass, the inter-reflection of long wave radiation between the device and the adjacent glass, the solar radiation absorbed by the shading device, inter-reflection of solar radiation between the shading layer and glass layers, the convection from shading layer and glass to the air in the gap and from the exterior layer shading to the outside air [17].

The windows of the buildings modelled during this study consist of a single layer of glazing, a frame and a divider. The frame and divider materials depend on the buildings vintage and socio-economic level of its occupants. Solar protections were assumed to be completely opaque and located only on the exterior side of the windows. Their presence also depends on the buildings vintage and socio-economic level of its occupants as well as on the zone usage.

2.3.3 Infiltration and ventilation loads

Infiltration and ventilation are driven by the pressure differences between the air leakage components internal and external environments. These pressure differences may be caused by wind or air density variations due to differences in internal and external temperatures. There are some simplified models implemented in EnergyPlus for solving the infiltration and ventilation air flow rates and thermal loads, all of which model the entire building as a single zone and assume a unique inside temperature. These models are the `DesignFlowRate`, the `EffectiveLeakageArea` and the `FlowCoefficient` for infiltration and also the `DesignFlowRate` and the `WindAndStackWithOpenArea` for ventilation. In all of them, the air flow rates are assumed to depend on some user defined parameters, the temperature difference between zone air and outdoor air and the local wind speed. On the other hand, more detailed infiltration and ventilation calculations are possible using the `AirflowNetwork` (AFN) model also imple-

mented in EnergyPlus. By using this model, not only the air flows between the interior and exterior are solved but also among the thermal zones defined within the building. Besides, the wind direction is taken into consideration in this model along with the wind speed.

As part of the work carried out in the project FSE_1_2017_1_144779 [4], the research team studied these different models and performed an analysis to determine which was the best alternative for the purposes of the project. Based on the idea that infiltration and ventilation loads would represent a relevant portion of the total heat exchanged between a zone and its surroundings, it was concluded that the better accuracy provided by the AFN model was worth the extra effort required for using a far more detailed model. This recommendation was also followed in this thesis. So in order to determine the infiltration and ventilation loads either from outside air or from adjacent zones, the AFN model implemented in EnergyPlus was used.

This model is capable of determining air flow through cracks in exterior or interior surfaces and also of solving the flow due to natural ventilation. Besides, it allows to set either a zone level or an opening level control for natural ventilation based on temperature, enthalpy or some of the defined comfort criteria. On the other hand, the model does not consider air circulation or air temperature stratification within a thermal zone [24]. Its solving method consists of a set of nodes, with a certain temperature, humidity and pressure, connected by airflow components through linkages. Each thermal zone in the building represents an airflow node whereas for the exterior there is one airflow node for each air leakage component. These components such as openings and cracks correspond to the airflow linkages.

The airflow calculations are highly dependent on the air pressures surrounding the building due to wind [25]. These wind pressures are calculated for each exterior node according to Equation 2.10:

$$p_w = C_p \rho \frac{V_{ref}^2}{2} \tag{2.10}$$

where p_w in Pa is the wind surface pressure relative to static pressure in undisturbed flow, ρ is the air density (kg/m^3), V_{ref} is the reference wind speed at local height (m/s) and C_p is the wind pressure coefficient of the corresponding facade.

The local wind speed for each external node is determined with Equation 2.11, where the height used for its calculation (z in Eq. 2.11) is that of the corresponding component centroid. For the pressure coefficients, the model allows for them either being set by the user or automatically calculated. In this thesis the second option was selected meaning that, for each time step, the program calculates a surface-average wind pressure coefficient for the building facades and the roof according to Equation 2.12.

$$V_z = V_{met} \left(\frac{\delta_{met}}{z_{met}} \right)^{\alpha_{met}} \left(\frac{z}{\delta} \right)^{\alpha} \tag{2.11}$$

In Eq. 2.11 subindexes z and met represent the desired location and the meteorological station, respectively. V is the wind speed, z the height above the ground and δ and α are the wind speed profile boundary layer thickness and exponent, respectively. δ, δ_{met}, α and α_{met} take values according to the terrain type selected by the user.

$$\begin{aligned} C_p = 0.6 \ln[1.248 - 0.703 \sin(\theta/2) - 1.175 \sin^2(\theta) + 0.131 \sin^3(2\theta G) + \\ + 0.769 \cos(\theta/2) + 0.07 G^2 \sin^2(\theta/2) + 0.717 \cos^2(\theta/2)] \end{aligned} \tag{2.12}$$

In Eq. 2.12 C_p is the average pressure coefficient for a given facade, θ is the angle between wind direction and outward normal of the facade under consideration and $G = ln(L_1/L_2)$ with L_1 being the width of the wall under consideration and L_2 the width of the adjacent wall.

Then, based on the calculated wind pressures and forced airflows (if present), the model proceeds to pressures and airflows calculations. Each component such as openings and cracks has a relationship between airflow and pressure drop. Therefore, for solving the pressure in each node and airflow through each linkage, a system of equations is assembled consisting of one equation for each linkage, based on the type of component that conforms it.

In this work, the infiltrations are assumed to be through cracks in the roof, through every opening (exterior and interior doors and windows) and through the stairwell in the two-storey houses. The models used to characterize these type of air pathways in terms of the airflow through them as a function of pressure difference, are the `Crack`, the `SimpleOpening` and the `HorizontalOpening`. The airflow through a crack and through closed vertical

and horizontal openings are characterized by Equation 2.13 with the exception that for the openings there is no $CrackFactor$ and the temperature correction factor is not considered.

$$\dot{m} = (CrackFactor)C_T C_Q (\Delta P)^n \tag{2.13}$$

Where $\dot{m}$ is the air mass flow (kg/s), the $CrackFactor$ is set by the user, C_Q is the air mass flow coefficient at 1 Pa, ΔP the pressure difference across the crack and n the air flow exponent. $C_T = \left[\frac{\rho_0}{\rho}\right]^{n-1} \left[\frac{\nu_0}{\nu}\right]^{2n-1}$ is a dimensionless reference condition temperature correction factor, where ρ and ν are the air density and kinetic viscosity at the specific air temperature condition whereas ρ_0 and ν_0 are those at the reference air conditions: 20°C and 101325 Pa.

When windows and doors are open the `SimpleOpening` model establishes the pressure difference at any level z of a vertical opening based on reference pressures, assuming Bernoulli hypothesis on both sides of the opening and including a turbulence term as shown in Equation 2.14:

$$P_1(z) - P_2(z) = (P_{1,ref} - P_{2,ref}) - g(\rho_1 z - \rho_2 z) + \Delta P_t \tag{2.14}$$

where subindexes 1 and 2 refer to each side of the opening, P is the air pressure, P_{ref} is a known air pressure at $z = 0$ and ΔP_t is a pressure difference which simulates the effect of turbulence.

Then, the airflow velocity at any given z is given by Equation 2.15:

$$v(z) = \sqrt{2\frac{P_1(z) - P_2(z)}{\rho}} \tag{2.15}$$

Finally, by knowing the airflow velocity profile, the airmass flow is calculated as shown in Equation 2.16.

$$\dot{m} = C_d \theta \int_{z=0}^{z=H} \rho v(z) W dz \tag{2.16}$$

Where $\dot{m}$ is the airmass flow (kg/s), C_d is the discharge coefficient set by the user, θ is the area reduction factor which defines the effective opening of the window or door, W is the opening width and H the opening height.

The `SimpleOpening` model, also considers that Eq. 2.14 may have a root in $0 < z < H$ meaning that there is a neutral plane and that there would be two-way flow through the opening.

On the other hand, the `HorizontalOpening` model considers the superposition of the forced (due to the pressure difference across the opening) and the buoyancy flow. This model formulation is explained in [17] and its results for the relationship between airmass flow and pressure difference through a horizontal opening are presented in Equations 2.17 and 2.18.

$$\dot{m}_U = \begin{cases} \dot{m}_{buo} & \text{if } P_L \geq P_U \\ -\rho_U A_{eff} C_d \left(\frac{2|\Delta P|}{\rho_{ave}}\right)^{0.5} + \dot{m}_{buo} & \text{if } P_L < P_U \end{cases} \tag{2.17}$$

$$\dot{m}_L = \begin{cases} \dot{m}_{buo} & \text{if } P_U \geq P_L \\ -\rho_L A_{eff} C_d \left(\frac{2\Delta P}{\rho_{ave}}\right)^{0.5} + \dot{m}_{buo} & \text{if } P_U < P_L \end{cases} \tag{2.18}$$

Where subindexes U and L refer to the upper and lower zones, $\dot{m}_U$ is the air mass flow from the lower to the upper zone whereas $\dot{m}_L$ is the air mass flow from the upper to the lower zone. A_{eff} is the effective opening area, C_d the discharge coefficient set by the user, ρ_{ave} the average air density between the lower and the upper zone and $\dot{m}_{buo}$ is the buoyancy flow which is calculated as shown in Equation 2.19.

$$\dot{m}_{buo} = \begin{cases} \dot{m}_{buo,max}\left(1 - \frac{|\Delta P|}{|\Delta P_{Flood}|}\right) & \text{if } \Delta\rho > 0 \text{ and } \frac{|\Delta P|}{|\Delta P_{Flood}|} < 1 \\ 0 & \text{Otherwise} \end{cases} \tag{2.19}$$

Where $\dot{m}_{buo,max} = \rho_{ave} 0.055 \left(\frac{g|\Delta\rho|D_H^5}{\rho_{ave}}\right)^{0.5}$ with D_H the hydraulic diameter and $\Delta P_{Flood} = |C_{shape}^2 \frac{g\Delta\rho D_H^5}{2A_{eff}^2}|$ with $C_{shape} = 0.942\text{width/depth}$ for a rectangular opening.

Therefore, based on the `Crack`, `SimpleOpening` and `HorizontalOpening` models, the information of the components discharge coefficient, airmass flow coefficient and exponent, and with the wind data provided in the weather file, the AFN model solves the pressures in each node and airmass through each linkage. Then, with the airflow calculated for each linkage, the infiltration and ventilation loads can be determined.

2.3.4 HVAC system

There are several HVAC equipments and forced air units implemented in EnergyPlus. By means of the Building System Simulation Manager, the supply

air stream is calculated and the system thermal load is included in the zone air heat balance equation as $\dot{Q}_{sys}$ which is determined as shown in Equation 2.20.

$$\dot{Q}_{sys} = \dot{m}_{sys} C_p (T_{supply} - T_z) \tag{2.20}$$

Where $\dot{m}_{sys}$ is the airmass stream, C_p is the air specific heat, T_{supply} is the specified supply air temperature and T_z is the zone temperature.

In order to determine $\dot{Q}_{sys}$, EnergyPlus uses a predictor-corrector scheme which first estimates it assuming stationary conditions and zone air temperature equal to the set point temperature. Then, with that energy quantity as a demand, the system is simulated by the Building System Simulation Manager and its actual capability is determined.

In this study, the HVAC template: `IdealLoadsHVAC` was used. This is the simplest HVAC model and consists of an ideal system which supplies conditioned air to the zone by mixing air at the zone exhaust condition with the specified amount of outdoor air (none in this study) and then adds or removes heat and moisture at 100% efficiency. This model is usually used in situations where the user wishes to study the building requirements without modelling a full HVAC system [24]. It provides an understanding of the quantity of energy required to maintain certain conditions in a given zone and so it provides a way to characterise the buildings and its zones thermal performances. As a consequence, it allows to compare different zones within a building and also different buildings with each other. These comparisons may result in determining the impact of the building characteristics such as enclosure materials, openings sizes and quality, geographic location and usage patterns on its thermal energy requirements.

Therefore, in this thesis, the obtained heating and cooling loads refer to thermal energy requirements. Their conversion to final energy consumed would depend on to which extent these requirements are satisfied and the characteristics of the actual HVAC system (efficiency and energy source).

2.4 Results processing

For each case simulated results were processed with the intention of converting output data into meaningful information. In this study, the goal of this process was to characterize each building modelled in terms of their thermal

energy requirements. Besides, and aiming at identifying areas of improvement, energy gains and losses through each building component such as its enclosure, windows, internal gains and those due to infiltration and ventilation were identified. In order to determine the contribution of each term to the heating or cooling demand, different EnergyPlus variables were considered based on the corresponding heat balance.

All processed results for each building are presented on a monthly scale. Moreover, in order to easily identify major drivers of thermal energy demand, the relative contribution of each term to the total is determined. This calculation is done for the cooling and heating periods, which were considered to be from the 1st of December to the 28th of February and from the 1st of June to the 31th of August, respectively.

In the following sections a description of all the processed results is provided. It includes the explanation of the results meaning, along with the EnergyPlus output variables used to determine them. Based on the large amount of simulations that were carried out for the analyses presented in the next two chapters, the process of calculating the desired results from the simulations output variables was automatized. In order to do so, Python functions were developed and Eppy scripting library [26] was used. This library is based on Python and has the capability to manipulate EnergyPlus files. The automation process is described in Chapter 4 including details regarding inputs and outputs and an insight into the most relevant functions developed.

2.4.1 HVAC loads

This result includes the monthly heating and cooling energy provided by the HVAC systems in order to ensure thermal comfort to the occupants. Taking into consideration the characteristics of the model used for the HVAC system mentioned in Section 2.3.4, these loads represent thermal energy requirements (and not energy demand) for occupants comfort.

These heating and cooling loads are for the whole building, meaning that all the present HVAC systems loads are added. There is one system per conditioned building zone, yet, not all zones within a building are conditioned. This varies across the different buildings depending on the zones usage and the total amount of occupants with the objective of the model to be as realistic as possible. Even though there are some households in which thermal condi-

tioning is done regardless of the zone usage and the occupants presence (such as older residential building apartments with central heating), these are the minority in the Uruguayan housing stock. Therefore, and aiming at gaining generality, these type of households were not taken into consideration.

EnergyPlus output variables used to obtain these results are: *Zone Ideal Loads Zone Sensible Cooling Rate* and *Zone Ideal Loads Zone Sensible Heating Rate*. During the simulation, these variables are determined hourly for each zone ideal loads air system. Therefore, its processing involved adding all zones rates and then converting them into monthly energy.

2.4.2 Enclosure

In order to analyse the heat transfer through the building enclosure, it is separated into gains and losses through walls, roof and floor. Besides, for the gains through walls and roof, it is distinguished between those due to solar radiation absorbed by the surface and conducted into the construction, and those due to other sources. These other sources include long wave radiation from the environment and convective exchange with outside air.

To provide a better understanding of these results, the heat balance for a wall outside surface, the output variables processed and the obtained results are presented in Figure 2.5. The same would apply for a roof outside surface.

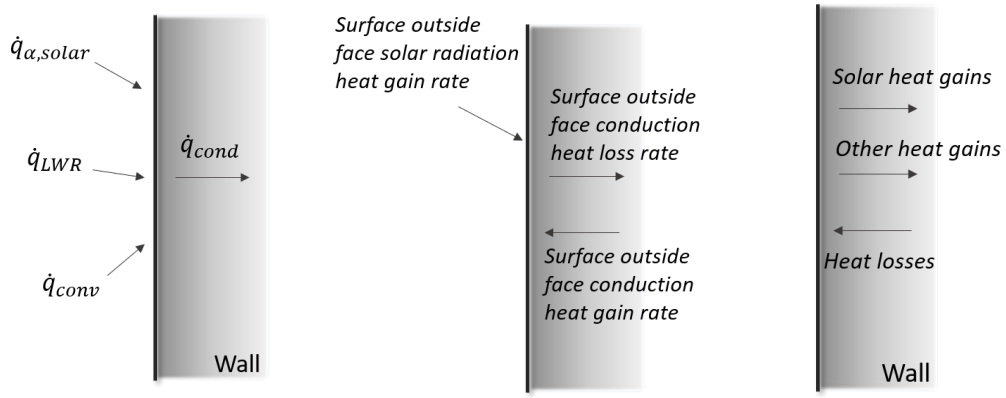

(a) Heat balance. **(b)** EnergyPlus output variables. **(c)** Results.

Figure 2.5: Outside surfaces variables.

The heat balance on an outside surface (Fig. 2.5a) is that presented in Equation 2.21:

$$\dot{q}_{\alpha,solar} + \dot{q}_{LWR} + \dot{q}_{conv} = \dot{q}_{cond} \tag{2.21}$$

where $\dot{q}_{\alpha,solar}$ is the absorbed solar radiation, $\dot{q}_{LWR}$ is the net long wavelength radiation exchange, $\dot{q}_{conv}$ is the convective exchange with outside air and $\dot{q}_{cond}$ is the heat conducted into the wall.

The EnergyPlus output variables processed in order to get the desired results are those shown in Fig. 2.5b. They are provided hourly and for each outside surface of the building. *Surface outside face solar radiation heat gain rate* is the heat gained by the outside surface due to the absorption of solar radiation, which is equivalent to $\dot{q}_{\alpha,solar}$ of both Fig. 2.5a and Eq. 2.21. It is important to note that this heat does not necessarily ends up as heat gained by the zone, on the grounds that it can be lost from the surface to the outside as long wavelength radiation and/or convection.

On the other hand, there are the *Surface outside face conduction heat loss rate* and the *Surface outside face conduction heat gain rate* which are considered to be the heat entering and leaving the zone, respectively. Note that these two variables names are thought from the outside surface point of view, entailing that the heat lost from the surface is the one gained by the zone and vice versa[1]. $\dot{q}_{cond}$ of Fig. 2.5a and Eq. 2.21 is equivalent to *Surface outside face conduction heat loss rate* when it is a positive value and to *Surface outside face conduction heat gain rate* when it is a negative value.

Finally, the desired results shown in Fig. 2.5c are the *Solar heat gains* which, differently from *Surface outside face solar radiation heat gain rate*, represent the heat actually gained by the zone that is due to the solar radiation absorption in the outside surface. Then, there are the *Other heat gains* which are also heat entering the zone due to long wavelength radiation or convection and the *Heat losses* which are the heat lost from the zone to the outside.

These results are calculated based on the output variables mentioned as shown in Equations 2.22, 2.23, 2.24 and 2.25:

$$\Delta = \dot{q}_{cond,in} - \dot{q}_{\alpha,solar} \tag{2.22}$$

$$Solar\ heat\ gains = \begin{cases} \dot{q}_{\alpha,solar} & \text{if } \Delta \geqslant 0 \\ \dot{q}_{cond,in} & \text{if } \Delta < 0 \end{cases} \tag{2.23}$$

$$Other\ heat\ gains = \begin{cases} \Delta & \text{if } \Delta \geqslant 0 \\ 0 & \text{if } \Delta < 0 \end{cases} \tag{2.24}$$

[1]Note that in this analysis, the walls thickness is considered as part of the zone.

$$Heat\ losses = \dot{q}_{cond,out} \tag{2.25}$$

where $\dot{q}_{cond,in}$ is the hourly value of *Surface outside face conduction heat loss rate*, $\dot{q}_{\alpha,solar}$ is the hourly value of *Surface outside face solar radiation heat gain rate* and $\dot{q}_{cond,out}$ is the hourly value of *Surface outside face conduction heat gain rate*.

These results are calculated hourly and for each outside surface of the building. Then they are added distinguishing between type of surface (walls or roof) and those obtained total hourly results are converted into monthly energy. For the case of the heat transferred through the floor, even though the heat balance would differ from that shown in 2.5a, the output variables analysed and its post process is the same as for walls and roof. In this case, solar heat gains are always null and the only distinction made is between gains and losses.

2.4.3 Windows

The desired results for the windows heat gains include distinguishing between transmitted solar radiation through the glazing and other heat gains, which include convective heat transfer from the glazing, frame and divider into the zone. For the case of heat losses, the distinction is between the heat lost through the glazing and that lost through the frame and divider. Based on the supposition that transmitted solar radiation would be a significant portion of the total heat entering the zone, and given that the windows orientation plays a major role in the value of this variable, all windows results are given for each orientation.

The output variables processed for the windows heat transfer and the obtained results are presented in Figure 2.6. In Fig. 2.6a, there are the EnergyPlus output variables used in order to obtain the desired results for the heat entering or leaving the zone through the windows. *Surface window transmitted solar radiation rate* and *Surface window shortwave from zone back out window heat transfer rate* are the transmitted radiation through the glazing in both directions. Taking into consideration the hypotheses assumed for glazings (see Section 2.3.2) these transmitted radiations are only short wavelength, and are the solar radiation for the transmitted into the zone and both reflected solar and electric lighting for the transmitted out from the zone. Then, there are the

Surface window inside face glazing net infrared heat transfer rate and *Surface window inside face glazing zone convection heat gain rate*, which represent the net exchange of infrared radiation and convection heat transfer from the glazing to the zone. Finally, *Surface window inside face frame and divider zone heat gain rate* is the heat transfer from any frames and dividers to the zone.

The desired results are the *Solar transmitted heat gains*, *Other heat gains*, *Glazing heat losses* and *Frame and divider heat losses* and are shown in Fig. 2.6b. These results are calculated for each hour and each window based on the output variables as presented in Equations 2.26 to 2.28.

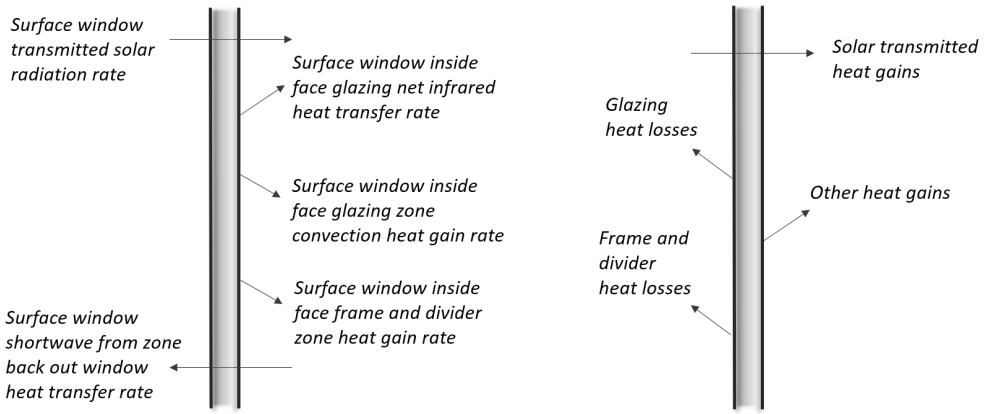

(a) EnergyPlus output variables. **(b)** Results.

Figure 2.6: Windows variables.

$$Solar\ transmitted\ heat\ gains = \dot{q}_{\tau,solar} \tag{2.26}$$

$$Other\ heat\ gains = \dot{q}^{+}_{conv,glazing} + \dot{q}^{+}_{net,IR} + \dot{q}^{+}_{f\&d} \tag{2.27}$$

$$Glazing\ heat\ losses = -\dot{q}^{-}_{conv,glazing} - \dot{q}^{-}_{net,IR} + \dot{q}_{\tau,out} \tag{2.28}$$

$$Frame\ and\ divider\ heat\ losses = -\dot{q}^{-}_{f\&d} \tag{2.29}$$

Where $\dot{q}_{\tau,solar}$ is the hourly value of *Surface window transmitted solar radiation rate*, $\dot{q}^{+}_{conv,glazing}$ ($\dot{q}^{-}_{conv,glazing}$), $\dot{q}^{+}_{net,IR}$ ($\dot{q}^{-}_{net,IR}$) and $\dot{q}^{+}_{f\&d}$ ($\dot{q}^{-}_{f\&d}$) are the hourly values of *Surface window inside face glazing net infrared heat transfer rate*, *Surface window inside face glazing zone convection heat gain rate* and *Surface window inside face frame and divider zone heat gain rate* when they

are positive (negative) and 0 when they are negative (positive). Finally, $\dot{q}_{\tau,out}$ is the hourly value of *Surface window shortwave from zone back out window heat transfer rate*.

These results are calculated hourly and for each outside window of the building. Then they are added distinguishing between the window orientation and those obtained total hourly results are converted into monthly energy.

2.4.4 Infiltrations and ventilation

In EnergyPlus 8.7 outputs there is no distinction between heat transfer due to infiltration or due to natural ventilation. Therefore, the obtained results only distinguish between gains and losses. Besides, in this work only sensible heat is studied on the grounds that the HVAC system is only controlled by temperature and that the model used for solving the surfaces heat balance provides sensible heat only solutions.

The output variables used to study the infiltrations and ventilation loads are *Zone infiltration sensible heat gain rate*, *Zone infiltration sensible heat loss rate*, *Zone mixing sensible heat gain rate*, *Zone mixing sensible heat loss rate*. Their values are the hourly gains and losses due to outside air infiltrations and ventilation in each zone and the hourly gains and losses due to adjacent zones air mixing.

By adding the gains and subtracting the losses for every zone and for every hour in each month, the monthly total energy entering and leaving the building due to infiltration and ventilation can be obtained.

2.4.5 Internal gains

Other sources of heat are the internal gains which only contribute to the heat entering the zone. The internal gains considered in this study are those due to the occupants metabolic rate, the electric equipment and the lighting. As done for infiltration and ventilation, only sensible heat is considered.

The output variables used to study the internal gains are *Zone people sensible heating rate*, *Zone electric equipment total heating rate* and *Zone lights total heating rate*. Their values are directly the hourly gains due to these internal loads in each zone. As for infiltration and ventilation loads, the only required processing involved adding them for all zones and expressing the results as monthly energy.

2.4.6 Relative contributions

In order to identify major drivers of thermal energy demand in each building, all the previously obtained results were post processed so as to determine the relative contribution of each component to the total. By doing so, it is possible to develop more effective retrofit measures in the search of reducing energy requirements. This relative contributions analysis was performed for the cooling and heating periods considered and it consisted of determining the net heat gains or losses through each component.

The different components considered to contribute to the total thermal requirements were separated into walls, floor, roof, windows, infiltrations and ventilation, people, equipment and lighting. Therefore, for the cooling period the walls net contribution would be the heat gained by the building through them minus the heat lost through them; and the same for the other components. For the heating period the calculation would be the opposite. In Equations 2.30, 2.31 and 2.32 the calculations for the walls cooling and heating net loads are presented as an example. For the rest of the components the procedure would be analogous.

$$\text{Walls net} = \text{Walls solar gains} + \text{Walls other gains} - \text{Walls losses} \tag{2.30}$$

$$Walls\ net\ cooling\ load = \begin{cases} Walls\ net & \text{if } Walls\ net \geqslant 0 \\ 0 & \text{if } Walls\ net < 0 \end{cases} \tag{2.31}$$

$$Walls\ net\ heating\ load = \begin{cases} -Walls\ net & \text{if } Walls\ net \leqslant 0 \\ 0 & \text{if } Walls\ net > 0 \end{cases} \tag{2.32}$$

Then, the total net cooling load is determined by adding the net cooling load of every component during the cooling period and the same for the total net heating load during the heating period. Finally, by knowing the components net loads and the total net loads, the relative contribution of each component can be determined.

2.5 Final remarks

In this chapter, EnergyPlus software was presented as the tool selected for running the buildings simulations in this thesis. Also, an overall understanding of the program structure was provided as well as the main models used in this study and the reasons behind their selection. All of the models used were already implemented in EnergyPlus and so no ad hoc developments were required.

Concerning surfaces heat balances, EnergyPlus default models were used for convection coefficients calculations: `TARP` for inside and `DOE-2` for outside coefficients. For the case of walls and roofs the `ConductionTransferFunction` was used as the algorithm for solving the conduction heat fluxes. To determine conduction through the ground, the model selected was `GroundDomain:Slab` combined with `Site:GroundTemperature:Undisturbed:KusudaAchenbach` model for the undisturbed ground temperatures, as they proved to be the most accurate from those available. For windows heat transfer, the layer-by-layer approach was followed whereas infiltration and ventilation loads were solved by means of the `AirflowNetwork` model. Finally, the HVAC system was modelled with `HVACTemplate:Zone:IdelLoadsAirSystem`.

Finally, the results identified as relevant in the search of characterizing buildings thermal performances were presented. For each of the required results, there is a description of the EnergyPlus output variables required to calculate them. There is also an explanation of how the variables were operated for obtaining the desired results. These results are the ones which will be analysed in the next two chapters.

Chapter 3

Analysis of variability impact in an example case

3.1 Introduction

In Chapter 2, EnergyPlus was presented as the software selected for the buildings thermal performance analyses, and so were the results that will be processed after each household simulation. For this thesis, the intention is that those results of all the individual building simulations to be executed, can be combined to represent the whole residential sector as accurately as possible. In order to achieve this goal, a housing stock characterisation process (described in Chapter 4) was performed, where typical Uruguayan buildings were identified. These typical buildings, or archetypes, are those which will be modelled and simulated in EnergyPlus.

Hence, archetypes are used in this thesis to represent different households which share some characteristics such as size, materials, openings quality and number of occupants. However, despite their common characteristics, these buildings are all different, and these differences may have an impact on their thermal performance. Examples of these variations are the front facade orientation, the presence of objects shadowing facades and windows, the amount of attached walls, etc.

In this regard, Morrisey et al. [27] considered building orientation and obstruction by surrounding buildings to be among the key parameters for appropriate passive building design; which will then lead to less thermal requirements. Concerning the orientation, Anderson et al. [28] carried out a study

for 25 climates in the United States (US) in which thermal loads were calculated for a prototype residential building at different orientations. They found that the orientation of the largest glazed area in the colder regions had a great impact on the results as, compared to a house oriented at south, the house oriented at east/west required 12-20% more energy and the one oriented at north required 6-17% more energy. Differently, for the warmer zones, the house oriented at east/west required 30-71% more energy and the one oriented at north required 5-12% less energy than the house oriented at south. Vasov et al. [29] also studied the impact of orientation on energy consumption but in an office building case of study in Serbia. By means of EnergyPlus simulations, the authors concluded on the importance of considering the orientation in the early stages of a building design process due to its high impact on energy consumption. They found that even small changes in building orientation ($\pm 15°$) resulted in variations of up to 13.73% in heating energy demand and of 13.26% in cooling energy demand. Spanos et al. [30] found that good building orientation and glazing location can reduce energy requirements of a typical residential building in the United Kingdom by 20%.

Regarding the surroundings, Liu et al. [31] analysed the impact of other buildings shading a household facades on its energy consumption. They simulated a rectangular enclosed space surrounded by four buildings (one in each side of the rectangle) and found that cooling energy consumption of buildings in the enclosed space was $7 - 15\%$ lower than that of the same buildings but located in an open space. Chagolla et al. [32], on the other hand, studied the effect of a tree shading on thermal energy demand of a house located in a warm zone in Mexico. The tree under study was a very tall one with dense foliage and so its shading covered almost three facades and a large proportion of the roof. The results obtained in this study show a reduction of 76.6% in the energy requirements due to the presence of this tree. Hwang et al. [33] also analysed the effect of trees on residential energy consumption in different US cities. They concluded that shade tree impact depends on the local weather, the type of tree and the position of the tree relative to the building. For cities with long cooling seasons, they found that a tree located west from the building could decrease annual demand by up to 160 kWh whereas in colder cities a tree located south from the building could increase annual demand by up to 134 kWh.

Given that in the previously mentioned studies building orientation and surroundings have proven to have an important impact on energy consumption, in this chapter the effect of considering variations in these characteristics is analysed for the case of Uruguayan climate and constructions. The objective is to determine the relevance of considering this variability within each archetype when aiming at using it to represent different buildings in terms of thermal performance. The methodology used to achieve this goal involved considering an example case of an archetype and defining different case scenarios where the variations are incorporated. Then, the obtained results for each case scenario were compared and the impact of each variation was analysed. The variations considered within each archetype are the front facade orientation, the presence of shadows due to trees, the presence of shadows due to other buildings and the amount of attached walls. Besides, when modelling apartments also the floor level is considered as a possible variation as it affects wind profiles and it determines whether roof and/or floor are attached or exposed.

3.2 Example case definition

The example case selected in order to perform the analysis corresponds to the archetype used to represent houses with an area between $40m^2$ and $70m^2$ which are more than 30 years old and with occupants socio economic status characterised by deciles 5 to 7. This case was selected due to the fact that among the archetypes defined, this one has one of the higher prevalences while at the same time it has the most typical constructions for the enclosure. These two characteristics might result in a more relevant analysis as some of its conclusions could be extrapolated to the majority of the Uruguayan residential buildings.

The weather file used for the simulations is Montevideo's EnergyPlus weather file (EPW) generated by Lawrie and Crawley [34] based on the Typical Meteorological Year (TMY) developed by Alonso-Suárez et al. [35]. The exception is that the EPW wind data was replaced with data measured by the Administración Nacional de Usinas y Transmisiones Eléctricas (UTE) [1] which can also be found in [35]. Besides, the wind speed was then affected by a shelter factor of 0.5 to consider the effect of surroundings (more informa-

[1] UTE is a vertically integrated, state-owned company in the national power sector.

tion regarding the weather files used in this thesis is presented in Chapter 4). Also, as part of this work, this EPW file was corrected on the grounds that a mismatch between the TMY and the EPW timestamps was detected (details regarding this issue can be found in Appendix C).

The enclosure, interior walls and doors constructions thermal properties are summarized in Table 3.1. Regarding windows, this archetype has casement windows consisting of a single layer of 4mm glazing and an iron frame. Their thermal properties are condensed in Table 3.2. Details about the construction materials can be found in Appendix A in Tables A.1 to A.9. Besides, solar protections are considered to be present in the living room and the bedrooms windows and they consist of PVC roller shutters which are assumed to be completely opaque.

Table 3.1: Opaque constructions thermal properties.

Construction	**U (W/m²K)**	$\alpha_{\mathbf{SWR,i}}$	$\alpha_{\mathbf{SWR,o}}$	$\alpha_{\mathbf{LWR,i}}$	$\alpha_{\mathbf{LWR,o}}$
Exterior wall	3.02	0.20	0.20	0.90	0.90
Interior wall	4.66	0.20	0.20	0.90	0.90
Roof	4.28	0.20	0.55	0.90	0.93
Floor	9.02	0.45	-	0.95	-
Bedrooms floor	5.47	0.90	-	0.60	-
Exterior door	3.42	0.90	0.90	0.60	0.60
Interior door	1.12	0.90	0.90	0.60	0.60

Table 3.2: Non-opaque constructions thermal properties.

Construction	**U (W/m²K)**	$\tau_{\mathbf{SWR}}$	$\tau_{\mathbf{LWR}}$	$\rho_{\mathbf{SWR}}$	$\varepsilon_{\mathbf{LWR}}$
Windows	312.5	0.88	0.00	0.08	0.84

Regarding air leakages in this archetype, they are assumed to be through all openings and also through cracks which are considered to be exclusively on the building roof. As mentioned in Chapter 2, in order to solve the infiltration and ventilation air flow rates and loads, the `AirflowNetwork` (AFN) model requires each component to be characterized by its C_Q and n of Eq. 2.13. Defining these parameters is non trivial as they depend not only on the components materials and design but also on their assembly, installation and maintenance status.

As part of the studies carried out in FSE_1_2017_1_144779 [4], some typical openings were defined in terms of their air leakage properties (relative to the openings perimeter) and they were assigned to the different archetypes according to their vintage and decile. Besides, in order to solve airmass flow through

door and windows when they are open (Eqs. 2.16), a discharge coefficient of 1 was set, for the results to be on the safe side, due to the lack of measured data from where to determine the actual ratio between real discharge and theoretical discharge.

The windows and doors infiltration properties of this archetype are presented in Table 3.3. For the case of roofs, also in FSE_1_2017_1_144779 [4], they were categorized into lightweight and heavyweight and their air leakage properties were defined according to these categories as well as the roof area and its exposed perimeter. This archetype roof is a heavyweight and in Table 3.4 there are the C''_Q and C'_Q corresponding to this category. The final C_Q is then calculated according to Equation 3.1:

$$C_Q = C''_Q A_{roof} + C'_Q P_{roof} \tag{3.1}$$

where A_{roof} is the area of the roof surface and P_{roof} is its exposed perimeter.

Table 3.3: Windows and doors air leakage properties relative to perimeter.

Construction	C'_Q (g/smPa^n)	n
Window	0.898	0.682
Door	1.896	0.590
Door	0.046	0.660

Table 3.4: Roof air leakage properties.

Construction	Type	C''_Q (g/sm^{2}Pa^n)	C'_Q (g/smPa^n)	n
Roof	Heavyweight	0.156	0.132	0.7

From the geometries defined to represent this archetype "Model 11" was selected on the grounds that it is a rather simple geometry which might help to avoid getting results too dependent on the example case peculiarities ("Model 11" data sheet can be found in Appendix B). This entails not only a simpler analysis but also allows for more general conclusions. In Figure 3.1 there is the geometry plan whereas its representation in EnergyPlus is shown in Figure 3.2. "Model 11" total glazed area is 6.91 m^2, of which 4.22 m^2 are on the front facade, 1.54 m^2 are on the back facade and 1.15 m^2 are on the facade which is 90° clockwise from the front one.

Besides, this archetype is characterized by three people living in the house who operate the openings, solar protections and HVAC systems in order to

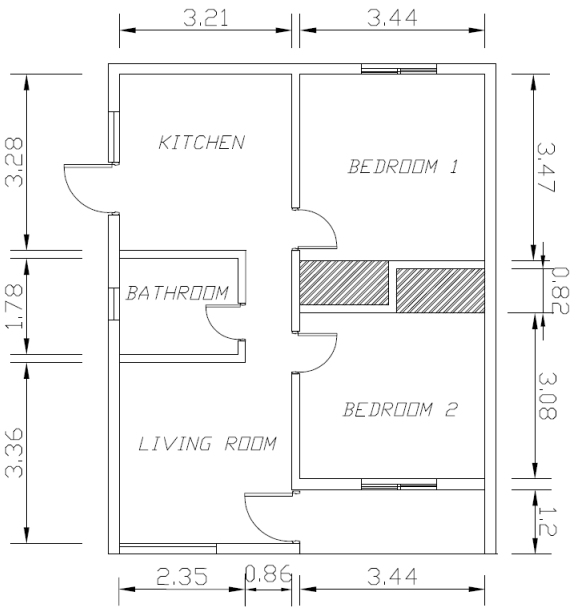

Figure 3.1: "Model 11" geometry.

achieve thermal comfort. In this thesis thermal comfort is defined according to ASHRAE 55 [36], where the comfort temperature for each day is determined as shown in Equation 3.2. EnergyPlus calculates this daily comfort temperature and determines whether the zone is within the comfort limits criteria, which are $T_{confort} \pm 3.5°C$ for the 80% acceptability limits defined in ASHRAE 55 and used in this work.

$$T_{ot} = 0.31 T_{pma,out} + 17.8 \tag{3.2}$$

T_{ot} in Eq. 3.2 refers to the zone operative temperature calculated as the average of the indoor air temperature and the mean radiant temperature of the zone interior surfaces. $T_{pma,out}$ on the other hand, refers to the prevailing mean outdoor air temperature and is calculated as an exponentially weighted, running mean of a sequence of daily outdoor temperatures prior to the day in question. Its calculation is shown in Equation 3.3.

$$\begin{aligned} T_{pma,out} &= (1-\alpha)(T_{e,d-1} + \alpha T_{e,d-2} + \alpha^2 T_{e,d-3} + ...) \\ &= (1-\alpha) T_{e,d-1} + \alpha T_{pma,out,d-1} \end{aligned} \tag{3.3}$$

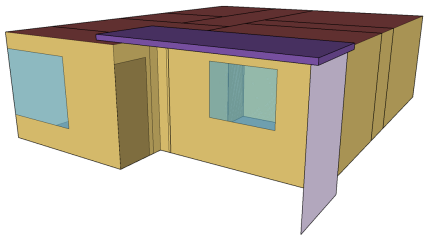

(a) Front facade.

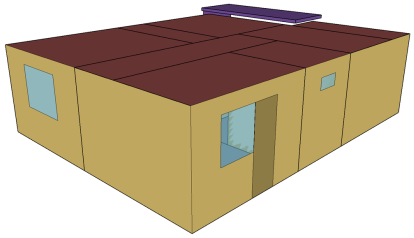

(b) Back facade.

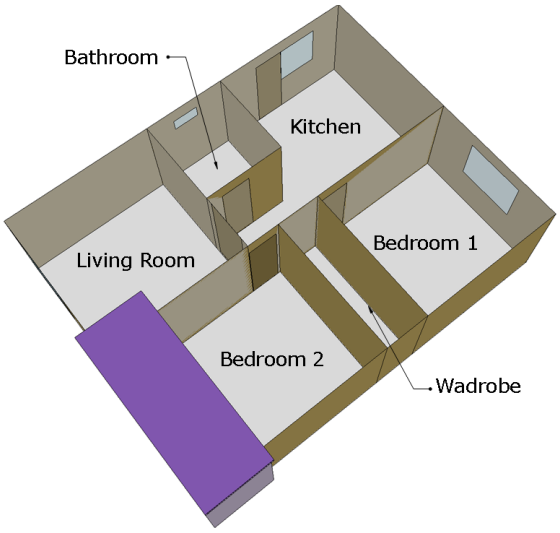

(c) Thermal zones.

Figure 3.2: "Model 11" representation in EnergyPlus.

In Eq. 3.3 α is a constant between 0 and 1 which controls the speed at which the running mean responds to changes in weather (EnergyPlus uses $\alpha = 29/30$). $T_{e,d-1}$ represents the mean daily outdoor temperature of the day before the day in question, $T_{e,d-2}$ is the mean daily outdoor temperature of the day before that and so on. $T_{pma,out,d-1}$, on the other hand, is the prevailing mean outdoor air temperature of the day before the day in question.

Thus, the occupants take advantage of natural ventilation by opening the windows when the zone operative temperature is higher than the comfort one but within the ASHRAE 55 80% acceptability limits (±3.5°C). When this condition is not met, they turn the HVAC on. Besides, whenever the HVAC is active on cooling mode, if incident solar radiation on a window is more than 300 W/m^2, solar protections are used.

HVAC, windows and solar protections operation is restricted to the occupied zones which are the living room from 14:00 to 22:00 hs and the bedrooms

from 22:00 to 08:00 hs. The kitchen and the bathroom are never occupied and their windows are always open during the time there are occupants in the house (from 14:00 to 08:00 hs) and closed otherwise.

As mentioned in Chapter 2, the model of the HVAC systems used, actually provide information regarding thermal requirements and these requirements are only accounted for in the occupied zones. Therefore, in the example case, the HVAC heating and cooling loads obtained are, in fact, the required energy for these efficient occupants to be in thermal comfort in the living room and the bedrooms during the occupied hours.

All these considerations regarding the occupants behaviour and thermal requirements are due to the lack of data from which the Uruguayan households occupants could be characterised in terms of their schedules and behaviours. The schedules and occupied zones definitions were taken from NBR 15575 [37]. Then, the decision of only accounting for thermal requirements in the occupied zones relies on the idea that thermal comfort considerations only make sense in the presence of people. Moreover, as mentioned in Chapter 2, if the occupants were to use an HVAC system to meet these requirements, they would only do so in the occupied zones. Finally, the occupants behaviour defined regarding windows and solar protections operation is an ideal one and the results would therefore show the house thermal performance under efficient operation of its openings and solar protections.

3.3 Case scenarios

Given the fact that in this thesis this archetype will be used to represent several buildings, it is important to analyse how certain differences among those buildings impact the thermal performance of the archetype. As already mentioned, in this study those differences have been narrowed down to: front facade orientation, presence of trees shadowing the building, presence of another building shadowing one of the facades and amount of attached walls.

As the studied archetype is located in Montevideo, where the streets direction -and therefore the city blocks orientation- are highly dependant on the neighbourhood, the front facade orientation can take any value from 0° to 360°; where a value of 0° indicates that the front facade is facing north and increases clockwise (see Figure 3.3 with orientation examples). Taking this into consideration, case scenarios were defined by setting the parameters concerning the

surroundings (shadows and attached walls) and then they were simulated for orientations varying every 5° from 0° to 360°. Therefore, 72 simulations were carried out for each case scenario defined.

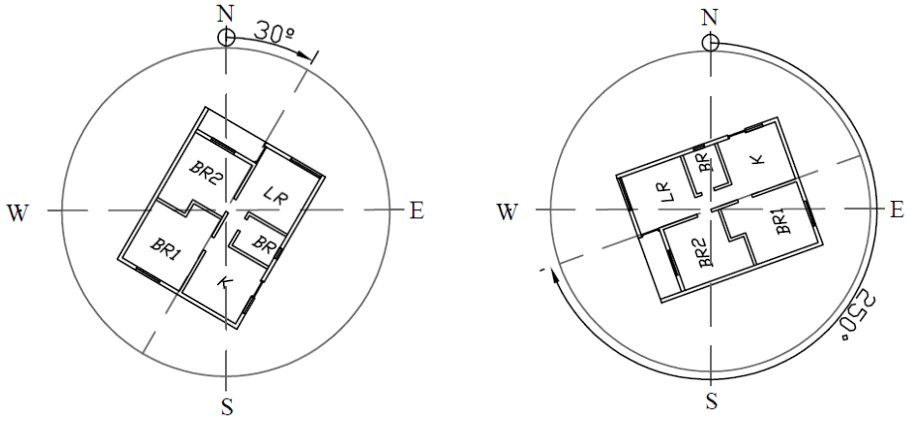

(a) 30°. **(b)** 250°.

Figure 3.3: Orientation examples.

Regarding the presence of shadows due to trees, given the archetype characteristics, only two variations were considered: either there are no trees shadowing the building enclosure or there is one tree in front of the front facade as shown in Figure 3.4a. Similarly, for the case of shadows due to other buildings the possibilities are: no shadows due to buildings or one building shadowing the side facade located 90° clockwise from the front one, as shown in Figure 3.4b.

Given the archetype geometry and the openings location, there is only one facade that can be attached to another building. Consequently, also two configurations were considered in this regard: either the archetype is detached or it is attached on a single facade (the one located 270° clockwise from the front one), as shown in Figure 3.4c. In this thesis attached walls were modelled as adiabatic, which is a reasonable supposition when the attached building inside temperatures are similar to those in the studied building.

Table 3.5 shows the case scenarios defined, where these variations were incorporated. EnergyPlus was used for performing the simulations and the models selected within the software for solving the heat balance equations as well as the results to process for each case are those detailed in Chapter 2. Having defined 5 case scenarios to be run for each of the 72 possible orientations, result in a total of 360 models to generate and simulate. Thus, Eppy

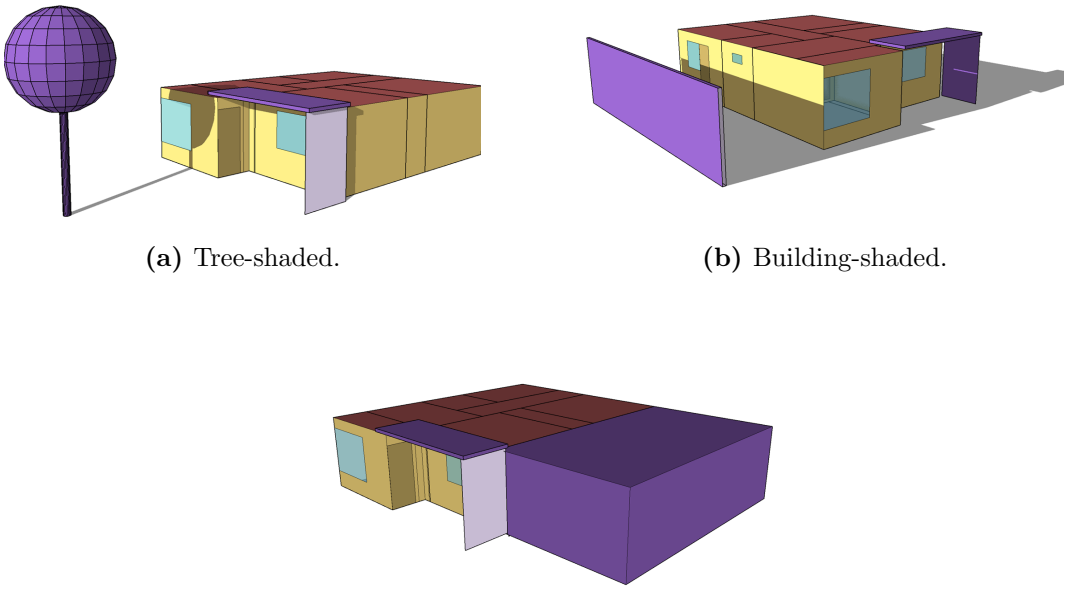

(a) Tree-shaded.

(b) Building-shaded.

(c) Attached.

Figure 3.4: Possible variations regarding shading and exposed facades.

scripting language, based on Python, was used so as to automatically generate the IDFs, simulate them and process the results. This whole process took 11 h 40 min on a personal computer with Intel Core i7 processor and 16,0 GB RAM.

Table 3.5: Case scenarios defined.

Case scenario	Tree	Building	Attached
I	No	No	No
T	Yes	No	No
B	No	Yes	No
A	No	No	Yes
TBA	Yes	Yes	Yes

3.4 Results and discussion

The resulting annual total HVAC loads for each case scenario as a function of the building orientation are shown in Figure 3.5. By observing this figure, and remembering that HVAC loads in this work actually refer to energy re-

quirements for thermal comfort, it becomes evident that the dependence of the house thermal requirements on the case scenario and the front facade orientation is relevant. These requirements vary from 1458kWh for an attached house oriented at 355° to 1967kWh for an isolated detached house oriented at 310°. This means that an error of 35% could be committed if the simple detached geometry were to be used to determine thermal performance of an attached building, even though they are both characterised by the same archetype.

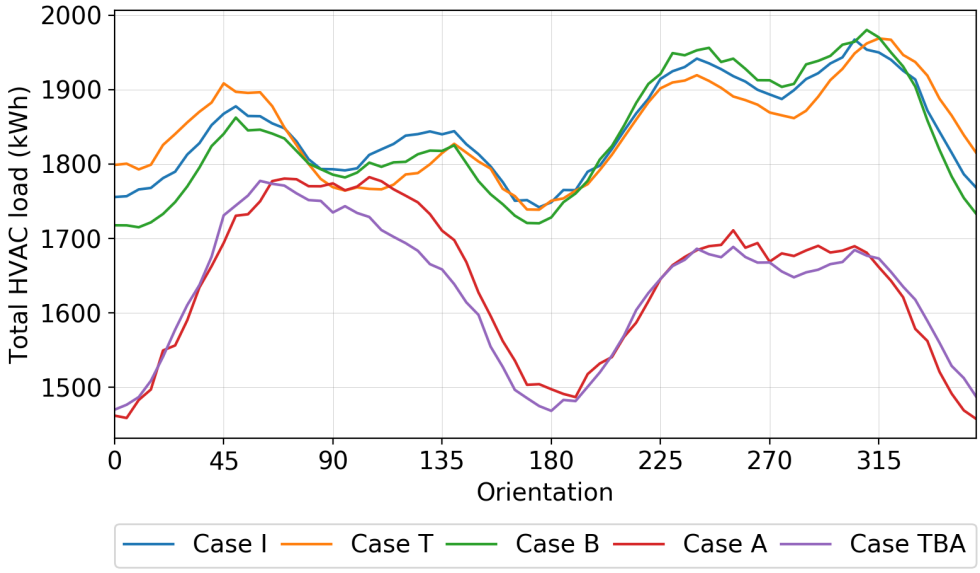

Figure 3.5: Annual total thermal load.

Moreover, different cases and orientations could result in different contributions of each component to the total cooling and heating requirements. Taking into consideration these differences in components relative contributions might be important when aiming at improving the building thermal performance, as the most effective retrofit measures could not be the same for different case scenarios and orientations.

For example, in Figures 3.6a and 3.6b, the relative contributions for cooling requirements of Case I oriented at 130° and Case A oriented at 355° are shown. In both charts it can be observed that the roof and the windows have the bigger shares but in Fig. 3.6a their contributions are very similar whereas in Fig. 3.6b the roof is responsible of 54.4% of the cooling load and the windows of 28.6%. The "Other" category is conformed by those components with relative contributions of less than 3%, which in these cases are the floor and equipment and lighting loads. In these examples the walls net contribution to cooling loads

is negative (meaning the net heat transferred through the walls is from the zone to the outside) and this is why the walls have no contribution to cooling loads, and the same happens with the infiltration and ventilation loads.

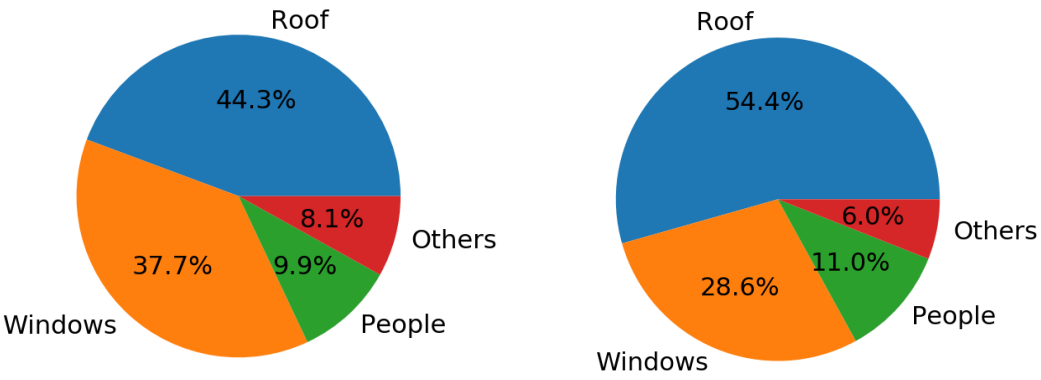

(a) Case I at 130°. **(b)** Case A at 355°.

Figure 3.6: Cooling loads relative contributions. Case I: isolated house with no objects shadowing it. Case A: attached house with no objects shadowing it.

The same analysis on contributions differences can be performed for heating requirements. In Figures 3.7a and 3.7b there are the relative contributions for heating requirements of Case B oriented at 0° and Case TBA oriented at 250°, respectively. While in the former all three roof, walls and infiltrations have similar relevance, in the later the walls only contribute with 11.6% of the total heating load. In these cases the windows, floor and internal loads actually reduce heating loads as their net contribution is positive, meaning that the zone gains heat through them. This is the reason why they have no contribution to heating loads and do not appear in the charts.

The impact of the surroundings on thermal requirements is explained by differences in the building's area exposed to the sun and to the outside environment. The defined case scenarios will hence have differences in solar gains as well as in losses through the enclosure. By observing Fig. 3.5, the effect of the surroundings is quite clear. From the different case scenarios defined, it can be noted that the characteristic which has the biggest influence on the thermal requirements is the number of attached facades. At almost every orientation the attached cases perform better than the detached ones. The only exception is at orientations near east (90°) where all the case scenarios have very similar thermal requirements.

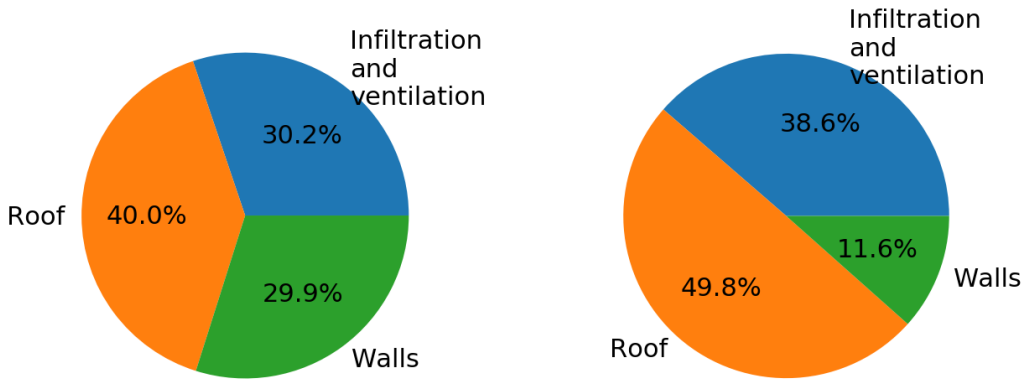

(a) Case B at 0°. **(b)** Case TBA at 250°.

Figure 3.7: Heating loads relative contributions. Case B: detached house with a building shadowing one of its facades. Case TBA: attached house with tree and building shadows.

Regarding orientation, its impact on buildings thermal performances is mainly explained by the position of the sun relative to the buildings facades and windows and, to a lesser extent, by differences in infiltration and ventilation loads. Consequently, the influence of orientation on the example case thermal requirements will be studied through the variations of solar gains and infiltration and ventilation loads.

With the intention of providing a better understanding on how the surroundings and the orientation impact on the example case thermal performance, a more profound analysis on the effect of both characteristics is performed in the following sections. The study is focused on their influence on solar gains and infiltration and ventilation losses. The enclosure losses were not specifically analysed as they vary with the orientation quite similarly as solar gains (the higher the solar gains, the higher the enclosure outside surfaces temperatures and, consequently, the higher the losses through them). Also, their variation with the case scenario is rather obvious as the attached cases have one adiabatic facade whereas the detached ones have all the facades exposed to the outside environment.

Given that what is desirable during heating season is the opposite in cooling season, and that both the solar gains and the infiltration and ventilation loads would be rather different during those periods, the analysis will be performed separately for heating and cooling loads. The periods considered are from May

to September for heating and from November to March for cooling; which is when the great majority of the corresponding thermal energy is demanded.

3.4.1 Impact of orientation and surroundings on solar gains

Concerning the sun position, and given that in the southern hemisphere the sun path is mainly in the northern sky, the north facing facades and windows capture more direct solar radiation during winter, when the sun is lower in the sky. The opposite is true for the south facing facades. For east and west facing facades, they capture more solar radiation during summer when solar altitudes are higher. These statements can be verified in Figure 3.8, where there is the incident beam solar radiation rate per area on a wall according to its orientation. These values are EnergyPlus results for the Montevideo EPW used in this analysis. Their obtention involved simulating a cube with side length 1m and requesting the monthly average beam solar radiation as the simulation output variable.

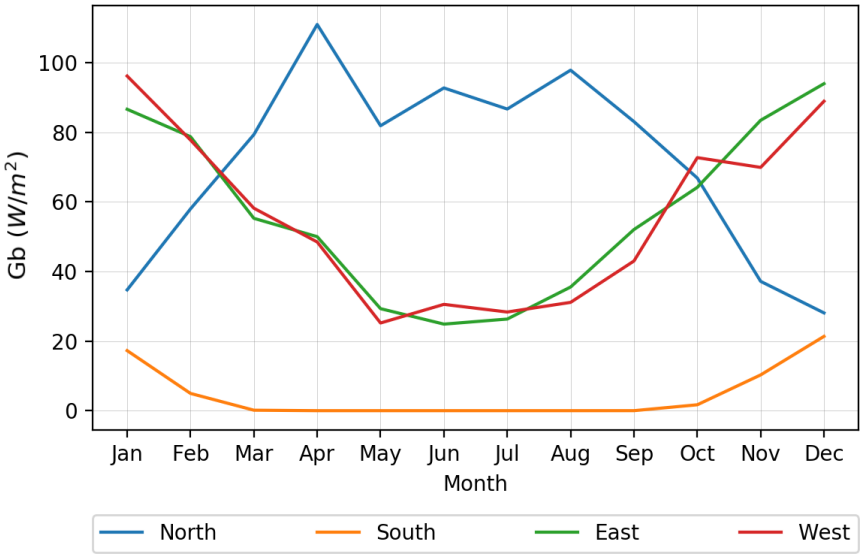

Figure 3.8: Incident beam solar radiation on a vertical plane in Montevideo.

So, from Fig. 3.8, it can be concluded that north is the preferable direction for walls and windows as they receive more solar radiation in winter -when it is desirable- than in summer -when it is not-. Besides, the position of the sun during summer allows for a simple shading of north facades with horizontal

devices, such as the roof overhang of the example case. East and west are the worst performing facades in terms of cooling requirements as they are the ones which receive the highest solar radiation during summertime, whereas south facing facades are the worst during heating period as they receive none of beam solar radiation.

In this regard, the example case front facade orientation has opposing effects on solar energy captured by the building. This is due to the fact that the biggest glazed area is on the front facade but the house lengthwise axis runs perpendicular to it, meaning that there is more thermal mass to absorb solar radiation in the facades perpendicular to the front one. Besides, for the different case scenarios there are the shading objects and the attached neighbours that affect solar gains differently depending on the orientation. It is therefore not simple to predict the relationship between solar gains and orientation for each case scenario, as there are several aspects that should be taken into consideration.

Heating period

The annual heating loads for each case scenario as a function of the front facade orientation are presented in Figure 3.9; once again, these loads are in fact heating energy requirements for the occupants to be in comfort. When comparing the detached cases (Case I, T and B) to the attached ones (Case A and TBA), not only do the values differ but also the graphs general patterns. The detached cases heating load is in its lowest level at 0° and increases with the front facade orientation until it reaches its peak at 225°. On the other hand, the attached cases heating load increases with the orientation until 105° in Case A and 115° in Case TBA, where it starts falling towards its minimum value at 325° in Case A and 280° in Case TBA.

Something similar happens with the house solar energy gains during heating period shown in Figure 3.10. It can be observed that their relationship with orientation is different for the attached and the detached cases. Whereas they have a strong dependence on orientation for the attached scenarios where variations are of up to 23%, that is not the case for the detached ones, where solar gains variations with orientation are less than 6%.

Based on the large differences observed in Figs. 3.9 and 3.10, and aiming at understanding solar gains variations, the attached and the detached cases will

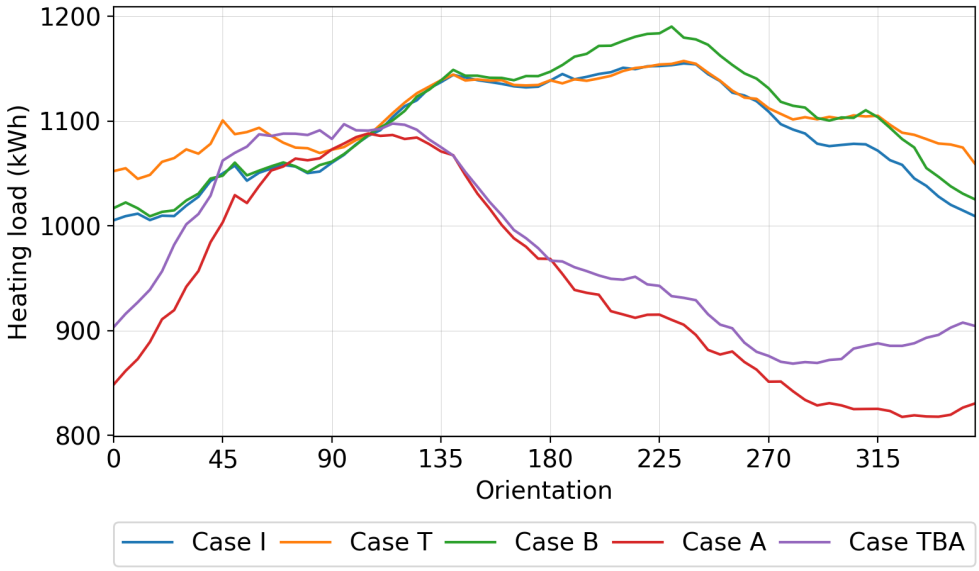

Figure 3.9: Annual heating load.

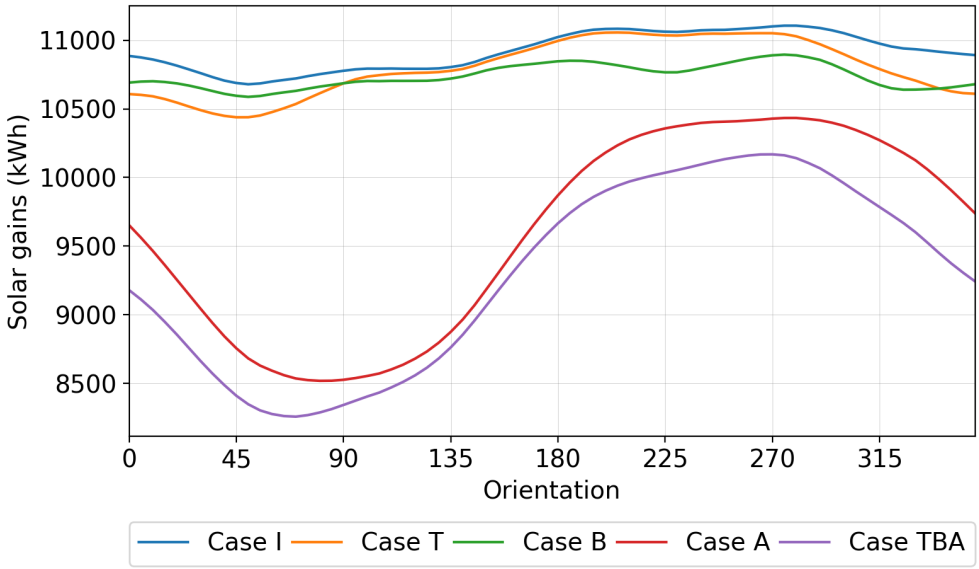

Figure 3.10: Solar heat gains during heating period.

be studied separately. For simplicity, Case I (the isolated geometry) will be the scenario used to analyse the former, while Case A (the attached geometry with no shading) will be the one used for the latter.

Case I solar heat gains through each component and the resulting total during heating period are in Figure 3.11. By contrasting Figs. 3.11a and 3.11b it can be observed the opposite effect of orientation on solar gains through win-

dows and through walls. While windows transmitted solar radiation reaches its peak at orientations near north and is at its lowest at orientations near south-east, the opposite happens with the heat gains due to the absorbed solar radiation in the walls.

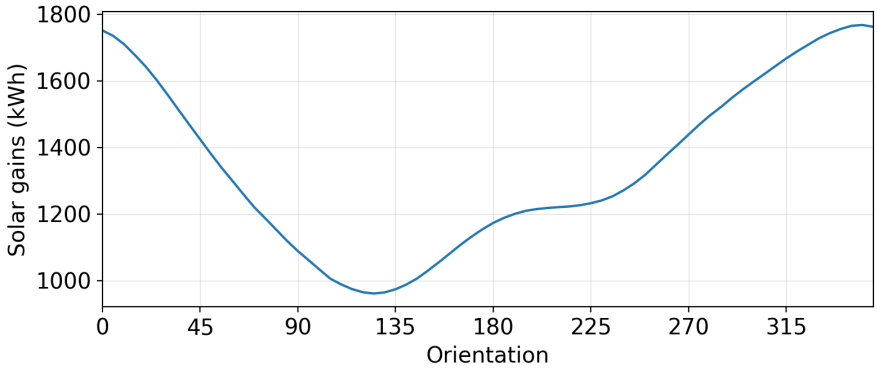

(a) Windows.

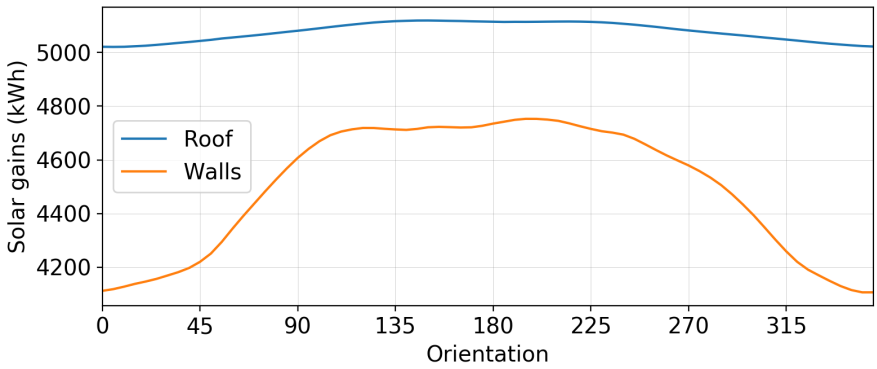

(b) Roof and walls.

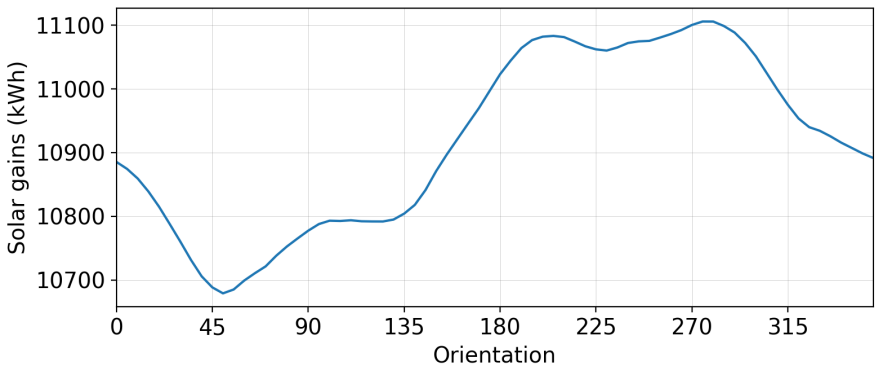

(c) Total.

Figure 3.11: Case I solar heat gains during heating period.

The Fig. 3.11a graph pattern is explained by the fact that the house largest glazed area is on the front facade while the facade located counter-clockwise from the front one has no windows. Accordingly, when the house is facing north the largest glazed area is facing north whereas when the house is facing east there is zero glazed area facing north. Moreover, at 125°, not only would there be almost none glazed area facing north but also the largest glazed area would be rotated towards south, minimizing windows solar gains.

To illustrate these differences, the transmitted solar radiation through the windows during solar midday of the 21st of June can be observed in Figure 3.12. At that time, for the house oriented at 0° (Fig. 3.12a), the sun is facing directly the largest windows which are in the living room and one of the bedrooms. Differently, for the house oriented at 125° (Fig. 3.12b), the midday sun only reaches the other bedroom window and with an incidence angle of 55°.

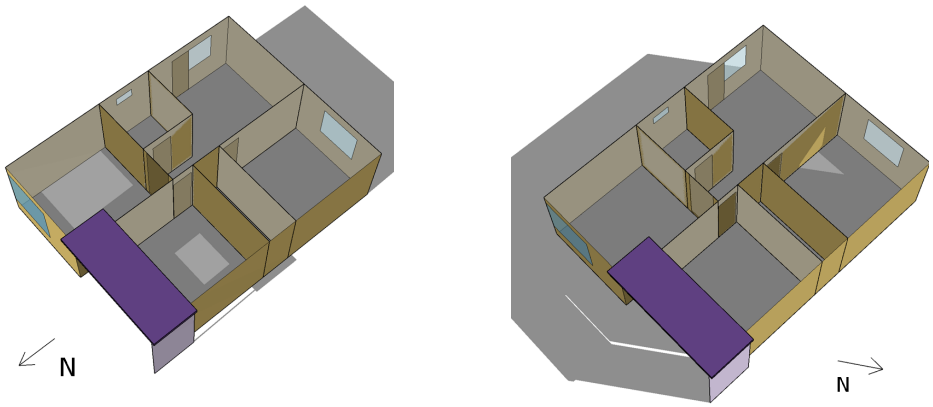

(a) Oriented at 0°. **(b)** Oriented at 125°.

Figure 3.12: Case I window transmitted solar radiation for orientations at 0° and 125° on 21st of June at solar midday.

On the other hand, walls solar gains are the highest -and very similar- from orientations of 95° to 265° and the lowest at 0° as shown in Fig. 3.11b. This puts in evidence that the roof overhang is what has the greatest impact on the walls solar gains rather than the lengthwise axis orientation. When the front facade is facing north (orientation=0°), the roof overhang shades it, and when it is facing south (orientation=180°) the overhang has no effect as there is no incident beam solar radiation on the front facade. There is also the fact that the house plant is not exactly a rectangle as the living front wall is not aligned to that in the bedroom next to it (see Fig. 3.1). This results in even more shading on the front bedroom wall when the building is oriented at 0°.

Moreover, holding the largest glazed area, entails that the front facade is the least massive of the house. This also contributes to the walls absorbed solar radiation being at its lowest when the building is facing north.

The effects of the roof overhang and the house plant shape for the house oriented at 0° can be observed in Figure 3.13. The images also are for the 21st of June but for 10:00 hs (Fig. 3.13a) and for 15:00 hs (Fig. 3.13b). It can be noted that the front facade is partially shaded all throughout the day. During morning hours it is due to both the roof overhang as well as the living room side wall whereas during afternoon it is only due to the roof overhang and its support.

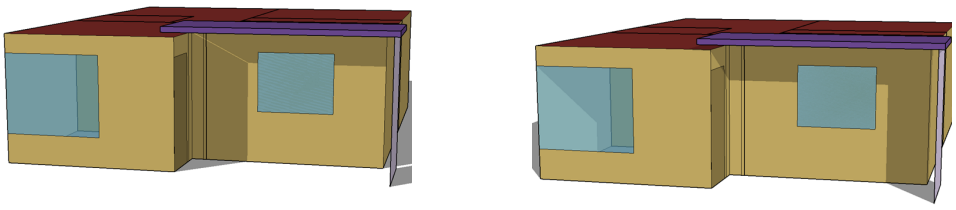

(a) 10:00 hs. **(b)** 15:00 hs.

Figure 3.13: Case I at 0° front facade shading.

The roof solar gains shown in Figure 3.11b are the highest at any orientation and, as it is a horizontal surface, its incident solar radiation does not depend on the building's orientation. The subtle variations observed must be due to the depth of the roof overhang shading part of the roof surface, as the upper plane of the overhang is slightly higher than the upper plane of the roof. This shading occurs when the overhang is located north of the roof, explaining the graph pattern.

Finally, in Figure 3.11c the Case I total solar heat gains are presented, which reach their peak at 280° and are at their lowest at 50°. As a consequence of the opposite variations of solar gains through windows and walls, and the almost zero variation in the higher gains, the dependence of the total solar heat gains on the orientation is quite more subtle than that of the windows or the walls. Whereas in windows and in walls the variations are of up to 84% and 16%, respectively; the maximum total variation is of 4.5%. This explains the pattern observed in Fig. 3.10 for the detached cases.

However, the relationship between total solar heat gains and orientation of Fig. 3.11c does not seem to correlate with the heating requirements presented

in Fig. 3.9 for Case I. For example, at 225° solar gains are higher than at 0° but so are the heating requirements. This is due to the fact that heating requirements in this study were only considered in occupied areas. Given that the example case archetype is only occupied in the living room and the bedrooms, the most favourable orientations would be those which capitalize on more solar gains in those zones.

In this regard, Case I solar gains in the living room and the bedrooms during heating season are shown in Figure 3.14a. In this case, when comparing them to the heating requirements of Fig. 3.9, the relationship between solar gains and heating requirements is clearly noted. The differences between the orientations with better and worst performances in each graph are due to the fact that the occupation schedules (which are used to determine thermal requirements) were not considered in Fig. 3.14a, where there are the total solar gains in the living room and the bedrooms. Knowing that during day time the occupied zone is mostly the living room, it can be accepted that the orientation with the lowest heating requirements would be somewhere in between those which maximize solar gains in the occupied zones as a whole and in the living room alone (see Fig. 3.14b)[1].

The other unattached cases heating load requirements vary with orientation similarly to Case I. Case T has higher requirements than Case I at orientations from 270° to 90° which is when the tree is shading the living room window and wall. The main difference is at 355° which is when the tree is almost north to the living room facade and the Case T heating load exceeds the Case I by 6%. On the other hand, Case B has higher requirements at orientations where the shading has more impact on the living room side wall and bathroom and kitchen windows solar gains. Those orientations are from 160° up to 20°, and the difference between Case I and Case B is maximum at 225° when Case B heating load is 3% higher than that of Case I.

For the attached cases, as there is less exposed area, the solar heat gains would be lower but so would be the heat losses through the walls. Given that in heating season heat losses are higher than gains, it can be admitted in a rather straight forward way that the attached cases would require less heating loads than the detached ones. By observing Fig. 3.9, it can be concluded that

[1]Note the different scales in Figs. 3.14a and 3.14b y-axes as the first adds up solar gains in the living room and the two bedrooms while in the second one there are only the living room solar gains.

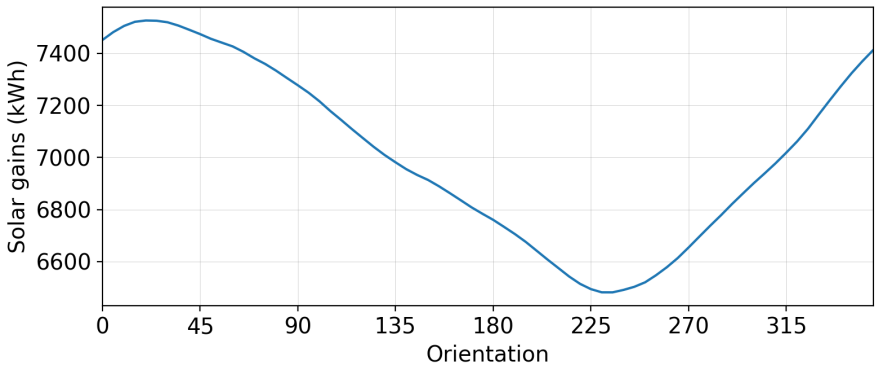

(a) Living room and bedrooms.

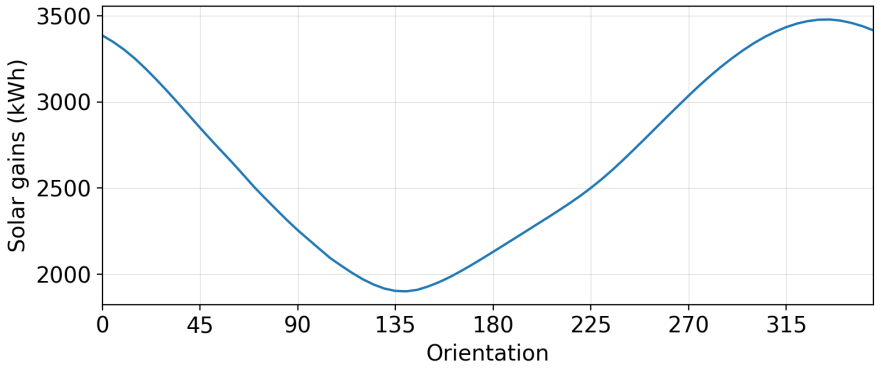

(b) Living room.

Figure 3.14: Case I solar heat gains in occupied zones during heating period.

this affirmation is true for every orientation except at orientations near 90°, where the attached facade is facing north and the non-capitalized solar heat gains surpass the lower losses.

So, intuitively, the attached cases would perform better at orientations where the attached facade is facing somewhere near south (house oriented at around 270°), where the incident solar radiation wasted is less relevant, and worst at orientations where it is facing approximately north (house oriented at around 90°), where it is more relevant. Yet, as done for the detached cases, in order to relate solar gains variability with that in heating requirements; only gains in the occupied zones should be considered.

In this regard, Case A solar gains in the living room and the bedrooms during heating season are shown in Figure 3.15a whereas gains exclusively on the living room are shown in Fig. 3.15b. By comparing these graphs with those in Fig. 3.14 it can be noted that while the solar gains in the occupied zones as

a whole are quite lower in the attached case, in the living room they are the same. This is reasonable as the attached facade only affects bedrooms walls.

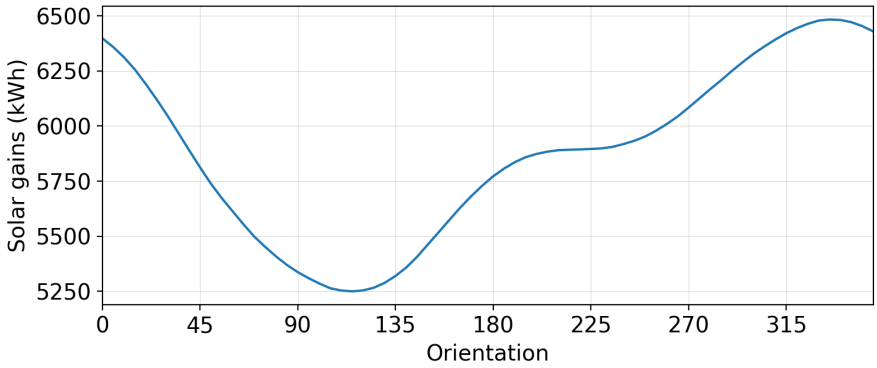

(a) Living room and bedrooms.

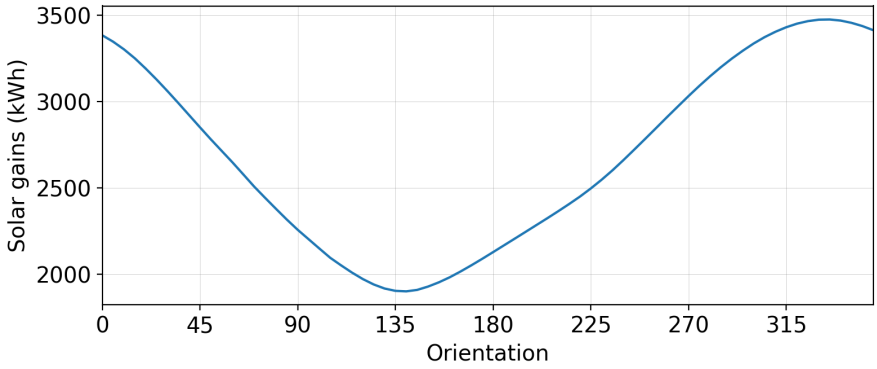

(b) Living room.

Figure 3.15: Case A solar heat gains in occupied zones during heating period.

Once again, the variations in the occupied zones solar gains explain the pattern of the heating requirements. The highest solar gains in the occupied zones are for the attached house oriented at 325° which corresponds to the orientation with the lowest heating requirements. The lowest solar gains on the other hand are at orientations around 110° which have the highest thermal requirements (see Fig. 3.9). It can therefore be concluded that, for both the attached and the detached cases, the occupied zones position relative to the sun path ends up being the key factor for the relationship between the heating requirements and the orientation.

Cooling period

Up to now, all the discussion regarding solar gains variations was for the heating loads, so, in order to complete the analysis, the cooling period should be studied. Thermal requirements for the cooling period considered are shown in Figure 3.16 as a function of the house orientation and the case scenario. Contrarily to what happened with heating loads, in this case the different scenarios seem to vary similarly with changes in the orientation. This is because during cooling period solar altitudes are higher, and so the walls and windows contribution to the total solar gains loses relevance compared to that in the roof.

For all case scenarios, the orientation which minimizes cooling loads is at around 175° whereas the one which maximizes them is at around 305°. Yet, as with the heating loads, the attached cases perform better than the detached ones, except at orientations from 230° to 290° approximately. Which is when the attached facade is facing somewhere around south.

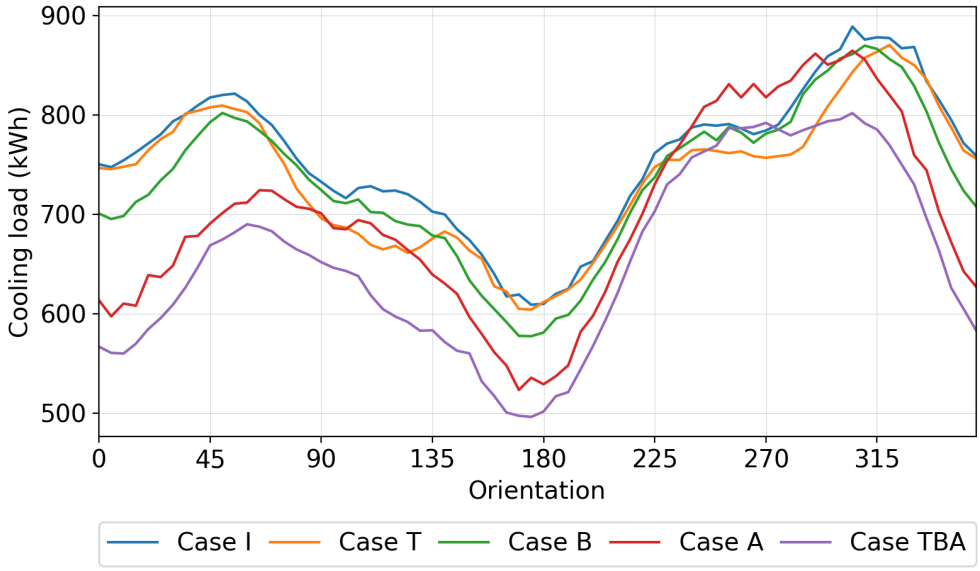

Figure 3.16: Annual cooling load.

The household total solar gains during cooling season are in Figure 3.17. Comparing this graph with that in Fig. 3.10 it can be noted that solar gains are much higher during cooling season, which is reasonable as so it is the incident solar radiation. Also, it can be observed the differences in the graphs patterns, specially for the attached cases. As mentioned, these are due to the differences

in the sun paths during both seasons; as in summer solar altitudes are higher, the northern facade being attached has less impact than during winter.

Similarly to heating season, the attached cases solar gains seem to depend much more strongly on orientation than those in the detached ones (see Fig. 3.17). Once again, these solar gains graphs do not explain the cooling loads and orientation relationship as there is no correlation between them and the graphs patterns of Fig. 3.16, specially for the detached cases.

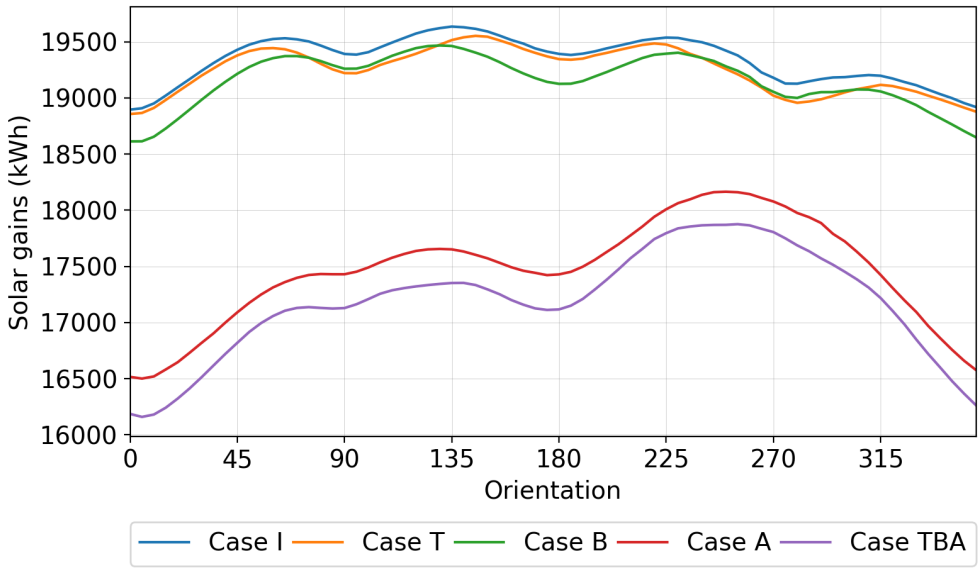

Figure 3.17: Solar heat gains during cooling period.

So, as done for heating loads, Case I solar heat gains variation with orientation is shown in Figure 3.18a exclusively for the occupied zones. Now the relationship between solar gains and cooling loads is starting to be noted. Yet, there are still differences for orientations around west, where cooling loads are as high as for east orientations but solar gains are not. As before, this difference is because in Fig. 3.18a there are the total solar gains in the living room and the bedrooms without considering whether they are occupied or not. The cooling loads on the other hand, are the thermal requirements which are only accounted for during the occupied hours in each zone.

Thus, once again, solar gains in the living room have a greater impact on the cooling loads than those in the bedrooms on the grounds that the living room is the occupied zone during the hours of high irradiance. Case I living room solar gains are in Figure 3.18b where it can be observed that they are

higher at orientations around west, and that is the reason why cooling loads at these orientations are also high.

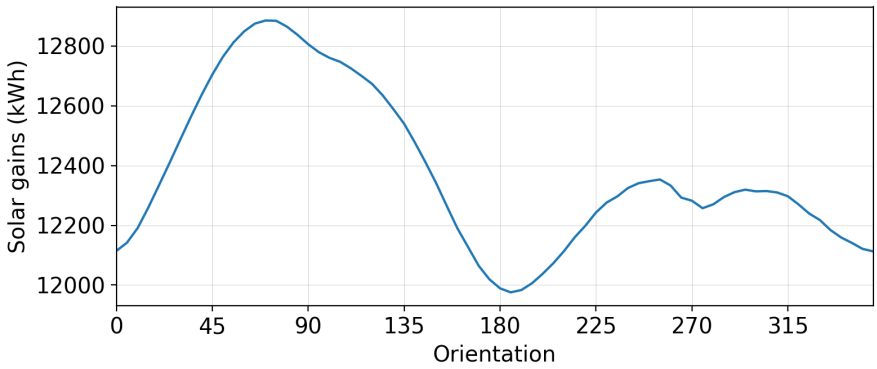

(a) Living room and bedrooms.

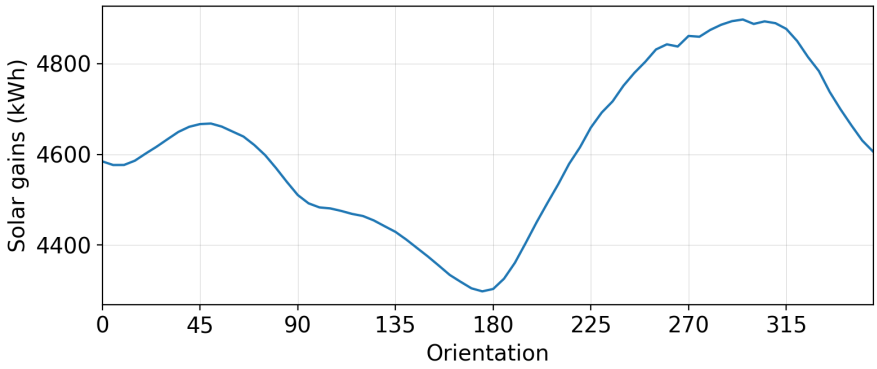

(b) Living room.

Figure 3.18: Case I solar heat gains in occupied zones during cooling period.

Proceeding accordingly for the attached scenarios, Case A solar gains were obtained exclusively for the occupied zones and are shown in Figure 3.19. These graphs also have the same pattern as cooling loads, orientations with higher solar gains correspond to higher cooling loads and vice versa.

So both for heating and cooling periods, the variations in solar gains with the orientation and the surroundings can be explained by the position of the exposed walls, windows and shading objects relative to the sun. However, when aiming at relating the variations in solar gains with those in thermal requirements, the occupancy schedules have to be considered.

All in all, in order to understand the impact of orientation on buildings thermal performance, not only should solar gains be considered but also the building zones usage patterns. Actually, these usage patterns end up being the key aspect when trying to relate solar gains with heating and cooling require-

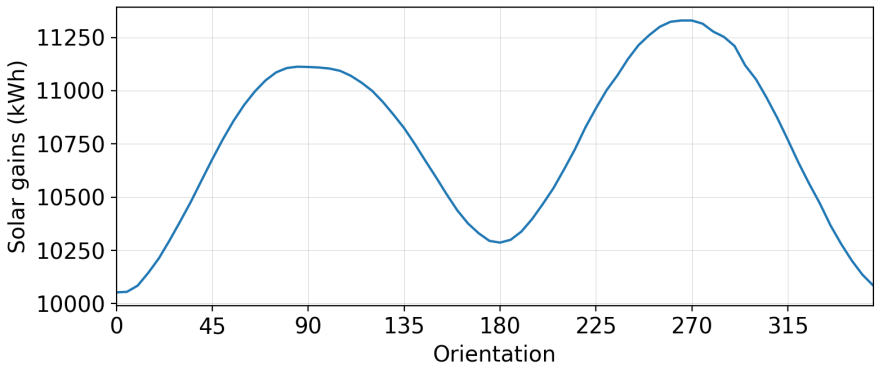

(a) Living room and bedrooms.

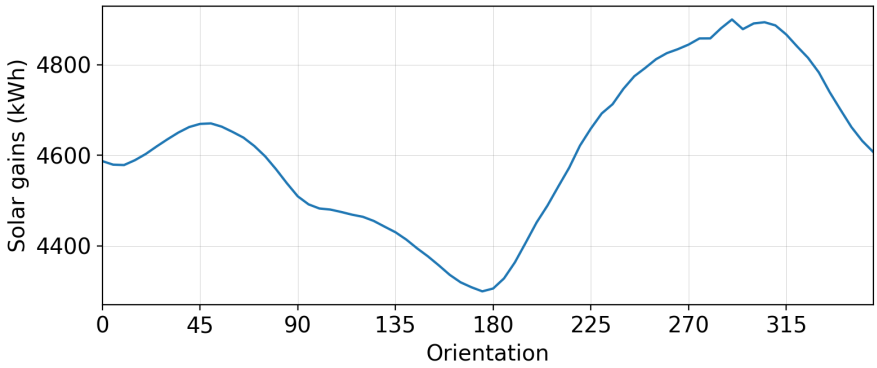

(b) Living room.

Figure 3.19: Case A solar heat gains in occupied zones during cooling period.

ments. The reason behind this is that in this study thermal requirements were only taken into account in occupied zones. This seems to be a quite reasonable hypothesis for buildings thermal performance simulations on the grounds that thermal comfort considerations only make sense in the presence of people.

3.4.2 Impact of orientation and surroundings on infiltration and ventilation losses

Infiltration and ventilation loads depend both on the airmass flows entering (and leaving) the building through cracks and openings and on the temperature difference between the thermal zones and the outside environment. Analysing how these loads vary with the house orientation and its surroundings is rather complicated as there are several aspects that should be considered. First, there are the airmass flows which vary with the building orientation and surroundings as they depend on the local wind profiles. Also, the temperature

difference might present variations as, even though the outside temperatures do not depend on the building orientation nor on the case scenario, the inside temperatures might, specially in those unoccupied zones where there are no HVAC systems modelled. Moreover, these differences in the inside temperatures may result in different operations of the windows, which in turn will drastically affect the airmass flows. Above all, there is the issue that EnergyPlus outputs do not distinguish between infiltration and ventilation. This makes it very difficult to identify the drivers of the variations in the infiltration and ventilation thermal loads, as they could be attributed to changes either in the wind profiles, the zone temperature or in the occupants windows opening behaviours.

As a workaround for these issues, the approach followed to proceed with the analysis involved studying simpler cases in order to understand the different aspects separately and the weight that each would have in the total. In the following sections, there are the different stages of the analysis. First of all, the study was narrowed down to infiltration airmass variations, then the same was done but for the case of ventilation airmass. Next, the differences in the windows opening behaviours are presented. Finally, the results for the original case are presented and related to the studied aspects.

Infiltration airmass

Infiltration airmass flows are a function of the pressure difference across the cracks, where the outside pressures are characterised by the building geometry and the wind speed and direction relative to the facades. Hence, and knowing that Montevideo's wind profile has some preferred directions with either higher wind speed or higher frequency, infiltration airmass would vary with the building orientation. Regarding the surroundings, they would also affect the airmass leaked into the building as they locally influence the wind profile. However, the EnergyPlus model used does not consider the impact of the surroundings on the wind speed nor on the pressure coefficients and so the analysis will be focused on the impact of orientation.

For any given wind direction, the higher the wind speed, the bigger the airmass leaked. The impact of wind direction on the other hand is not as obvious, as it depends on the building geometry and the cracks characteristics and location. Consequently, to study the effect of the wind direction relative

to the building facades, a one year simulation was performed for the example case geometry in which the wind speed was fixed (at 5 m/s) and wind direction was left as it was in the EPW file[1]. By doing so, the effect of wind direction could be isolated so as to analyse its impact on airmass leaking into the house. As the intention is to study the variations in the infiltration airmass, all the exterior openings were forced to be closed for every hour. The obtained results would therefore show the variation of the infiltrations with the wind direction relative to the front facade for the example case geometry.

The resulting hourly air change rates as a function of wind direction are shown in Figure 3.20, where each dot corresponds to one hour of the year. There, it can be noted that infiltrations are maximum for wind directions from 0° to 55° relative to the front facade, have a minimum at 90°, a maximum at around 130° and are at their lowest at wind directions of 270° relative to the front facade. Two aspects should be considered when trying to understand this graph pattern: the cracks distribution across the building enclosure and the facade pressure coefficients variations with wind direction.

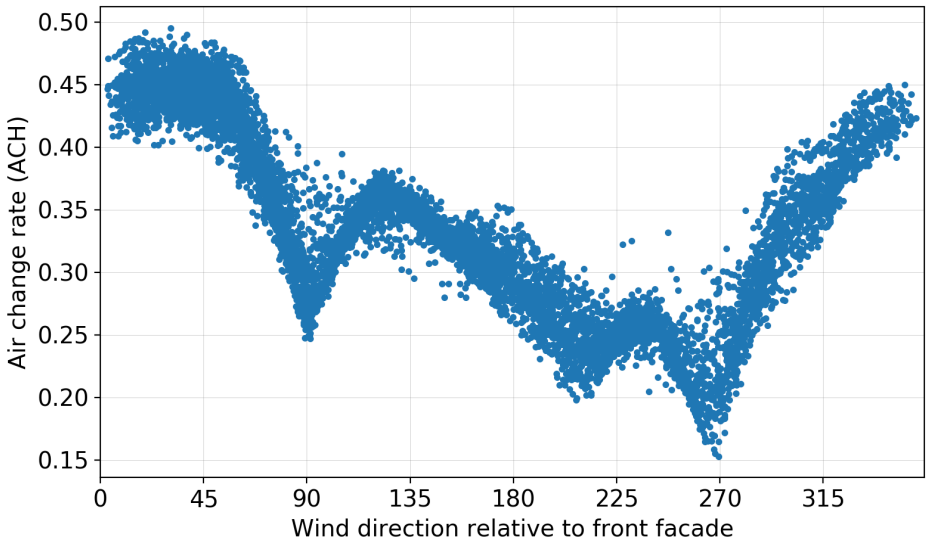

Figure 3.20: Air change rates due to infiltration with fix wind speed (5 m/s).

The first aspect can be observed in Figure 3.21, where there is the example case geometry and the openings highlighted in bold. The openings perimeters are of 17.3m in the front facade, 11.2m in the one at 90°, 5m in the back facade

[1]Given that the EPW contains hourly data for the wind direction, a one year simulation should be enough to cover all possible wind directions.

and none in the one at 270°. The second aspect can be studied by calculating the pressure coefficients on each facade (see Eq. 2.12) and knowing that airmass depends on the difference between those pressure coefficients (ΔC_p) across each crack inlet and outlet.

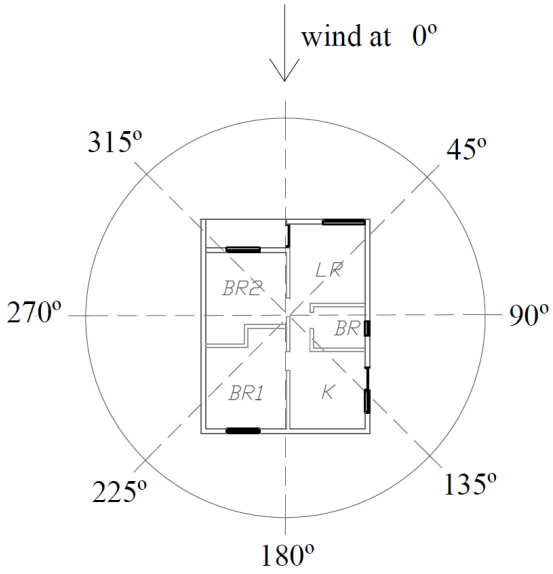

Figure 3.21: Building geometry and openings position for wind directions relative to front facade.

Given that in the example case the cracks are located along each opening perimeter and also on the roof, the relevant C_p are those on the facades at 0°, 90° and 180° and on the roof. These C_p are shown in Figure 3.22a as functions of the wind direction relative to the front facade. Besides, in Figure 3.22b there is the weighted average ΔC_p where each term was weighted according to the corresponding C_Q (see Eq.3.4).

$$\Delta C_p = \frac{\sum_n (C_{p,n} - C_{p,i}) C_{Q,n}}{\sum_n C_{Q,n}} \tag{3.4}$$

Where n represents each facade where there are air paths and $C_{p,i}$ is the interior pressure coefficient, which for this analysis was approximated as the weighted average of the outside ones ($C_{p,i} = \frac{\sum_n C_{p,n} C_{Q,n}}{\sum_n C_{Q,n}}$). The C_Q are determined for each facade and the roof according to the openings distribution observed in Fig. 3.21 and the openings and roof characteristics presented in Tabs. 3.3 and 3.4.

Observing Fig. 3.22b it can be noted that the air change rate of Fig. 3.20 varies with wind direction accordingly to the variation of the average ΔC_p

defined. This shows that the infiltration airmass depends on wind direction through the pressure coefficients and the cracks location and characteristics.

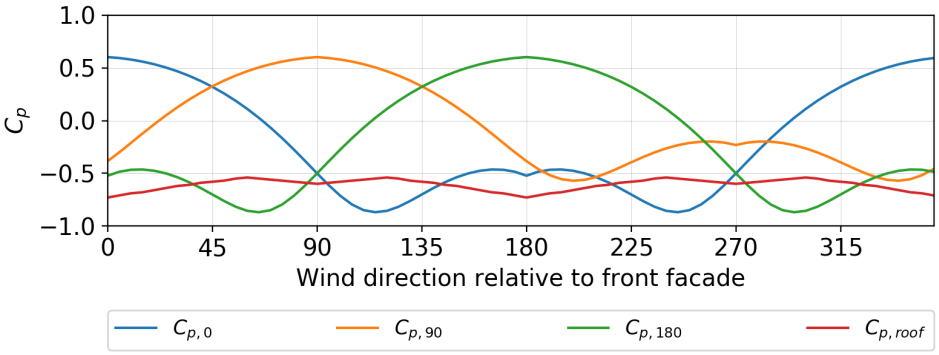

(a) Pressure coefficient on relevant facades.

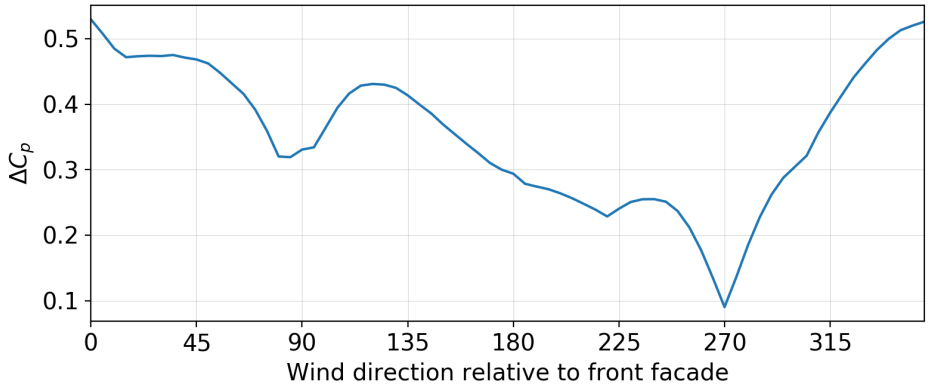

(b) Weighted average pressure coefficients difference.

Figure 3.22: Pressure coefficients variation.

Finally, and in order to complete the analysis, this same case with all the windows and doors closed was simulated varying the house orientation and for the original EPW (this is, not fixing the wind speed). By doing this, and knowing how the infiltration airmass varies with wind speed and direction for the studied geometry, the obtained infiltration air change rates could be related to the EPW wind profiles.

The resulting annual average air change rates as a function of the house orientation are shown in Figure 3.23. It can be observed that they grow with the building orientation until their peak at 100° where they start decreasing towards their minimum at 305°. Given that infiltration airmass depends on both wind speed and direction, and that the wind pressure varies with the square of wind speed, the EPW wind profile is presented in Figure 3.24 as a wind rose where the radius value is calculated as the relative frequency of each

direction multiplied by the square of the mean wind speed in each particular direction. The result was then normalized to add up to 100%.

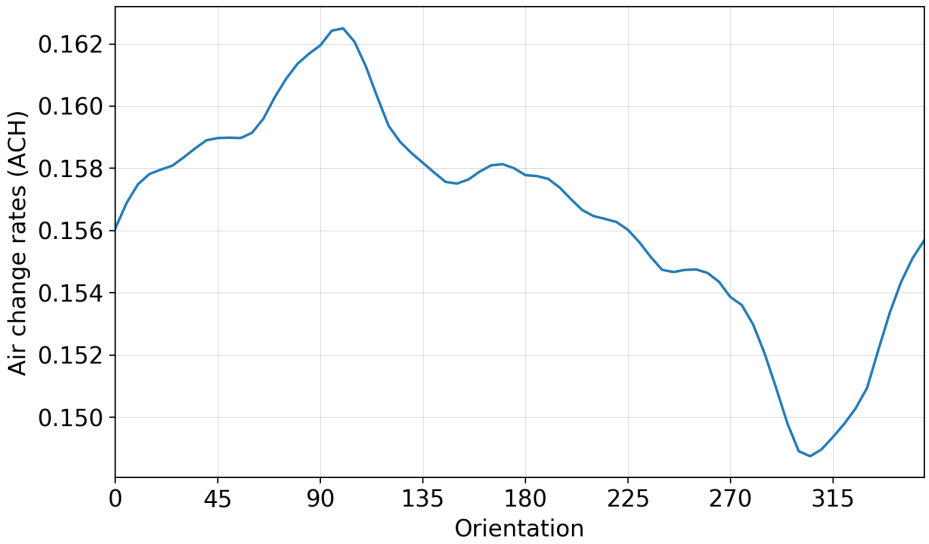

Figure 3.23: Infiltration annual average air change rates.

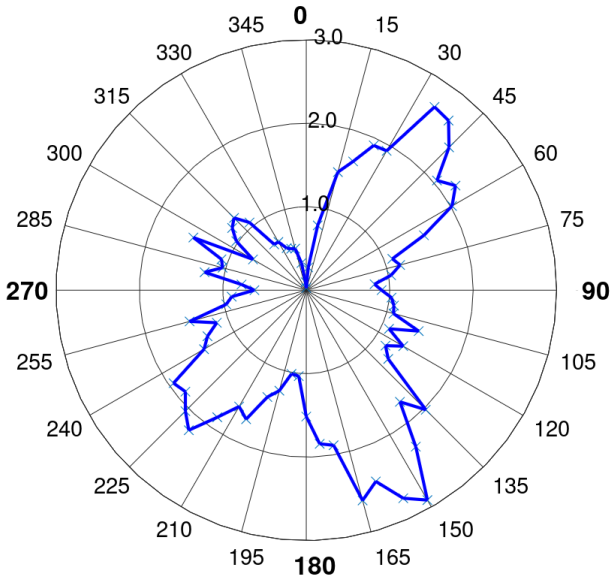

Figure 3.24: Wind rose of direction frequency by the square of wind speed.

The obtained relationship between average annual air change rates and house orientation can be understood by knowing how the infiltrations vary

with the wind hitting the different facades (Fig. 3.20) and the annual most (and least) prevalent winds (Fig. 3.24). For example, in Fig. 3.20 some of the maximum infiltrations happen at wind directions of 50° relative to the front facade; for a house oriented at 100°, this would be for winds direction of 150° which is actually the direction with the highest prevalence in the wind rose (Fig. 3.24). For winds at around 130° relative to the building there are also high air change rates in Fig. 3.20. For a house oriented at 100°, this corresponds to an absolute wind direction of around 230° where are also quite relevant winds according to Fig. 3.24. Finally, if the lowest values in Fig. 3.20 are converted into absolute wind directions for a house oriented at 100°, they would be at around 10° and 300° where there is very little wind in Fig. 3.24. It therefore seems reasonable for the house oriented at 100° to have high infiltrations.

On the other hand, for a house facing at 305° the maximums infiltrations would come from directions at around 355° and, to a lesser extent, at 75° (these correspond to relative directions of 50° and 130°, which have the maximum infiltrations according to Fig. 3.20). Observing the wind rose, those are the directions with the lowest prevalences. Contrarily, the minimum infiltrations would be related to directions at around 215° and 145° (270° and 200° relative to the building front) which are relevant wind directions in Fig. 3.24. Hence, it is also reasonable for the house oriented at 305° to have the lowest annual infiltrations.

All in all, the relationship between infiltration airmass and the house orientation for the case scenario is that shown in Fig. 3.23. The function graph pattern can be understood by relating the pressure coefficients differences and the openings locations along the enclosure, with the local wind profiles used for the simulations.

Ventilation airmass

The ventilation airmass variations analysis was approached equally as the infiltrations study. Once again, the impact of wind speed on ventilation airmass is quite clear (the higher the speed, the larger the airmass) whereas the impact of wind direction is highly dependant on the windows location and areas. First of all, a one year simulation was performed fixing wind speed (at 5 m/s) and leaving wind direction to vary as in the original EPW file, so as to isolate the effect of wind direction. As in this case the intention is to study the variations

in the ventilation airmass, all the exterior windows were forced to be open for every hour.

The resulting hourly air change rates as a function of wind direction are shown in Figure 3.25, where each dot corresponds to one hour of the year. The maximums ventilation airmass are at directions of around 0° and 120° relative to the front facade and there is also a relative maximum at 240°. The minimums on the other hand are for winds at around 270° and 90° (see Fig. 3.25). By comparing this graph with that in Fig. 3.20, it can be observed that ventilation airmass variations with wind direction are rather different than those for infiltration. More importantly, it can be noted the large difference in the air change rates values in each case as, while the infiltration ones are of around 0.35 ACH, the ventilation rates are around 40 ACH.

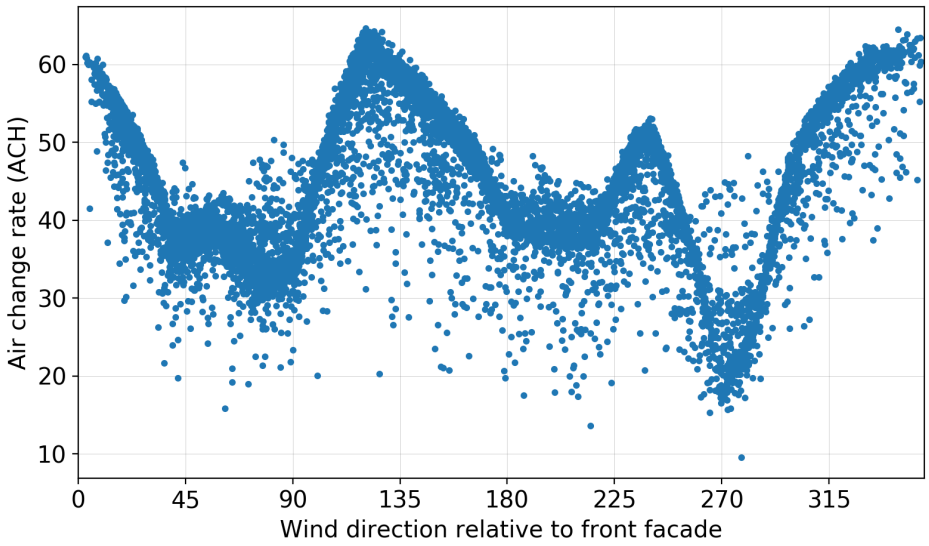

Figure 3.25: Air change rates due to ventilation with fix wind speed ($5m/s$).

Differently than for infiltration, the ventilation airmass depends on the openings areas rather than on their C_Q. Thus, in order to relate the pattern of Fig. 3.25 with the pressure coefficients differences across the building facades, the distribution of the openings areas should be considered. These areas are of 4.22 m^2 in the front, 1.15 m^2 in the one at 90° and 1.54 m^2 in the back facade. Besides, in this case the pressure coefficients differences that would have the greatest impact on the ventilation airmass would be those between the facades where there are windows, which are between the front and back facade and between each of them and the facade at 90°. Once again, the weighted average

ΔC_p was determined and its variation with relative wind direction is shown in Figure 3.26. The calculation procedure is almost the same as Eq. 3.4 with the exception that, instead of the C_Q, the sum was done weighting the terms according to the windows areas.

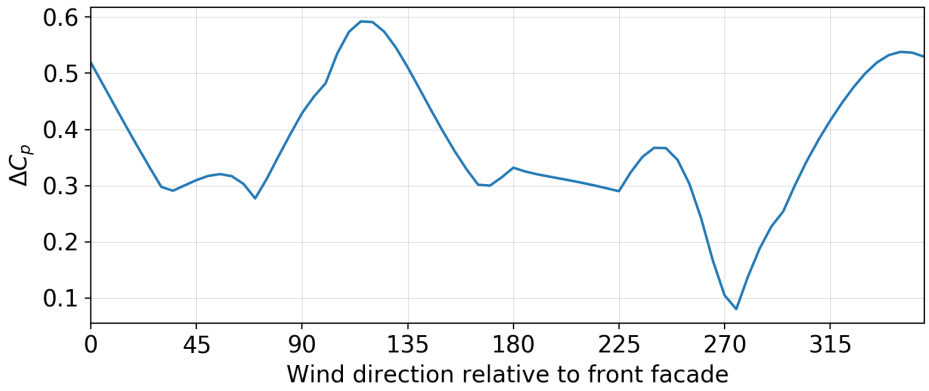

Figure 3.26: Weighted average pressure coefficients difference.

Comparing the graph of Figs. 3.25 and 3.26 it can be observed how both graph patterns are very similar. This shows how the AFN model used in this work relates ventilation airmass with wind direction according to the pressure coefficients difference across the house facades and the windows distribution on the enclosure.

As done for the infiltration analysis, this case with all the windows opened was again simulated but for the original EPW and varying the house orientation. Once again, by doing this, and knowing how the ventilation airmass varies with wind speed and direction for the studied geometry, the obtained ventilation air change rates could be related to the EPW wind profiles. The resulting annual average air change rates as a function of the house orientation are shown in Figure 3.27. The maximums in this case can be found at building's orientations of 60° and 270° and the minimum is for a building facing 325°.

This graph in Fig. 3.27 can be explained by analysing Figs. 3.25 and 3.24 for the different building orientations. For example, the higher air change rates according to Fig. 3.25 are for wind directions from 300° to 30° and from 105° to 165° relative to the front facade. These, for a building oriented at 60°, correspond to absolute wind directions from 0° to 90° and from 165° to 225°; which according to the wind rose of Fig. 3.24 include orientations with quite high prevalences. Besides, the lower air change rates happen at relative wind

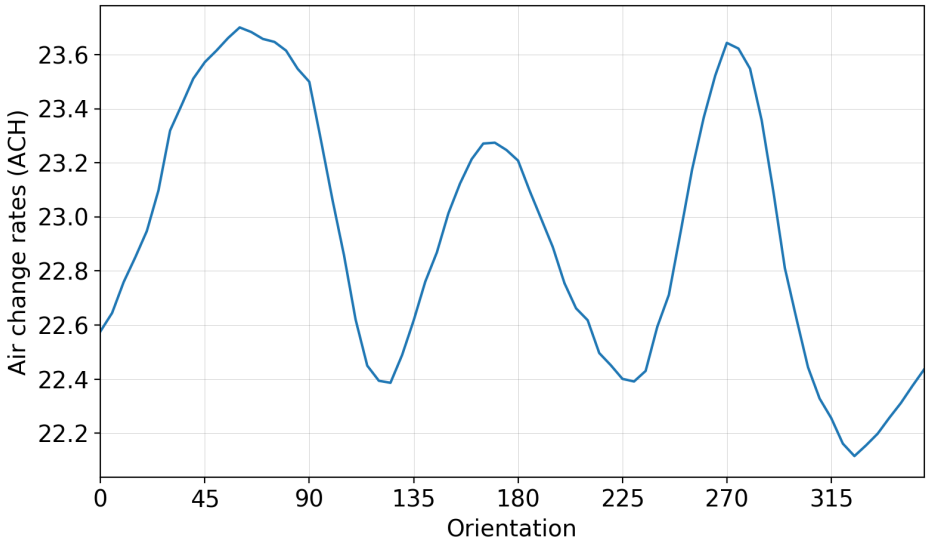

Figure 3.27: Ventilation annual average air change rates.

directions from 260° to 285° (see Fig. 3.25). For a building oriented at 60°, these correspond to absolute wind directions from 320° to 345° which have very little frequency and/or wind speed according to the wind rose in Fig. 3.24.

So, equally as for infiltration, the relationship between ventilation airmass and the house orientation for the case scenario (see Fig. 3.27) can be understood by relating the pressure coefficients differences and the openings areas and locations along the enclosure, with the local wind profiles used for the simulations. However, the drastic differences between infiltration and ventilation air change rates suggest that the aspect that would have the greatest impact on infiltration and ventilation thermal loads is the occupants behaviour regarding windows operation.

Occupants behaviour

In the example case scenario, the occupants operate the windows so as to achieve thermal comfort with the lowest possible HVAC consumption. All throughout this work, the comfort criteria is determined in accordance with ASHRAE 55 [36] and is based on whether the zone operative temperature is within a certain range. This zone operative temperature depends on the zone air as well as the walls temperatures.

If the zone operative temperature is higher than the comfort one, but within the upper and lower ASHRAE 55 acceptability limits, the occupant opens the

windows instead of using the HVAC system. Conversely, if the zone operative temperature is beyond the acceptability limits, the windows are closed and the HVAC system is turned on. This entails that the occupants behaviour regarding windows operation depends on the walls temperatures (as well as on the zone air temperature) which vary with orientation and case scenario similarly as solar gains.

However, this is only true for the occupied zones (living room and bedrooms) and only during the hours in which they are occupied. For the hours when they are not, the windows remain closed. Contrarily, the kitchen and bathroom windows are always open as long as there are people in the house, and are closed otherwise. So in order to analyse the influence of building orientation on the occupants behaviour, the study will be focused on the living room and the bedrooms.

Enclosure temperatures vary not only with building orientation but also with the surroundings, thus, the same will happen to the occupants behaviour. Nevertheless, for simplicity, only Case I will be studied. In this case, the analysis is based on the original simulation. This means that the original EPW file was used and also that the house windows were not forced to be closed nor open but left to be operated by the occupants according to the mentioned criteria.

The amount of time (as a percentage) that the living room and/or bedrooms windows were open is shown in Figure 3.28 as a function of the building orientation. 100% would mean all of the windows were open during the whole period. Due to the great difference that there would be for the two periods considered, heating and cooling seasons are presented separately in Figs. 3.28a and 3.28b, respectively.

If the graphs in Fig. 3.28 are compared to the corresponding solar gains it can be noted that the time the windows are open during heating season varies with building orientation equally as the living room solar gains shown in Fig. 3.14b. This is on the grounds that during winter, the more solar radiation on the walls, the higher the operative temperature and, consequently, the more time the operative temperature is higher than the comfort temperature but within the ASHRAE 55 limits. Also, this will happen mostly in hours near midday when the only occupied zone is the living room, which is why the windows opening pattern depends on living room solar gains. During summer the exact opposite happens: the more radiation on the walls, the less time

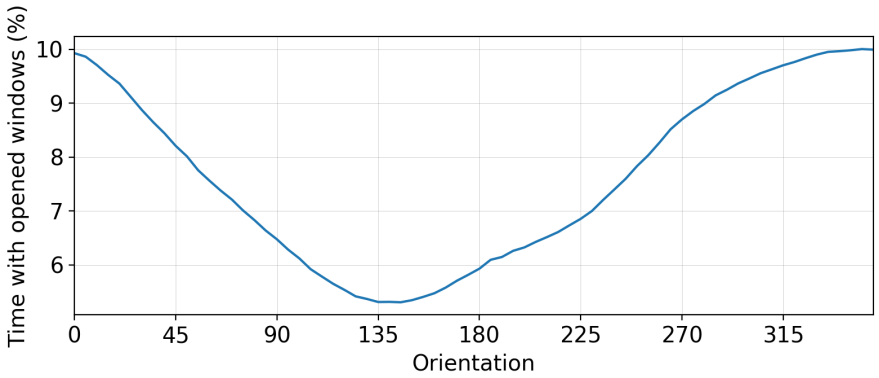

(a) Heating period.

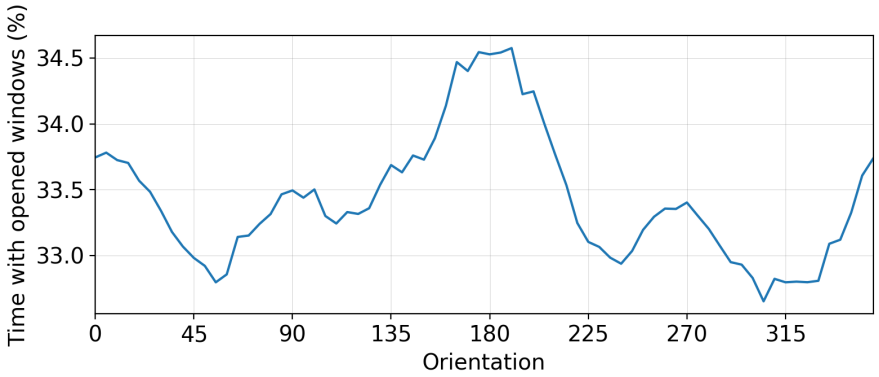

(b) Cooling period.

Figure 3.28: Amount of time with opened windows in occupied zones.

within comfort limits. Accordingly, during cooling season the variation of the time with opened windows is opposite as the variation in the total solar gains (Fig. 3.17).

As concluded when comparing infiltration and ventilation air change rates values, these variations in the amount of time in which the windows are open would have the greatest impact on the example case infiltration and ventilation airmass. This can be seen in Figure 3.29, where the resulting air change rates for heating and cooling periods are shown. These graphs patterns are very similar to those in Figs. 3.28a and 3.28b as the more time the windows are open, the grater the airmass entering the house.

Figs. 3.29a and 3.28a vary similarly except at orientations around 0° whereas the same happens with Figs. 3.29b and 3.28b that are different at orientations near 45°. These differences can be understood by taking into consideration the ventilation airmass relationship with building orientation of Fig. 3.27; air change rates are quite low at 0° and rather high at 45°. This

provides evidence for the importance of using a quite detailed model such as AFN as if fixed values for ventilation and infiltration air change rates were to be used this dependence on orientation would be dismissed.

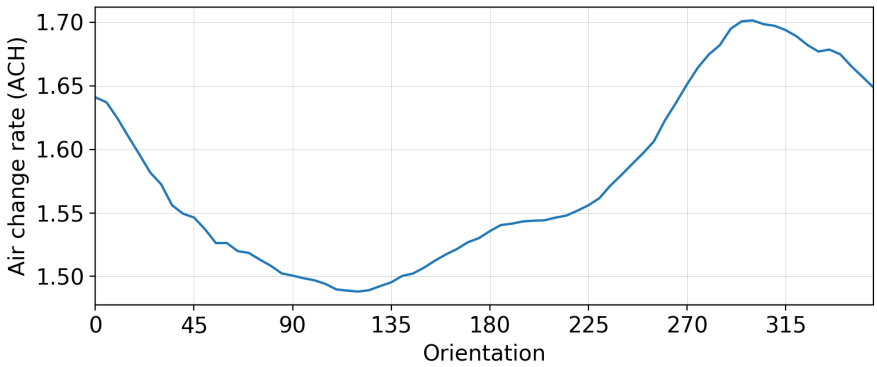

(a) Heating period.

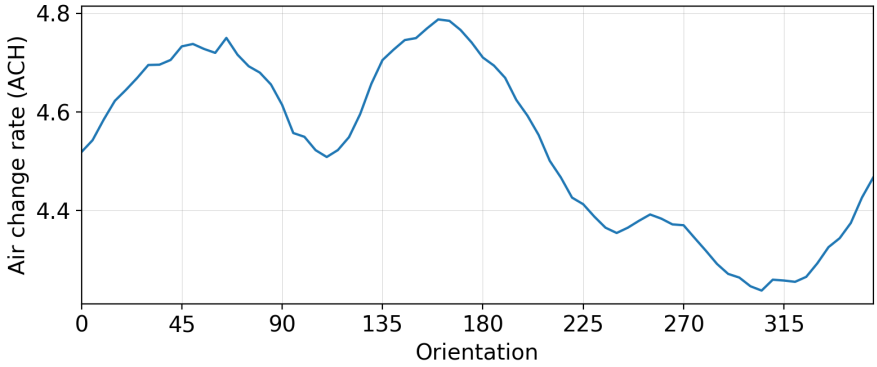

(b) Cooling period.

Figure 3.29: Average air change rates for heating and cooling periods.

So the relationship between the example case infiltration and ventilation airmass and the building orientation can be explained by the influence of orientation on the occupants windows opening behaviour and the variations in ventilation air change rates. Since the first aspect is highly dependant on solar gains, which as studied in Section 3.4.1 vary both with the orientation and the surroundings, the outside airmass entering the house through the openings would also depend on the case scenario.

Infiltration and ventilation thermal loads

Up to now, all the analyses were only focused on understanding the relationship between the infiltration and ventilation airmass and the building orientation.

In order to complete the study, the infiltration and ventilation thermal loads should be considered. As mentioned, these thermal loads are a function of the airmass and the temperature difference between the zone and the outside environment.

For a given window opening factor the leaked airmass will be the same for the different case scenarios given that the EnergyPlus model used does not consider the impact of the surroundings on the wind profiles. However, the occupants behaviour would vary with the surroundings and so the actual airmass entering the house would also vary with the case scenario. Due to this and also to the fact that the zone temperatures may slightly vary for the different case scenarios, so would the infiltration and ventilation energy losses.

The infiltration and ventilation energy losses during heating and cooling periods for the case scenarios and the orientations considered are those shown in Figure 3.30. It can be observed that there is a strong resemblance between these graphs and those in Fig. 3.29, which is reasonable as the temperature difference should not vary as much as airmass with the orientation. Besides, the differences among the case scenarios are more noticeable during the cooling period and between the detached and the attached situations. This is because the major impact of the surroundings on the walls temperature is when there is an attached facade. As the attached facade is that containing the bedrooms walls, the influence is not very relevant during heating period when the ventilation varies mainly with the living room operative temperatures.

When analysing infiltration and ventilation thermal loads, there are several aspects that should be taken into consideration such as occupants schedules, windows opening behaviours, HVAC operation, etc. For instance, even during heating period, there could be some hours in which operative temperatures are higher than comfort and, consequently, infiltration and ventilation losses are desired and do not affect heating loads. Thus, relating these energy losses to heating and cooling requirements would require further analyses; which exceed the objectives of this chapter.

3.5 Conclusions

This chapter provides evidence for the importance of considering some variability within a given archetype when using it to represent different households. It was found that, for the example archetype, an error of up to 35% could be

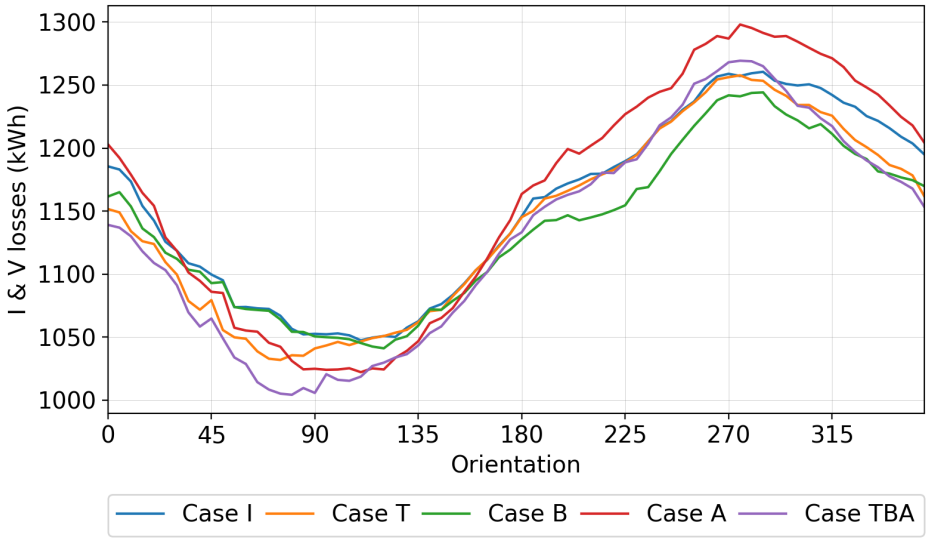

(a) Heating period.

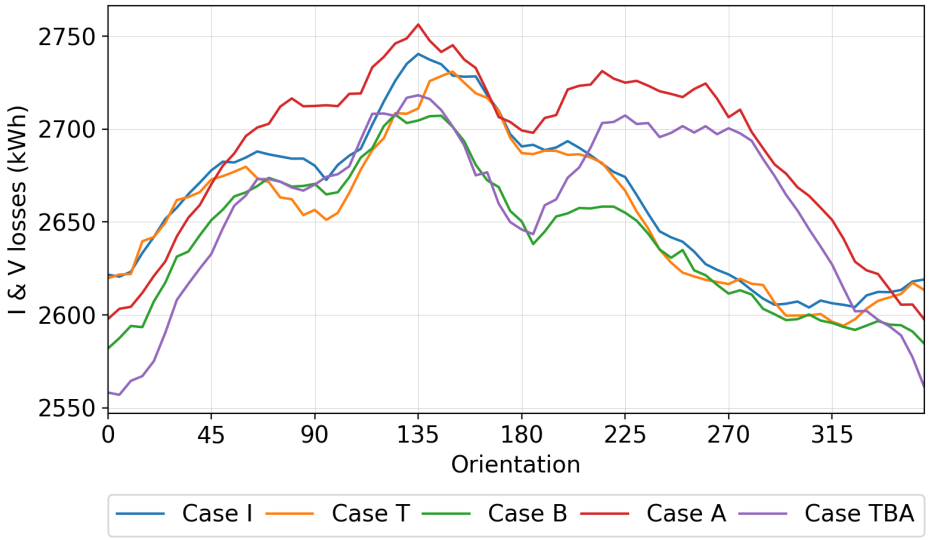

(b) Cooling period.

Figure 3.30: Infiltration and ventilation losses.

committed if the isolated house were to be used to characterise the thermal requirements of a house with an attached facade. Moreover, there are also differences in the relative contribution of each component such as roof, walls, windows, infiltration and ventilation, etc. to the heating and cooling requirements. This puts in evidence that, even within the same archetype, if retrofit measures were to be designed, the most effective options may not be the same for different households.

As far as total thermal requirements are concerned, from the different scenarios considered, the attached cases showed a better performance than the detached ones for every orientation. The only exception is at orientations where the attached facade is facing north, where all the case scenarios performed very similarly. For all the surroundings considered, the most favourable orientation is when the house is facing around north, although south orientation is also very similar. Focusing on heating period, the best orientations are also around north whereas the worst are around south for the detached scenarios and near east for the attached ones (when the attached facade is facing north). Conversely, during cooling period south is the best orientation whereas north-west is the worst as it is the one which maximizes solar gains in the living room. Both during heating and cooling periods, the attached cases performed better for the majority of the orientations. Nevertheless, the differences are much more relevant during heating period on the grounds that solar altitudes are lower and the walls and windows contributions to solar gains are more relevant.

These differences in thermal performances are mostly due to the strong dependence solar gains have on the building orientation and its surroundings. In this regard, the obtained results show that when aiming at relating the variations in solar gains with those in thermal requirements, the zones usage patterns end up playing the most relevant role. This means that during heating period, the most favourable orientation would be that which capitalizes on more solar gains in the occupied zones, specially in those occupied during day time. For the detached cases this is when the house is oriented at 0° whereas for the attached ones is at 325° or 280° if there is also the effect of shading. Contrarily, for cooling period, the better orientation is that which receives less solar gains in the occupied zones and that is at 180° for all case scenarios.

Apart from solar gains, the other thermal loads that vary with orientation and the surroundings are those due to infiltration and ventilation. Given that there are several factors affecting their variability with orientation and case scenario, the analysis was divided into three stages. In the first, the dependence of infiltration airmass on building orientation was understood by relating the pressure coefficients variations and the cracks characteristics to the local wind profiles. Secondly, the same was done for the ventilation airmass but in this case the pressure coefficients and the openings areas were related to the local wind profiles. In this two first stages, only the impact of orientation was studied on the grounds that the model used to solve infiltration and ventilation

airmass does not consider the impact of the surroundings. Finally, the occupants behaviour regarding opening factors was studied and related to solar gains through the operative temperatures. Due to the large differences between infiltration and ventilation airmass, the variation of the infiltration and ventilation thermal loads with the building orientation resulted very similar to the variation of the percentage of time with the windows open.

Even though this study was based on an example case, it can be acknowledged that building orientation and its surroundings would influence the results in any given archetype and geometry. This hence demonstrates the importance of considering this variability within each archetype when aiming at characterising a whole housing stock relying on them. Besides, and given that the effect of these variations depended on the building geometry, the zones usage patterns, the openings characteristics and the local weather, the relationship between thermal requirements and building orientation and surroundings scenario would be different in each geographic location and for each combination of archetype and geometry. This results in the need of performing as many simulations as possible, upon each archetype in each geographic location, so as to contemplate these variations and obtain results as accurate as possible.

Chapter 4

Automation of the modelling process and simulation of the Uruguayan housing stock

4.1 Introduction

In recent years, different building energy models have been developed with the purpose of effectively understanding, assessing and managing energy consumption in residential building sector. The reason behind this is the relevant proportion in which residential buildings contribute to the world total final energy demand, combined with the objectives of numerous countries of reducing energy consumption and greenhouse gases (GHG) emissions.

Within this context, urban scale building energy models are gaining relevance as they appear to be a promising tool for quantifying buildings energy requirements for whole cities. Li et al. [38] presented a review on Urban Building Energy Modelling (UBEM) where two main modelling approaches are distinguished: top-down and bottom-up. The former utilizes the estimate of total building sector energy consumption and other pertinent variables to attribute the energy consumption to characteristics of the entire sector. On the contrary, the latter calculates the energy consumption of individual buildings and then extrapolates these results to represent a region or nation [39]. Therefore, each technique requires different levels of detail for the input data and produces results with different applicability.

In top-down models, residential buildings are treated as a single energy entity and their consumption is usually represented in terms of types of energy used (electricity, natural gas, fuel oil, LGP, wood) but with no regard for individual buildings or end-uses. With this approach, demand prospective is determined by relating energy use and associated major drivers such as changes in gross domestic product (GDP), energy price, population, household size, technologies, weather conditions, etc. [38]. This relationship is established with historical data series and through econometric models based on price and income, or technological models which estimate energy consumption in the entire housing stock according to appliance ownership tendencies [39].

Top-down models inputs hence include long term historical data series and the variables considered are macroeconomic indicators (such as GDP, employment rates and price indices), climatic conditions, housing construction rates and estimates of appliance ownership. The strengths of this technique are that it requires a limited set of input information (still, historical data series must be reliable which is non-trivial) and that it is capable of assessing short term effects of prices policies. On the other hand, the main shortcomings of this type of models are that they are not suitable for evaluating technology changes and, as there is no detail regarding energy end-uses, they are not capable of identifying areas of improvements. Also, significant errors may arise when using them for long-term predictions given that the relationship between energy consumption and economic indicators is likely to change over time due to new developments or climate change [40].

Pérez-García and Moral-Carcedo [41] used an econometric top-down model to determine the relationship between electricity consumption and economic growth for the case of Spain. In this work, historical time series from 1970 to 2012 for both electricity demand and Gross Value Added (GVA) were used to develop a forecasting model for electricity demand, conditioned to the macroeconomic scenario. Likewise, Zhang [42] used this technique to establish the relation between energy consumption and heating degree-days for the United States of America (USA), Canada, Japan and China. For this purpose, a top-down approach was followed but with the addition of a physical factor such as climatic conditions. More precisely, statistics on energy consumption were used for the different climate regions identified and, for the case of electricity, data series of the penetration of household electric appliances were also considered.

Contrarily, in bottom-up models energy consumption is determined based on individual building data and then the results are extrapolated to represent the whole, based on the prevalence of the modelled sample in the stock. This implies the abstraction of the building stock into archetypes, which consist of building definitions that are used to represent a group of buildings with similar properties. This bottom-up technique is used to assess the contribution of each end-use towards the aggregate energy demand of the building sector. Among this approach there are some models which process individual building data through statistical methods by analysing sample buildings and others through simulation of physic-based models.

Statistical approaches relate relevant building characteristics such as vintage, usage and occupancy to measured building energy use, billing information or surveys data. This relation is determined by various techniques which can be categorized into three groups: regression analyses, conditional demand analyses (CDA) -where regressions are run based on end use appliances- and machine learning techniques, including neural network (NN) analyses. Advantages of this type of models include that simulations of energy use are at building level and also that end-uses as well as socio-demographic and macroeconomic effects are considered. Contrarily, their main disadvantages are that required billing or survey data may be difficult to get and that a large number of sampling subjects should be modelled for the results to be representative. Besides, as simulation results are highly dependant on historical trends, long term predictions would not be reliable.

Rafio et al. [43] developed a regression model of energy use versus weather conditions using information from utility bills and measured weather data. In the analysis, the model was applied for a case of study of about 300 residences in the USA. The aim was to target buildings for specific energy conservation retrofits and evaluate energy savings potential. Aydinalp and Ugursal [44] also used a statistical approach as they developed a CDA to model the end-use energy consumption in the Canadian residential sector. Using survey and weather data, an end-use energy consumption equation was developed for each end-use and each household to model; then the total energy consumption of a household would be the cumulative of all energy consumed for all end-uses considered. Aydinalp et al. [45], also applied NN for modelling energy consumption in the Canadian residential sector. In this case, survey data for

741 households was used to train the model whereas remaining data for 247 households was used to test its prediction performance.

The other type of bottom-up models involve a physic-based approach, where buildings simulations are run focusing on their physical characteristics and thermodynamic principles, which govern the interaction between a building and its surroundings. This type of approach is based on the modelling and simulations techniques developed by Building Energy Modelling (BEM). Most of these models rely on archetypes which represent the most frequent characteristics of a particular category. This is for the reason that case by case analysis using BEM would be unfeasible at city or even neighbourhood scale. Besides, considering the time consumed in the characterisation, generation and simulation of each individual archetype building model, automation also plays a key role in the applicability of this approach.

Physic-based bottom-up UBEMs allow the estimation of hourly energy demand loads down to the individual building level without the need of historical data and of knowing socio-economic parameters. The importance of determining energy demand in both temporal and spatial scales, relies on the fact that it could be an important input for developing predictions for energy demand. As a consequence, it might play a major part in generation capacity and power lines expansion planning. Moreover, these kind of models could be a quite capable tool when it comes to identifying areas of improvement or to evaluating the impact of the application of a certain policy in terms of hourly energy consumption and energy efficiency. These methods also have their weaknesses; among them there are the great level of detail needed for the input information and for calibrating the models. Also the computational cost associated with the need to run large simulations and the effort required to maintain the models. Besides, as many of these models are developed upon archetypes, their reliability is highly dependant on the definition and description of such archetypes.

Davila et al. [46] developed a full physic-based bottom-up UBEM for the city of Boston based on the Geographic Information Systems (GIS) datasets of the city and its Typical Meteorological Year (TMY). Simulations were performed for different scenarios with the intention of presenting how the model hourly resolution combined with its capability to study specific locations within the city, allow for many different analyses. The National Renewable Energy Laboratory (NREL) [47] also used this approach to analyse the energy ef-

ficiency potential in the United States (US) single-family detached housing stock. In order to do so, the authors used their self-developed analysis tool ResStock™ [48]. This tool consists of a physic-based bottom-up model that combines large public and private data sources with statistical sampling to characterise the housing stock. Then, it uses EnergyPlus to run detailed building simulations. Besides, as NREL high performance computing allows to run large number of simulations, 350,000 models were used to represent the US single family detached housing stock.

In Uruguay, quantifying energy demand for each end-use and identifying areas of improvement in residential sector are also gaining relevance given the important role energy efficiency plays in all short, mid and long-term energy policy objectives [49]. However, little has been done towards modelling national residential sector in detail. A top-down econometric model for the whole country was developed by the Dirección Nacional de Energía (DNE) [50] to elaborate energy demand projections for 2015-2035. In this study, the country was divided into residential, services, industry, primary activities (agriculture, mining and fishing) and transport sectors. However, each sector, except industry, was considered as a single energy entity.

Focusing on Uruguayan residential sector, the DNE [51] also carried out a study regarding residential buildings energy efficiency. The aim was to identify major areas of improvements and analyse retrofit cost-effectiveness. To achieve this goal, a quite simplified bottom-up physic-based model was developed for eight reference buildings located in two departments: Montevideo and Salto. Reference buildings consist of very simple geometries with no interior divisions. The model generated allows to analyse the impact of the location, orientation, compactness ratio, glazed percentage and enclosure construction on the energy requirements. Nevertheless, results obtained for the consumptions cannot be used to assess residential sector requirements on the grounds that housing stock is not characterised and could not be accurately represented by the reference buildings modelled.

In this regard, the present work aims at modelling energy requirements for thermal conditioning in the residential building sector in Uruguay. To address this challenge, a physic-based bottom-up approach was followed based on buildings identified as representative of the residential sector and their prevalence among the whole housing stock. The stages for developing this bottom-up model involved the housing stock characterisation, including the

definition of typical buildings and their prevalence in the residential sector. Then, the definition of hypotheses for the simulation such as selecting the weather files which best represent each Uruguayan department, occupation schedules for the buildings zones, occupants behaviour, comfort criteria, etc. Finally, there is the process automation stage, in which a tool was developed to characterise, generate and simulate the households models and, furthermore, process the results. EnergyPlus is the simulation engine used in which the energy calculation method relies on.

In the following sections, a description of the methodology followed to develop the model of the Uruguayan residential building sector is provided including the stages of housing stock characterisation, hypotheses definition and process automation. Then, the obtained results regarding thermal performance of Uruguayan housing stock are presented and analysed with the intention of assessing energy requirements for thermal comfort according to the buildings characteristics.

4.2 Methodology

To achieve the objective of assessing the energy requirements for thermal comfort in the Uruguayan residential building sector, a physic-based UBEM was generated using EnergyPlus version 8.7. The model development was part of the project FSE_1_2017_1_144779 [4] in which the author of this thesis collaborated and which involved three main stages: housing stock characterisation, simulation hypotheses definition and process automation. During the course of the project the author participated in all three stages but focusing mainly on the third one, as she developed the tool for the process automation. This is the reason why the main focus of this work is on the automation stage which will be thoroughly explained in this section. All three stages will be described nevertheless so as to provide an overall understanding of the whole process for the model generation and results analyses.

4.2.1 Housing stock characterisation

When following a physic-based approach, the first step is to know the building which would be modelled and simulated. Intending to represent all Uruguayan residential sector, and acknowledging that representing every building one by

one would be unfeasible, typical buildings were identified and characterised. In order to do so, the whole housing stock was categorised and grouped according to certain attributes upon which other building characteristics depend. These attributes are the building location, type (whether it is a house or an apartment), size, occupants socio-economic status and vintage. This study was executed in FSE_1_2017_1_144779 [4] and the present work uses the results.

"Type" category was divided into 2 groups while all "Size", "Decile rank" and "Vintage" categories were divided into 3 groups. Those are:

- Type
  - House
  - Apartment
- Size
  - Less than or equal to $40m^2$
  - Between $40m^2$ and $70m^2$
  - Greater than $70m^2$
- Decile rank
  - Deciles 1-4
  - Deciles 5-7
  - Deciles 8-10
- Vintage
  - Less than or equal to 10 years old
  - Between 10 and 30 years old
  - Greater than 30 years old

All buildings with a particular combination of decile and vintage parameters were determined to share the same characteristics in terms of materials, constructions, solar protections and air leakages through cracks and openings. The main results in this regard are summarized in Tables 4.1, 4.2 and 4.3, where the characteristics of the components are expressed in terms of variables defined in Chapter 2 (detailed information concerning materials and components can be found in Appendix D). Besides, in order to solve airmass flows through doors and windows when they are open and also through stairwells (Eqs. 2.16, 2.17 and 2.18), the `AirflowNetwork` (AFN) model requires the discharge coefficient and the stair sloping plane angle. For the first, a value of 1

was set for all cases due to the lack of measured data from which to determine the actual ratio between real discharge and theoretical discharge, and for the results to be on the safe side. For the second, a value of 35° was used as it corresponds to a standard staircase.

Table 4.1: Archetypes constructions main thermal properties.†

Decile	**Vintage**	**Exterior Walls**		**Roof**		**Floor**	
		U (W/m^{2}K)	α_{sol}	U (W/m^{2}K)	α_{sol}	U (W/m^{2}K)	
						Bedrooms	Other
1-4	$V \leqslant 10$	5.2	0.60	0.8	0.80	8.8	8.8
	$10 < V \leqslant 30$	5.2	0.60	0.8	0.80	8.8	8.8
	$V > 30$	4.4	0.60	22	0.60	8.8	8.8
5-7	$V \leqslant 10$	0.9	0.55	0.8	0.50	5.4	8.8
	$10 < V \leqslant 30$	3.6	0.55	1.4	0.50	5.4	8.8
	$V > 30$	3.0	0.60	4.5	0.50	5.4	8.8
8-10	$V \leqslant 10$	0.8	0.60	0.8	0.50	5.4	8.8
	$10 < V \leqslant 30$	1.8	0.55	1.4	0.50	5.4	8.8
	$V > 30$	2.4	0.60	4.5	0.50	5.4	8.8

† Film coefficients are not included in these U-factors

Table 4.2: Presence of solar protections in archetypes zones.

Decile	**Vintage**	**Living room**	**Bedrooms**	**Others**
1-4	$V \leqslant 10$	No	No	No
	$10 < V \leqslant 30$	No	No	No
	$V > 30$	No	No	No
5-7	$V \leqslant 10$	No	Yes	No
	$10 < V \leqslant 30$	No	Yes	No
	$V > 30$	Yes	Yes	No
8-10	$V \leqslant 10$	No	Yes	No
	$10 < V \leqslant 30$	No	Yes	No
	$V > 30$	Yes	Yes	No

Table 4.3: Archetypes openings and cracks air leakage properties.

Decile	**Vintage**	**Windows**		**Exterior doors**		**Roof**		
		C'_Q (g/sm)	n	C'_Q (g/sm)	n	C'_Q (g/sm)	C''_Q (g/sm^2)	n
1-4	$V \leqslant 10$	0.096	0.70	0.0456	0.66	0.636	0.156	0.70
	$10 < V \leqslant 30$	0.898	0.68	0.0456	0.66	0.636	0.156	0.70
	$V > 30$	0.898	0.68	0.0456	0.66	0.132	0.156	0.70
5-7	$V \leqslant 10$	0.096	0.70	0.0456	0.66	0.132	0.156	0.70
	$10 < V \leqslant 30$	0.898	0.68	0.0456	0.66	0.132	0.156	0.70
	$V > 30$	0.898	0.68	0.0456	0.66	0.132	0.156	0.70
8-10	$V \leqslant 10$	0.096	0.70	0.0456	0.66	0.132	0.156	0.70
	$10 < V \leqslant 30$	0.898	0.68	0.0456	0.66	0.132	0.156	0.70
	$V > 30$	0.898	0.68	0.0456	0.66	0.132	0.156	0.70

Table 4.4: Archetypes number of occupants.

Decile	Size	Number of occupants
1-4	$S \leqslant 40\text{m}^2$	3
	$40\text{m}^2 < S \leqslant 70\text{m}^2$	4
	$S > 70\text{m}^2$	5
5-7	$S \leqslant 40\text{m}^2$	1
	$40\text{m}^2 < S \leqslant 70\text{m}^2$	3
	$S > 70\text{m}^2$	4
8-10	$S \leqslant 40\text{m}^2$	1
	$40\text{m}^2 < S \leqslant 70\text{m}^2$	2
	$S > 70\text{m}^2$	2

The number of occupants on the other hand, depends on the household size and decile as shown in Table 4.4. Besides, the other characteristic which was decided to depend on that combination of type, size, decile and vintage is the building geometry. In this regard, a total of 32 representative geometries were defined and assigned according to which better represents each combination of those parameters. Hence, all possible combinations of type, size, decile and vintage define the 54 archetypes used to characterise the whole Uruguayan housing stock, and within each archetype there are some different options for the building geometry.

Regarding the buildings location, four subregions were considered according to climatic characteristics (see Figure 4.1). For the case of Montevideo, it on its own determined a subregion on the grounds that it holds a quite relevant proportion of the country's households (41%). Within each subregion, residential buildings are distributed into the departments according to certain known proportions shown in Table 4.5.

Each department would have its own weather characteristics as well as other attributes such as orientation of the cities blocks, amount of storeys in average in the apartment buildings and probabilities of having a tree in front of the house front facade, of having a building across the street and of the house being detached, semi-detached (sharing one or two walls with neighbours) or attached (sharing three walls with neighbours). Based on the results obtained in Chapter 3, this variability has a relevant impact on the buildings thermal requirements. Therefore, it will be considered within each archetype. Given that the values these variations may take depend on the department in which

the building is located, for each model to generate in each subregion, the department should be determined.

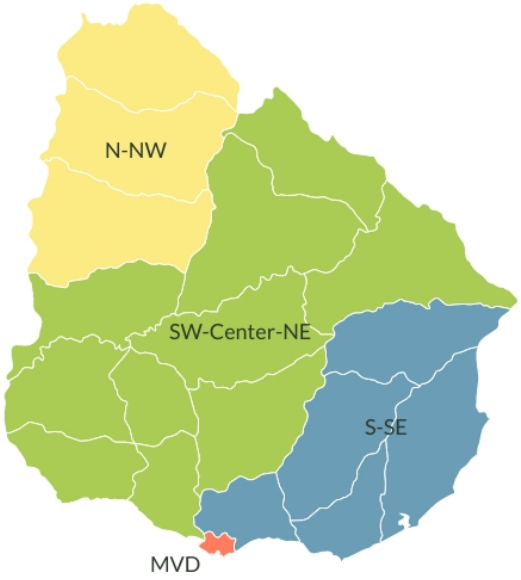

Figure 4.1: Regions considered.

Table 4.5: Distribution of departments within subregions.

N-NW	
Salto	39%
Paysandú	37%
Artigas	24%

SW-Center-NE	
Rivera	9%
Colonia	17%
San José	14%
Tacuarembó	12%
Cerro Largo	11%
Soriano	11%
Florida	9%
Durazno	7%
Río Negro	7%
Flores	3%

S-SE	
Canelones	59%
Maldonado	20%
Rocha	9%
Lavalleja	7%
Treinta y Tres	6%

MVD	
Montevideo	100%

Thus, the archetypes and its variations were used to characterise the whole Uruguayan housing stock. The remaining step to complete the characterisation is to know the proportion in which occupied residential buildings are distributed according to these archetypes and among the four geographic subregions. In order to calculate this proportions an analysis was performed in FSE_1_2017_1_144779 [4] based on reports and surveys about residential sector. Obtained results are summarized in Table 4.6, where the percentages in which the stock is distributed among the archetypes and subregions are presented.

Table 4.6: Housing stock distribution in the archetypes and subregions.

Type	Size (m^2)	Decile	Vintage (years)	N-NW	SW-Center-NE	S-SE	MVD	Subtotal	Subtotal	Subtotal	Total
House	S⩽40	1-4	V ⩽ 10	0,24%	0,70%	0,77%	0,67%	2,38%	11,00%	16,58%	84,67%
			10<V ⩽ 30	0,41%	1,17%	1,29%	1,13%	4,00%			
			V>30	0,34%	0,98%	1,08%	2,21%	4,62%			
		5-7	V ⩽ 10	0,06%	0,18%	0,20%	0,14%	0,58%	4,06%		
			10<V ⩽ 30	0,16%	0,46%	0,51%	0,34%	1,47%			
			X>30	0,17%	0,48%	0,53%	0,83%	2,00%			
		8-10	V ⩽ 10	0,04%	0,11%	0,12%	0,00%	0,27%	1,52%		
			10<V ⩽ 30	0,08%	0,23%	0,25%	0,00%	0,57%			
			X¿30	0,10%	0,28%	0,31%	0,01%	0,69%			
	40<S⩽70	1-4	V ⩽ 10	0,34%	0,99%	1,09%	0,92%	3,34%	16,09%	34,21%	
			10<V ⩽ 30	0,58%	1,66%	1,83%	1,56%	5,64%			
			V>30	0,49%	1,39%	1,54%	3,69%	7,10%			
		5-7	V ⩽ 10	0,18%	0,51%	0,57%	0,32%	1,58%	11,34%		
			10<V ⩽ 30	0,45%	1,29%	1,42%	0,85%	4,01%			
			V>30	0,47%	1,34%	1,48%	2,47%	5,75%			
		8-10	V ⩽ 10	0,14%	0,40%	0,44%	0,08%	1,07%	6,79%		
			10<V ⩽ 30	0,30%	0,86%	0,95%	0,17%	2,27%			
			V>30	0,36%	1,03%	1,14%	0,92%	3,45%			
	S>70	1-4	V ⩽ 10	0,23%	0,64%	0,71%	0,70%	2,28%	10,66%	33,88%	
			10<V ⩽ 30	0,38%	1,09%	1,20%	1,08%	3,74%			
			V>30	0,32%	0,91%	1,00%	2,41%	4,64%			
		5-7	V ⩽ 10	0,17%	0,48%	0,53%	0,37%	1,54%	11,23%		
			10<V ⩽ 30	0,42%	1,21%	1,33%	0,95%	3,91%			
			V>30	0,44%	1,25%	1,38%	2,71%	5,78%			
		8-10	V ⩽ 10	0,23%	0,67%	0,74%	0,24%	1,88%	11,99%		
			10<V ⩽ 30	0,50%	1,42%	1,57%	0,52%	4,01%			
			V>30	0,60%	1,71%	1,89%	1,90%	6,09%			
Apt.	S ⩽40	1-4	V ⩽ 10	0,001%	0,003%	0,003%	0,131%	0,138%	0,811%	3,00%	15,33%
			10<V ⩽ 30	0,002%	0,005%	0,005%	0,220%	0,232%			
			V>30	0,001%	0,004%	0,004%	0,432%	0,442%			
		5-7	V ⩽ 10	0,002%	0,006%	0,007%	0,067%	0,082%	0,734%		
			10<V ⩽ 30	0,005%	0,016%	0,017%	0,167%	0,205%			
			V>30	0,006%	0,016%	0,018%	0,408%	0,447%			
		8-10	V ⩽ 10	0,006%	0,018%	0,020%	0,131%	0,177%	1,456%		
			10<V ⩽ 30	0,014%	0,039%	0,043%	0,279%	0,376%			
			V>30	0,016%	0,047%	0,052%	0,788%	0,904%			
	40<S⩽70	1-4	V ⩽ 10	0,001%	0,004%	0,004%	0,215%	0,225%	0,669%	6,20%	
			10<V ⩽ 30	0,002%	0,007%	0,007%	0,347%	0,363%			
			V>30	0,002%	0,006%	0,006%	0,068%	0,081%			
		5-7	V ⩽ 10	0,000%	0,001%	0,001%	0,225%	0,227%	1,639%		
			10<V ⩽ 30	0,001%	0,002%	0,002%	0,524%	0,529%			
			V>30	0,001%	0,002%	0,003%	0,877%	0,883%			
		8-10	V ⩽ 10	0,018%	0,052%	0,058%	0,396%	0,525%	3,887%		
			10<V ⩽ 30	0,039%	0,111%	0,123%	0,836%	1,109%			
			V>30	0,047%	0,134%	0,148%	1,925%	2,253%			
	S>70	1-4	V ⩽ 10	0,000%	0,000%	0,000%	0,036%	0,036%	0,218%	6,13%	
			10<V ⩽ 30	0,000%	0,000%	0,000%	0,160%	0,160%			
			V>30	0,000%	0,000%	0,000%	0,022%	0,022%			
		5-7	V ⩽ 10	0,003%	0,008%	0,009%	0,151%	0,170%	1,089%		
			10<V ⩽ 30	0,007%	0,020%	0,022%	0,353%	0,402%			
			V>30	0,007%	0,021%	0,023%	0,467%	0,518%			
		8-10	V ⩽ 10	0,017%	0,048%	0,052%	0,507%	0,623%	4,828%		
			10<V ⩽ 30	0,035%	0,101%	0,112%	1,071%	1,319%			
			V>30	0,042%	0,122%	0,134%	2,587%	2,886%			

All in all, the main outcomes of this characterisation stage include a matrix containing the percentages in which residential buildings belong to a certain archetype and are located in a certain subregion (as in Tab. 4.6) along with the archetypes dependant characteristics (*stockDistribution.csv* in Appendix D). Also, the probabilities for a building in a given subregion to be located on each

department (*geoDistribution.csv* in App. D) as well as the departments characteristics regarding shading, neighbours, orientation, etc. (*departmentsProp.csv* in App. D). Not only will *stockDistribution.csv* play a key role during the simulation indicating the amount of cases to run for each archetype and subregion but also all these outcomes will be the main inputs for the models generation process. Finally, there is another matrix (*totalOccupied.csv* in App. D) where, based on the percentages from *stockDistribution.csv*, the total amount of residential buildings for each archetype and subregion are established. This matrix will be used for extrapolating the obtained results to the whole Uruguayan residential sector.

4.2.2 Definition of simulation hypotheses

After having characterised the whole residential sector, there are still some parameters to be defined before stepping into the simulation process. The reason behind this is that when generating the model for each building, there is more information to define other than its geometry, orientation, materials and construction characteristics. This extra information involves the definition of thermal comfort, occupancy, lighting and equipment schedules and thermal loads, occupants behaviours and weather information.

Integrating a thermal comfort model to the simulation is important as it sets the ground for evaluating and comparing buildings in terms of thermal performance. For the case of non-conditioned buildings, the analysis is usually performed based on the time not meeting the thermal comfort criteria, whereas for conditioned buildings it is done according to the energy consumed in achieving thermal comfort. Also, these parameters are useful so as to evaluate retrofits in terms of whether they reduced those unmet hours or energy consumption. In this work, the thermal comfort model considered was the ASHRAE 55 adaptive model [36], which is already integrated in EnergyPlus. Being an adaptive model implies that it relates indoor acceptable temperature ranges to outside meteorological parameters based on the idea that humans can adapt to different conditions during different times of the year.

As established in ASHRAE 55, the comfort temperature for each day is defined for the zone operative temperature which is the average of the indoor air temperature and the mean radiant temperature of the zone interior surfaces, and is calculated as shown in Equation 4.1. EnergyPlus calculates this

daily comfort temperature and determines whether the zone is within the comfort limits criteria. In this thesis, the comfort criteria considered is the 80% acceptability defined in ASHRAE 55 and its limits are $T_{confort} \pm 3.5°C$.

$$T_{ot} = 0.31 T_{pma,out} + 17.8 \tag{4.1}$$

T_{ot} in Eq. 3.2 refers to the zone operative temperature, $T_{pma,out}$ is the prevailing mean outdoor air temperature and is calculated as an exponentially weighted, running mean of a sequence of daily outdoor temperatures prior to the day in question. Its calculation is shown in Equation 4.2.

$$\begin{aligned} T_{pma,out} &= (1-\alpha)(T_{e,d-1} + \alpha T_{e,d-2} + \alpha^2 T_{e,d-3} + ...) \\ &= (1-\alpha) T_{e,d-1} + \alpha T_{pma,out,d-1} \end{aligned} \tag{4.2}$$

In Eq. 3.3 α is a constant between 0 and 1 which controls the speed at which the running mean responds to changes in weather (EnergyPlus uses $\alpha = 29/30$). $T_{e,d-1}$ represents the mean daily outdoor temperature of the day before the day in question, $T_{e,d-2}$ is the mean daily outdoor temperature of the day before that and so on. $T_{pma,out,d-1}$, on the other hand, is the prevailing mean outdoor air temperature of the day before the day in question.

For the software to solve the zones energy balance equations, information regarding all internal thermal loads should also be provided. For the occupancy, both metabolic rates and radiant fraction were determined for each occupied zone according to NBR 15575 [37], and the same was done for lighting and equipment loads (and radiant and visible fractions). All these internal gains are shown in Table 4.7. The occupancy, lighting and equipment schedules were also established as suggested in NBR 15575 [37] and are presented in Table 4.8.

Table 4.7: Internal gains.

Zone	**Occupants**		**Lighting**			**Equipment**	
	Metabolic rate (W)	Radiant fraction	Power (W/m^2)	Radiant fraction	Visible fraction	Power (W)	Radiant fraction
Bedrooms	81	0.30	5	0.32	0.23	-	-
Living room	108	0.30	5	0.32	0.23	120	0.30

As it can be noted, the only occupied areas are the living room and the bedrooms, and the household total amount of inhabitants depends on the

Table 4.8: Schedules.

Occupancy			
Bedrooms		Living room	
00-08	100%	00-14	0%
08-22	0%	14-18	50%
22-00	100%	18-22	100%
		22-00	0%

Lighting			
Bedrooms		Living room	
00-06	0%	00-16	0%
06-08	100%	16-22	100%
08-22	0%	22-00	0%
22-00	100%		

Equipment	
Living room	
00-14	0%
14-22	100%
22-00	0%

archetype as shown in Tab.4.4. Then, all the occupants use the living room according to the schedule of Tab.4.8 whereas the bedrooms are only occupied by some of the inhabitants. The criteria used in this regard is that there would be two occupants using the largest bedroom and the rest would be distributed in the remaining ones.

Weather files are also required inputs for EnergyPlus simulations. Their determination was also part of the work done in FSE_1_2017_1_144779 [4] and it implied deciding which of the available EnergyPlus weather files (EPW) would better represent local climate in each of the 19 Uruguayan departments. EPWs generated by Lawrie and Crawley [34] based on the Typical Meteorological Year (TMY) developed by Alonso-Suárez et al. [35] were selected as they have proven to be the most reliable from those EPWs available for Uruguay. However, and acknowledging that wind speed and direction may play an important role in the infiltration and ventilation loads, the EPWs wind data was replaced with UTE measured data for the same locations (UTE data series are also presented in [35]). This course of action was taken because UTE data series proved to be more consistent and representative of the Uruguayan wind map. Besides, and also during the course of the project FSE_1_2017_1_144779 [4], wind speeds were affected by a shelter factor of 0.5 due to the fact that the majority of the households are located in cities and in order to take into account the effect of surroundings in the wind speeds. However, during the analyses of Chapter 3, an error in the weather files was identified -and corrected- as there was a mismatch between the TMY and the EPWs timestamps (see Appendix C for further information regarding this error and the workaround followed).

The issue is that there are only five weather files based on the TMY which are for the departments of Colonia, Montevideo, Rivera, Rocha and Salto. For the rest of the departments, one of the five was assigned according to which better represents its local climate. This resulted in the distribution presented in Table 4.9.

Table 4.9: Weather file assignment.

Department	Subregion	Weather file
Artigas	N-NW	Salto
Paysandú	N-NW	Salto
Salto	N-NW	Salto
Colonia	SW-Center-NE	Colonia
Cerro Largo	SW-Center-NE	Colonia
Durazno	SW-Center-NE	Colonia
Flores	SW-Center-NE	Colonia
Florida	SW-Center-NE	Montevideo
Río Negro	SW-Center-NE	Colonia
Rivera	SW-Center-NE	Rivera
San José	SW-Center-NE	Montevideo
Soriano	SW-Center-NE	Colonia
Tacuarembó	SW-Center-NE	Rivera
Canelones	S-SE	Montevideo
Lavalleja	S-SE	Rocha
Maldonado	S-SE	Rocha
Rocha	S-SE	Rocha
Treinta y Tres	S-SE	Montevideo
Montevideo	MVD	Montevideo

One final aspect that has a relevant impact on the results is occupants behaviour. Not only does it affect energy requirements significantly but it also is the leading source of uncertainty in building energy use predictions according to Yan et al. [52]. Nevertheless, the job of accurately modelling occupants behaviours in Uruguayan households would imply a full study on its own, specially given the lack of data from surveys or interviews. Because of this, and in spite of its relevance, in the present work the modelling of occupants behaviour was narrowed down to a simplified representation that still allows analysing occupants impact on building performance.

To this end, two types of occupant were defined. The first consists of a user whose actions are all oriented towards efficiency in terms of energy consumption. While, on the other hand, the second one is the worst-case occupant scenario, whose behaviour has no regard for energy efficiency. This approach offers a means of considering occupants impact and also of determining the range in which real consumptions should be. As usage patterns for lighting and electric equipments were defined without user dependency, in this work user behaviour includes occupants interactions with operable windows and so-

lar protections. Whereas the efficient occupant takes advantage of natural ventilation and solar protections in order to achieve thermal comfort, the inefficient one does not.

4.2.3 Automation

The intention was to simulate as many households models as possible on the grounds that the quantity of archetypes modelled for each geographic region and the amount of variations considered within each archetype plays a major role in the accuracy of the housing stock characterisation; which is essential for the results to be representative. Therefore, efforts in generating a model as accurate as possible resulted in the need to run a rather big number of simulations, which set the path for automation as the final stage in the model development.

In this regard, Python scripts were developed so as to manage the large number of simulations. Also, Eppy scripting library [26], based on Python and with the capability to manipulate EnergyPlus files, was used to generate and run the buildings models. Eppy has been released under an open source license and it is a scripting language developed specifically for EnergyPlus input and output files. It allows the user to make a large number of changes in multiple EnergyPlus input data files (IDFs), as well as read data from the output files generated during a simulation. Consequently, results were also automatically processed using Eppy and Python itself.

This approach can be followed not only to build an UBEM as in [46], [47] and this work, but also to achieve other goals. For example, Bui et al. [53] also used Python and EnergyPlus -through Eppy- so as to develop an automated optimization process. Their aim was to enhance energy efficiency of two specific buildings by determining the optimal design of their facades. On the other hand, Glazer and Gard [54] used the same approach but with the objective of assessing the impact of applying some energy efficiency measures to different commercial building models.

In this work, a simulation platform was developed consisting of a sequence of Python functions, some of which interact with EnergyPlus through Eppy. The platform carries out the whole simulation process based on user defined parameters along with the housing stock characterisation outputs and the hypotheses detailed above. As the platform development and its capabilities are

some of the main focus of this work regarding the Uruguayan residential sector modelling, a rather detailed description is provided in the following sections. This includes the platform requested inputs, the simulation workflow and the resulting outputs.

Inputs

There is certain information the platform needs in order to proceed with the simulation process. Some of it is provided by the user when executing, whereas some other must be available in a certain directory established in the script. This distinction is done taking into consideration that there are some parameters the user can set when running the model depending on the simulation objectives, and that changing these parameters does not require knowing the model structure nor understanding the code. Contrarily, there is some information which has to do with the model structure, and that changes in this type of inputs require a deep understanding of the model as might imply changing or adding code.

When using the platform the user must establish the amount of models to simulate and among which archetypes and subregions. This provides the flexibility to analyse only a given type of building or desired deciles in certain locations. The user should also set for which type of occupant the simulations would be performed (could be one of the two defined or for both), and whether the analysis would be on conditioned or unconditioned buildings (it could also be for both). Then, the amount of models the user intends to simulate for each occupant and HVAC condition (Nc) multiplied by the number of occupant types (1 or 2) and by the number of scenarios regarding the presence of space conditioning (also 1 or 2) determines the total amount of simulations to be executed.

Then, among the information that has to do with the model structure and which should be locally available on certain directories, there are the results of the housing stock characterisation stage as well as some of the definitions commented in Section 4.2.2. Specifically, there is *stockDistribution.csv* containing the percentages in which the housing stock is distributed among the archetypes and subregions defined, along with the archetypes characteristics regarding constructions, amount of residents and possible geometries. Also, there are *geoDistribution.csv* and *departmentsProp.csv* which contain the probabilities

of a building in a given climate zone to be in one of the departments within the climate zone and the departments characteristics, respectively. All *stockDistribution.csv*, *geoDistribution.csv* and *departmentsProp.csv* can be found in App. D along with a more detailed explanation of their structure.

Besides, there are the five EPW files selected to represent the departments climate and an IDF file (*Template.idf*) containing definitions and general information such as simulation parameters, construction materials, construction definitions, schedules and output variables. Finally, there are the 32 geometries used to represent the whole residential sector (*geomXX.idf*). The EPW files, *Template.idf* and the 32 IDFs containing the different geometries can also be found in App. D.

Simulation workflow

The aim of this section is to provide an overall understanding of the steps followed in order to address the goal of modelling Uruguayan housing stock and assessing its thermal energy demand. In order to do so, the whole simulation workflow is described in terms of its main functions and logic sequence.

The workflow methodology distinguished between five steps: defining simulation parameters, model characterisation, model generation, model simulation and results processing. The first is carried out once at the beginning of the simulation, whereas the other four are executed as many times as the number of simulations to be run. In Figure 4.2 there is the general automation workflow with the most relevant functions; each of which approaches one of the five steps mentioned.

Manager is the main and most general function of the platform and it is the one executed by the user. It holds the input parameters established by the user before each simulation and also some others containing files paths and model definitions which should only be modified under certain structural changes. The purpose of this function is to determine simulation parameters according to the inputs set by the user. By doing so it completes the first step of the simulation workflow methodology which is the simulation definition.

In Table 4.10 the user defined variables that describe each simulation are listed. On the other hand, those variables which should only be modified under certain structural changes are: input files paths, lists of all possible occupant

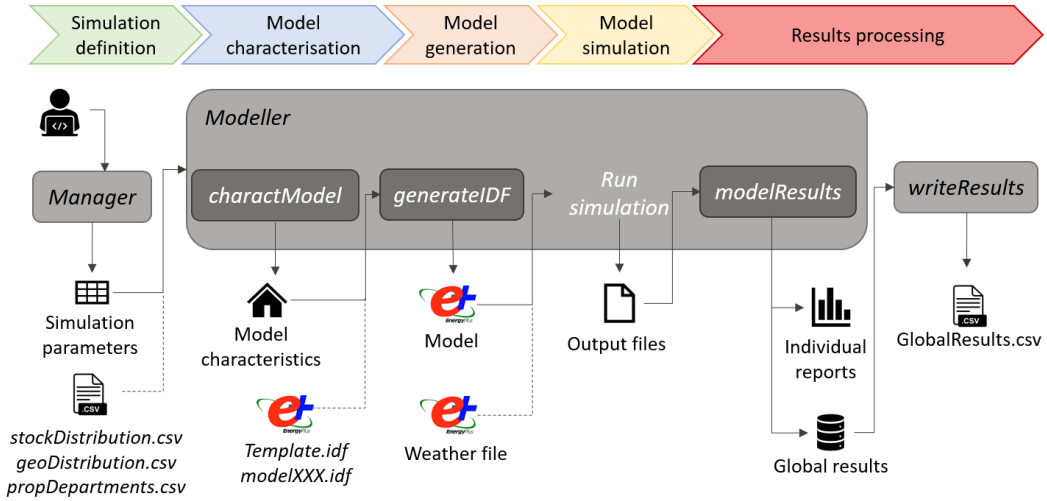

Figure 4.2: Simulation workflow.

types, space heating scenarios, subregions and archetypes and also a list of all the results to extract from each simulation.

Table 4.10: User defined variables.

Variable name	Description
Nc	Amount of models to simulate for each space conditioning scenario and each type of occupant.
users	List detailing the type of occupants for which to perform the simulations.
hvacs	List containing the space conditioning scenarios for which to perform the simulations (either with or without space conditioning, or both).
archetypes	List containing the archetypes for which to perform the simulations.
locations	List containing the subregions for which to perform the simulations.
indivReports	Establishes whether the results processing should be done both for each case and for the global simulation or only for the global simulation.

The next function is *Modeller*, which is called from *Manager*, and is the one which manages the total amount of simulations determined in its predecessor. Its inputs are all those parameters settled in *Manager* and needed to define the simulation. The objective of this function is to establish the task sequence for each case scenario and conduct the whole model characterisation, generation, simulation and results extraction processes.

This function logic sequence can be summarized as follows: for each subregion and for each archetype the function calls *charactModel*, which determines the model characteristics. Then, for each occupant type and space conditioning scenario, the *generateIDF* function is called and the EnergyPlus model is generated. The next step is to run the model simulation and process its results by calling the *modelResults* function. Finally, results are stored to be used afterwards to generate global reports.

Therefore, for each archetype and subregion *charactModel* is called to accomplish the task of model characterisation. This includes not only collecting all the characteristics for the given archetype but also considering its possible variations such as geometry and departments dependent characteristics (such as possible orientations, surroundings, number of attached facades, etc.). The amount of variations considered impacts on the accuracy of the archetype representation. However, the bigger the amount of variations the bigger the amount of models that should be generated and simulated and, consequently, the longer the time required. So, as a compromise between accuracy and computational cost, the amount of variations considered for a given archetype and subregion is determined distributing the total amount of models the user intends to simulate (Nc) into the archetypes and locations according to the percentages established in *stockDistribution.csv*. By doing so, the most prevalent archetype and subregion combinations are the ones for which more variations are considered resulting in a better representation of those cases of which results will have a greater impact.

Thus, for a given Nc, the function calculates from *stockDistribution.csv* the number of simulations to perform for each archetype in each subregion. For example, the archetype representing houses, between 40 and 70 m^2, more than 30 years old and deciles 1-4 in S-SE corresponds to 1.54% in Tab. 4.6. Therefore, for Nc=500, 8 models would be simulated for this archetype in this subregion. Then, the archetype characteristics that are the same for all the variations including constructions, amount of occupants, etc. are extracted from the same table *stockDistribution.csv*. Also all the possible geometries, from which the function then assigns one to each of the variations (8 in the example case). Then, a department is randomly designated to each variation based on the probabilities defined in *geoDistribution.csv* (and shown in Tab.4.5) for the given subregion. For the example archetype (which is located in the S-SE region), each of the 8 models to generate (considering Nc=500) has

a probability of 59% of being in Canelones, 20% in Maldonado, 9% in Rocha, 7% in Lavalleja and 6% in Treinta y Tres (see Tab.4.5). Using a random function and considering these probabilities a department is assigned to each one of the 8 models to generate for the given archetype in the given region. Finally, the characteristics dependant on the department are randomly defined for each variation according to the designated department and the probabilities established in *departmentsProp.csv*.

Hence, the outputs of *charactModel* are the number of models to generate for each archetype and subregion along with all their characteristics. This information completes the model characterisation step and gives way to the model generation one, carried out by *generateIDF*. This function generates an IDF for each one of the models to simulate based on the previously defined characteristics. The inputs requested to accomplish this task are the models characteristics, the corresponding geometry file (*geomXX.idf*) and the *Template.idf* from which objects containing general information are extracted.

The next step in the sequence is model simulation and it is carried out from *Modeller* itself, using the EnergyPlus model generated in *generateIDF*, and the corresponding weather file. Once the simulation is finished, *modelResults* processes each model results and elaborates individual reports and also stores averaged results for each archetype and subregion. Finally, *writeResults* generates a csv file with global results.

Outputs

Being the outcomes of the simulation process, the generated IDF along with its individual reports are stored after each model simulation. The IDF file holds all the information regarding the case: geometry, materials, constructions, schedules, internal loads, HVAC system if present, output variables, among others; and it could be run manually as a regular IDF file if desired. Besides, the individual reports are graphs in which relevant results for each case are shown and they are generated only if requested. The purpose of these reports is to allow the user to study any case individually and analyse the relative contribution of each term in the heat balance equation.

The graphs with the individual results, include all the results introduced in Chapter 2. Among them there are the heat losses and gains through building enclosure, windows and also those due to infiltration and ventilation. More-

over, monthly temperatures for each zone in the building are shown, as well as the monthly heating and cooling thermal requirements for the space conditioned models. Regarding the heat exchange through the building enclosure, it is disaggregated into floor, roofs and walls and, for the case of heat gains, solar radiation is distinguished from other type of gains. Windows on the other hand are divided according to their orientation and, for analysing heat exchanges through them, transmitted solar radiation is distinguished from other gains.

Besides, a text file for each case is also generated. In there, the main characteristics of the model are summarized so as the user can more easily analyse the results. These characteristics include: type (house or apartment), storey (if applicable), size, decile and vintage categories, subregion, department, geometry name out of the 32 possibles, type of occupant out of the two possibles, presence of HVAC system, presence of trees or buildings shading, quantity of attached facades and building orientation. There is also some geometric information such as enclosure area, amount of different thermal zones in the model and windows areas grouped by their orientation.

Finally, there is *GlobalResults.csv* containing global annual results for each type of occupant and each space conditioning scenario. These results are grouped and averaged according to archetype and subregion. They include all those results identified as relevant and described in Chapter 2. Besides, characteristics such as mean transmittance, attached percentage, glazed area, glazed area percentage, occupied area, etc. are also averaged for each archetype and subregion and included in *GlobalResults.csv* as they might be helpful for understanding the results. Then, by knowing the total amount of buildings in each archetype and subregion combination (from *totalOccupied.csv*), results for the whole residential sector can be determined for each type of occupant and each space conditioning scenario.

This file thus contains the information needed in order to determine energy requirements for space conditioning in Uruguayan residential sector for the two types of occupants defined. Furthermore, this assessment could be done distinguishing geographic locations, deciles or buildings characteristics such as type, size or vintage. This allows identifying major areas of improvements and also adopting different strategies for different households.

4.3 Results

A simulation was performed for 496 models among all archetypes and subregions, considering space conditioned buildings and for both user types defined. This resulted in a total amount of 992 simulations, which ran locally on a personal computer with an Intel Core i3 processor and 8 GB RAM. The whole simulation process took 36 hours and 48 minutes.

In this section, some relevant results will be reported so as to finally analyse energy requirements for thermal conditioning in Uruguayan residential sector and, at the same time, show the capabilities of the platform developed. These results are the simulation global results which are read from *GlobalResults.csv*, the output file described in the previous section and accessible in App. D. As mentioned, for each household model simulated there are also some individual results, some of which can also be found in App. D. All these results are highly dependent on the outcomes of the housing stock characterisation stage and the hypotheses considered, as they are the main inputs of the whole simulation process. It is therefore important to consider these aspects when analysing the results.

As mentioned in Chapter 2, and due to the HVAC model used, the obtained HVAC loads actually represent thermal requirements for maintaining thermal comfort in the occupied zones. Besides, and even though the thermal requirements determined are for the whole year, when heat gains and losses through different components are analysed, it is done for cooling and heating periods. These are from the 1st of December to the 28th of February and from the 1st of June to the 31th of August, respectively; as is during those months when the majority of thermal energy is demanded in every archetype.

First of all, an analysis is performed so as to test the results convergence for the number of models simulated. Then, global results are shown aggregated for the whole country and also grouped according to relevant buildings characteristics or geographic subregions. Both of these studies were done considering an efficient occupant. Finally, the impact of the occupant behaviour is discussed by comparing results for the two types defined.

4.3.1 Convergence analysis

As mentioned in Section 4.2.3, the platform developed allows the users to set the amount of simulations they intend to run for each type of occupant

and each HVAC configuration. This number of simulations would impact in the archetypes modelled for each region, and also in the number of models simulated within each archetype and subregion considering the variability in orientation, surroundings and geometries; both of which are determined according to the proportions of *stockDistribution.csv* (see App. D) shown in Tab. 4.6. This is, once the user has established the number of simulations to perform, the tool determines the amount of models to generate and simulate for each archetype and subregion according to the percentages shown in Tab. 4.6. Depending on the number of simulations and those percentages, a given archetype and subregion combination may not be modelled at all or may be modelled several times considering different orientations, surroundings scenario and geometries.

Given that the global results are determined extrapolating the obtained results to the whole housing stock, the archetypes modelled for each region and the different configurations considered within each archetype and region should be as many as possible for the global results to be representative. Hence, and first of all, the results convergence should be tested so as to determine whether the amount of simulations performed was enough to represent the housing stock as it was characterised in this work.

With the objective of assessing the global results convergence, simulations were performed only for the efficient occupant and number of simulations (N) of 6, 38, 87, 192, 295, 496 and 992[1]. Besides, and given that some characteristics of the models are determined according to probabilities (the geometry, the department and, as a consequence, the corresponding weather file, the orientation, surroundings scenario, etc.), each simulation was performed three times to have an idea of the dispersion of the results.

Resulting total annual thermal requirements extrapolated to the whole housing stock according to the characterisation used in this work are shown in Figure 4.3 as a function of N. On the other hand, the same results but disaggregated into cooling and heating requirements are shown in Figure 4.4.

The three graph patterns show that low N values overestimated the results, and that from N=192 onwards, the results seem to have converged. Regarding the dispersion, the results suggest that the highest the N, the lower the

[1]With the objective of them taking less time, these simulations were performed only for the efficient occupant and without processing individual results.

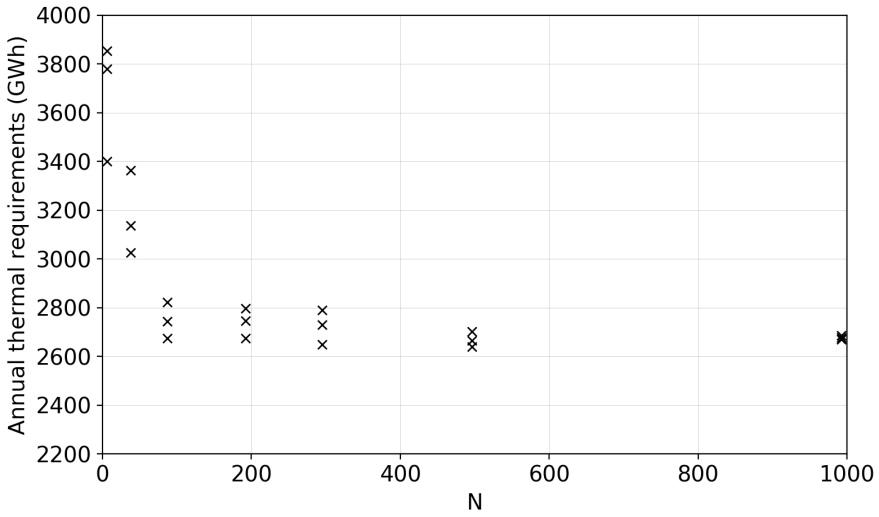

Figure 4.3: Global annual thermal requirements convergence with N for an efficient occupant.

dispersion. Nevertheless, more simulations for each N should be performed if aiming at a proper study of the results dispersion.

Given that all the results with N=496 differ from those with N=992 in less than 1.2% for total requirements, 0.8% for cooling requirements and 2.2% for heating requirements (all expressed relative to the average results of the three simulations performed for N=992); global results analyses will be performed for a simulation with N=496. This is on the grounds that the accuracy gained from N=496 to N=992 is not worthy of the extra computational effort required for simulating both types of occupants with N=992, which is double of that for N=496.

4.3.2 Global results for efficient occupants

Assuming efficiency-oriented occupants for the whole housing stock, the obtained annual thermal requirements of the Uruguayan residential sector are those shown in Table 4.11.

Table 4.11: Annual thermal requirements.

Cooling (GWh)	Heating (GWh)	Total (GWh)
1296	1345	2641

Given that these results represent thermal requirements and not energy demand, to determine whether they are close to reality would be a quite chal-

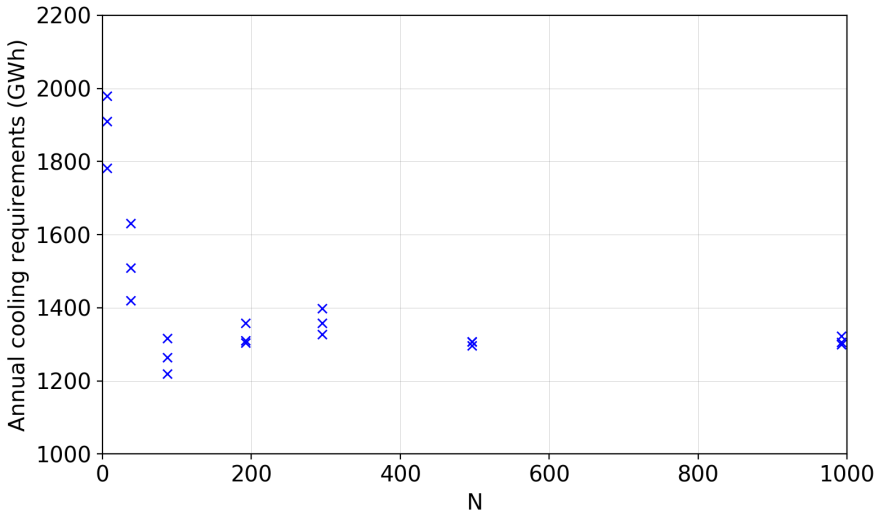

(a) Cooling.

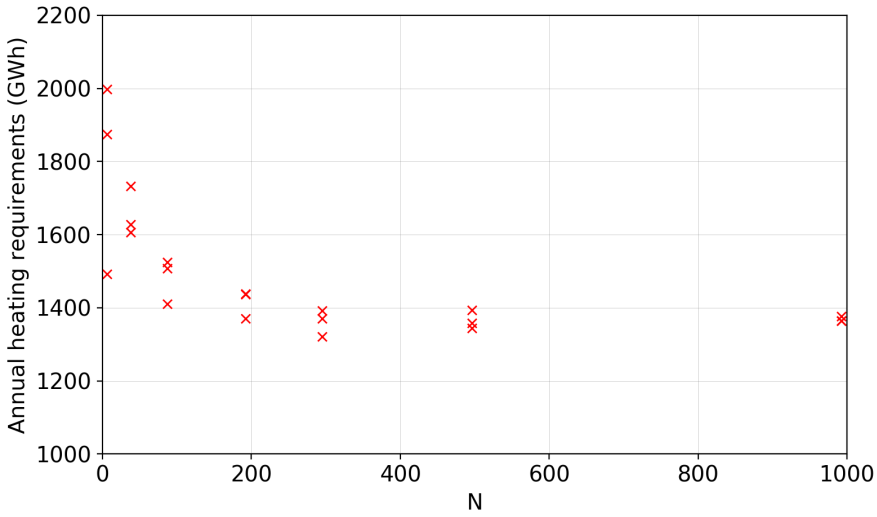

(b) Heating.

Figure 4.4: Global annual cooling and heating requirements convergence with N for an efficient occupant.

lenging task, and certainly an unfeasible one with the available data. Yet, in order to check their order of magnitude, the preliminary data from the Balance Energético Nacional (BEN) of 2019 [3] was used. There, it is established that the wood and coal used in the residential sector was of 3328GWh. Assuming a 30% efficiency in their conversion to useful energy (which is a reasonable efficiency for a traditional open fireplace), this wood and coal consumption results in 998GWh of useful energy.

On the other hand, in the Encuesta Continua de Hogares (ECH) of 2019 [55] it says that 90% of Uruguayan households use heating systems and that 43% use air conditioners. There is thus a 47% of households that use other heating systems. Assuming all these use wood, and that all wood and coal is consumed with heating purposes (note that neither of these hypotheses is completely realistic as there are gas heating systems and also not all the wood and nearly none of the coal in Uruguay is used for heating), would result in a heating thermal demand of $998/0.47 = 2123$GWh. Acknowledging that this value is a rough approximation due to the suppositions considered, and that the heating loads of Tab. 4.11 are for ideal occupants whose requirements are according to adaptive comfort and who make an ideal use of the openings and solar protections, the results seem reasonable.

So the results presented in Tab.4.11 are the Uruguayan residential sector requirements based on the housing stock characterisation and the hypotheses presented in Section 4.2. Though heating loads are a little higher than cooling ones, they are both very similar, at least for the whole country. Differences among regions and deciles would be analysed afterwards.

Remembering that in this work thermal requirements were only taken into account in the occupied areas (and only during the occupied hours), these whole country results could also be expressed relative to the households occupied area. Besides, and given that houses and apartments usually perform very differently, the results are also presented distinguishing between them both as shown in Table 4.12.

Table 4.12: Annual thermal requirements relative to occupied area.

Type	**Cooling (kWh/m^2)**	**Heating (kWh/m^2)**	**Total (kWh/m^2)**	$\mathbf{A_{occup}/A_{tot}}$ (%)
House	32.6	33.4	66.0	73.2
Apartment	20.5	14.2	34.7	64.7
Total	30.9	30.6	61.5	71.9

From Tab.4.12 it can be noted that apartments perform much better than houses since their requirements are nearly half. Despite apartments requiring less energy both for heating and cooling, the difference is more drastic in the former, as their heating demand is a 43% of that in houses. Another difference between the two types of household is the size of the occupied area relative to the total; which is larger in houses. This difference can be understood

when analysing how the deciles ranks considered are distributed among these types of household (see Figure 4.5). Knowing that households sizes are equally distributed among the two types (20% less than 40m^2, 40% between 40m^2 and 70m^2, 40% more than 70m^2) and considering the differences in number of inhabitants for the different deciles (Tab.4.4), it is clear that the apartments would have, in average, less occupants. Given that the bedrooms are occupied or not depending on the amount of occupants, it results in the apartments having less occupied area than the houses.

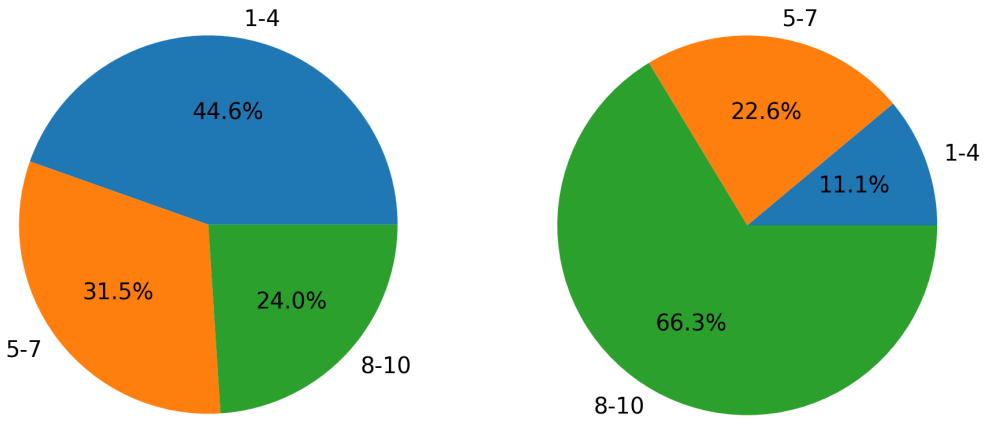

(a) Houses. **(b)** Apartments.

Figure 4.5: Deciles distribution among type of household.

Therefore, if the results were to be presented as the average thermal energy required per household (not relative to the occupied area), the differences in houses and apartments thermal performances would be even larger. However, if results were to be analysed relative to the number of occupants -which would represent the amount of energy each person needs to be comfortable- the differences would be smaller (see Table 4.13). Yet, in any case, apartments still have lower requirements .

Table 4.13: Annual thermal requirements relative to amount of occupants.

Type	Cooling (kWh/person)	Heating (kWh/person)	Total (kWh/person)	Occupants
House	380.0	493.2	873.3	3.2
Apartment	361.7	261.4	623.1	2.3
Total	377.4	459.8	837.2	3.1

Apartments performing better than houses is mainly due to the difference in the percentage of exposed area. Whereas in houses it is 87% on average,

in apartments is 32%. Besides, and based on the impact decile ranks have on constructions qualities, the deciles prevalence in each type of household also contributes to apartments requiring less thermal energy than houses.

One final aspect of these global results is that both in Tab. 4.12 and 4.13, the total requirements are very similar to those in houses. This is due to the fact that the houses share in the Uruguayan housing stock is 85%, meaning that there are nearly 6 houses for every apartment.

These results could also be analysed disaggregated by some of the households relevant characteristics. By doing so, a more profound understanding of the energy use patterns could be achieved. This understanding is relevant as it allows the design of targeted energy policies and building retrofit measures. Either of which will result in more effective and efficient actions towards increasing energy efficiency in Uruguayan residential sector.

Disaggregated by regions

The obtained results were first disaggregated by the defined subregions and are presented in Figure 4.6. There, it can be noted that MVD holds the bigger share of residential buildings and, consequently, of the energy requirements. Then there are S-SE and SW-Center-NE with similar shares of both and, finally, N-NW with the lowest shares of both number of households and energy requirements. However, whereas for MVD and S-SE thermal requirements share is lower than their housing stock share, the opposite is true for N-NW and SW-Center-NE (see Fig. 4.6a). This can be explained by observing Fig. 4.6b, where the energy demands relative to the occupied area are presented. In this case, the results relative to the amount of occupants would hold the same differences between the subregions given that household sizes and deciles are equally distributed among the subregions.

From Fig. 4.6b, it can be observed that MVD and S-SE total demand is less than 60kWh/m^2 whereas N-NW is around 80kWh/m^2 and SW-Center-NE is nearly 70kWh/m^2. For the case of N-NW, the difference is due to the cooling requirements which are double than in the other regions. SW-Center-NE on the other hand has both higher cooling and heating requirements than MVD and S-SE; yet the differences are much more subtle than those for N-NW.

Heating and cooling loads of Fig. 4.6b are in accordance with the differences in mean temperatures of Table 4.14 and also with Uruguay's solar and

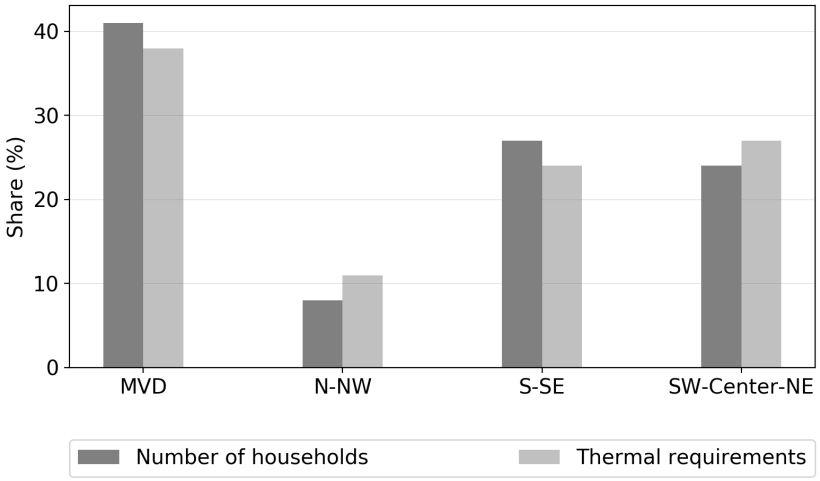

(a) Shares of stock and requirements in subregions.

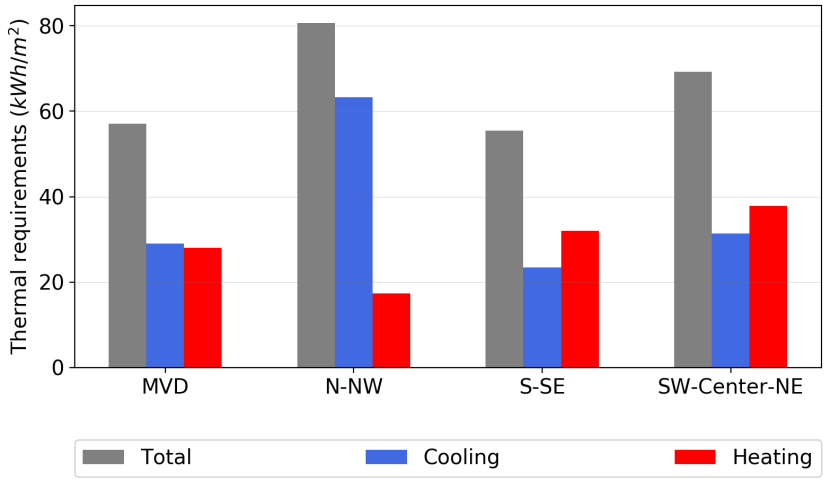

(b) Heating and cooling requirements in subregions.

Figure 4.6: Requirements disaggregated by subregions.

wind maps of Figure 4.7. Mean temperatures for each subregion were determined based on the EPWs used in this work. Note that SW-Center-NE region has the biggest temperature amplitude as there is the second highest average temperature during cooling season and the lowest during heating season. This explains why both heating and cooling requirements are higher, than for example MVD, in this subregion.

The fact that 88% of Uruguayan apartments are located in Montevideo, entails that while apartments share in MVD is 33%, in the rest of the subregions is 3.3%. As apartments perform better than houses regarding thermal requirements, this fact may be one of the reasons why MVD requirements are lower

Table 4.14: Subregions mean temperatures.

	Mean temperature (ºC)			
	MVD	**N-NW**	**S-SE**	**SW-Center-NE**
Cooling period	21.7	25.4	21.5	23.1
Heating period	10.8	13.7	11.0	10.7

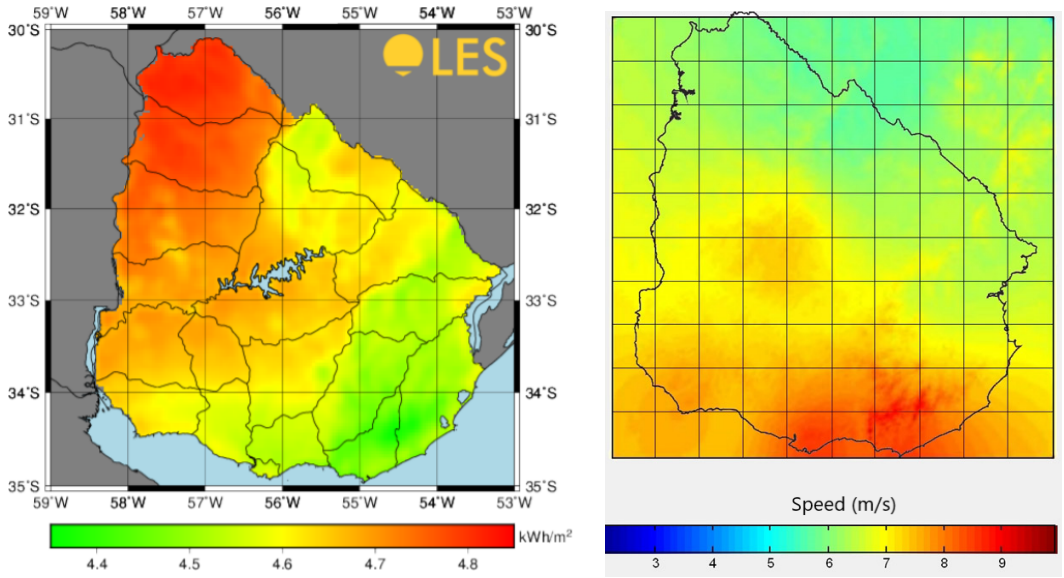

(a) Global horizontal irradiance (GHI)[56]. **(b)** Wind speed [57].

Figure 4.7: Solar and wind maps.

than those in N-NW and SW-Center-NE. More precisely, if only houses were to be considered, MVD total thermal requirements would grow from 57.1kWh/m^2 to 68.4 kWh/m^2. Hence, even only considering houses, MVD would still have lower demand than N-NW and SW-Center-NE (though very close to the later) but higher than S-SE.

In order to compare the differences in subregions and at the same time identify major drivers of thermal requirements, the heat gains and losses through different components during cooling and heating periods are presented in Figure 4.8 for MVD and N-NW subregions. These two subregions were chosen to be compared as they have very different requirements both during cooling and heating periods. Besides, due to the differences in houses and apartments performances, and with the aim of this comparison to be focused on the subregions characteristics, only houses were considered.

The categories in which energy gains and losses were distinguished in Fig. 4.8 are "Enclosure" which includes the heat transferred through walls,

roof and floor; "Windows" where there is both transmitted solar radiation and glazing and frame net heat exchange, "I&V" where there are the infiltration and ventilation loads and "Other" which includes the internal gains due to the occupants metabolic rate and lighting and equipment radiant fractions. Besides, the "Enclosure" category could then be disaggregated into "Walls", "Roof" and "Floor" which can in turn distinguish -for the walls and the roof- between solar gains and others such as long wave radiation exchange and convection. The "Windows" category on the other hand, can also be divided so as to quantify transmitted solar radiation and net heat exchange through the glazing and through frame and dividers separately.

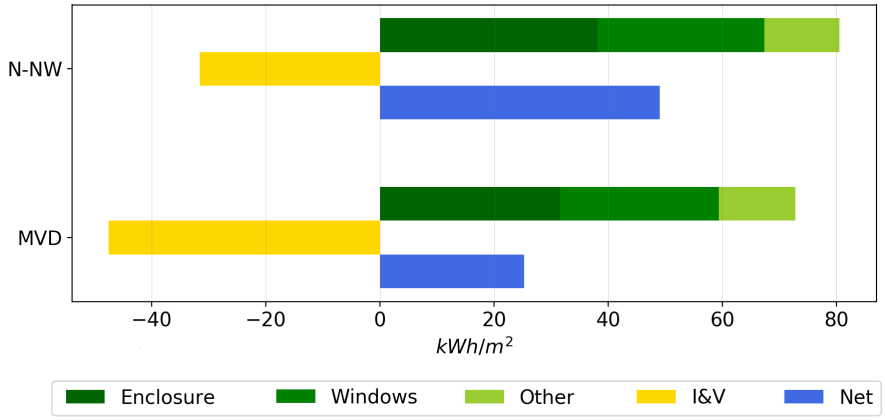

(a) Cooling period.

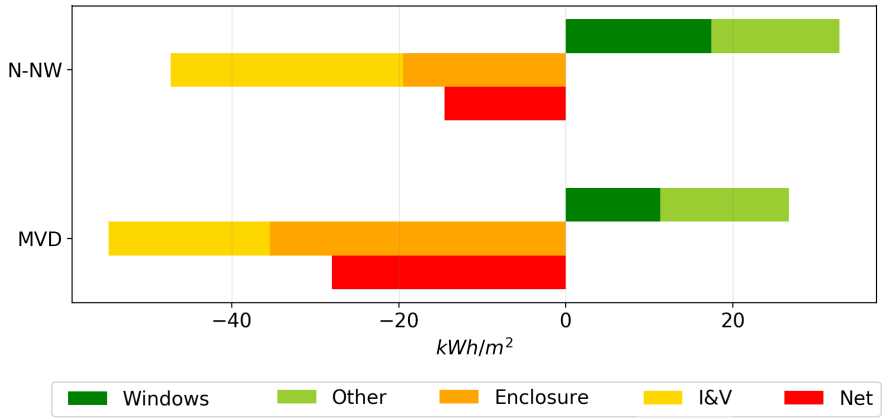

(b) Heating period.

Figure 4.8: Thermal energy gains and losses.

The higher N-NW requirements during cooling period are explained both by higher gains as well as lower losses as shown in Fig. 4.8a. The same happens for

MVD during heating period as there are higher losses and lower gains than in N-NW, which explain the more elevated heating requirements in this subregion. These differences are also related to the subregions mean temperatures, GHI and wind speeds (see Tab. 4.14 and Figs. 4.7a and 4.7b). The N-NW higher irradiance and temperatures result in bigger gains than in MVD, whereas MVD more elevated wind speeds induce higher infiltration and ventilation losses.

Focusing on cooling period, enclosure net gains are the highest for both subregions and are of 38 kWh/m^2 in N-NW against 32 kWh/m^2 in MVD. From those 38 kWh/m^2, there are 34 kWh/m^2 gained through the roof, 9 kWh/m^2 through the walls and there are 5 kWh/m^2 lost through the ground. So the major contribution to the enclosure gains in N-NW are from the roof and are all due to absorbed solar radiation.

Besides, given that the efficient occupant only takes advantage of natural ventilation when zone operative temperature is within certain limits (and uses the HVAC otherwise), the higher irradiance and outside temperatures in N-NW result in less time the temperature is within the comfort limits and, accordingly, in less time the house is being naturally ventilated. This, combined with the lower wind speeds, results in lower infiltration and ventilation losses in N-NW subregion.

During heating period, MVD highest losses are also through the enclosure and are of 36 kWh/m^2 whereas in N-NW are of 20 kWh/m^2. This difference is also due to the absorbed solar radiation in walls and roof as in N-NW is 34% higher than that in MVD. In this case, the bigger infiltration and ventilation losses in N-NW indicate that during heating period windows are more time open in the northern subregion.

Disaggregated by deciles ranks

Apart from the subregions, the results could also be analysed distinguishing between the decile ranks. The differences in this case may be related to different construction materials, amount of occupants, households sizes and percentages of occupied area. The comparison between the shares of each category in terms of the amount of households and the thermal energy required can be found in Figure 4.9 for the whole country, along with the categories thermal requirements relative to the occupied area.

In Fig. 4.9a it can be observed that the highest share in amount of households and even the higher share in energy requirements correspond to deciles 1-4. Also, that the remaining households are distributed equally between the other two decile ranks but not the energy requirements, which are higher for deciles 8-10. The only decile rank with a lower percentage in energy required than in number of buildings is the 5-7. Then, deciles 8-10 require thermal energy almost in the same proportion as the amount of households and 1-4 demands energy in a bigger proportion.

These differences are also clear in Fig. 4.6b where the thermal demands relative to occupied area are presented. While deciles 1-4 have the highest demands, deciles 5-7 have the lowest. Moreover, when distinguishing between cooling and heating, it remains clear that the reason of deciles 1-4 high requirements are the cooling loads whereas the opposite is true for deciles 8-10.

Following the same procedure as for the subregions, decile ranks 1-4 and 8-10 components contributions could be compared so as to analyse their large differences. Also, by studying the sources of energy gains and losses it could be detected the reason behind their high requirements and, consequently, allow the design of appropriate retrofit measures. The resulting gains and losses during cooling and heating periods for the deciles 1-4 and 8-10 are those shown in Figure 4.10. Once again, this analysis was performed only for the houses so as to isolate the effect of the decile rank.

Observing both Figs. 4.10a and 4.10b there is a large difference in the windows gains and also in the infiltration and ventilation losses for the two decile ranks in both periods. This is due to the quite different glazed areas that are there in each decile rank: while in deciles 1-4 average glazed area is 5.9 m^2, in deciles 8-10 it is 13.5 m^2. Contrarily, the internal gains (which are in the "Other" category) are higher for deciles 1-4 during both periods. This is due to the fact that there are more occupants in those deciles for every household size.

Another important difference between the two decile ranks, and one that should be taken into consideration when analysing the results, is the proportion of occupied area, which is 84.8% in deciles 1-4 and 50.9% in deciles 8-10. In Figs. 4.10a and 4.10b the energy contributions are the total gains and losses through each component expressed relative to the occupied area; this causes deciles 8-10 to have higher values as, for example, there would be more enclosure for the same occupied area.

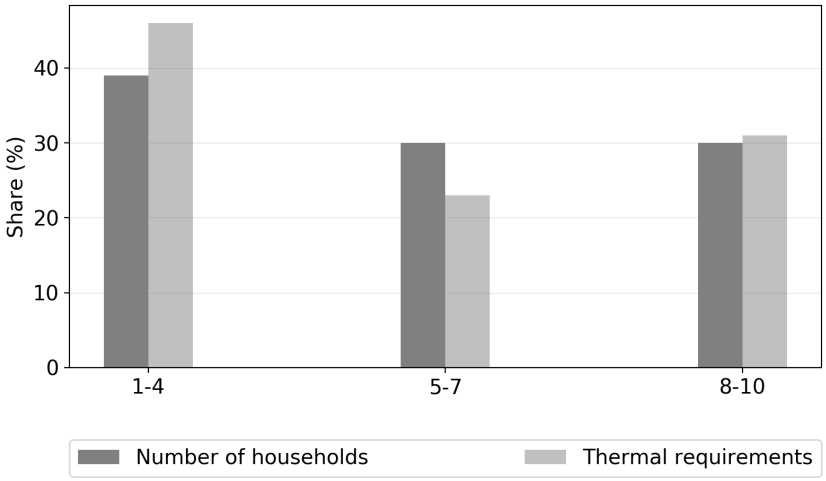

(a) Shares of stock and requirements in deciles.

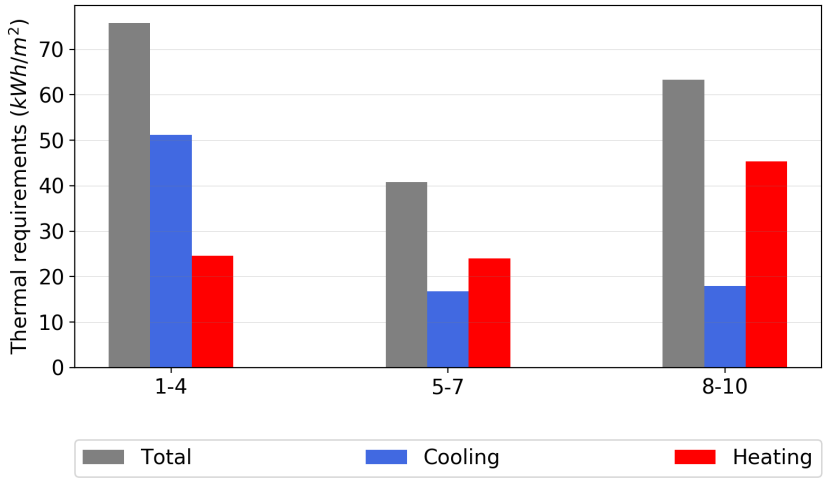

(b) Heating and cooling requirements in deciles.

Figure 4.9: Requirements disaggregated by deciles for the whole country.

Focusing on cooling period, deciles 1-4 have lower gains but also lower losses, resulting in net thermal energy gains of 38 kWh/m^2 against 12 kWh/m^2 in deciles 8-10. The main contribution to thermal gains in deciles 1-4 is the enclosure with 36 kWh/m^2 and, within the enclosure, the roof is the biggest responsible for the high cooling requirements. Deciles 1-4 having more gains through the enclosure than deciles 8-10, indicate the different construction qualities, specially considering that there is less enclosure per occupied square meter. By observing Tab. 4.1 it can be verified that deciles 1-4 constructions have both higher transmittances and higher solar absorptivity.

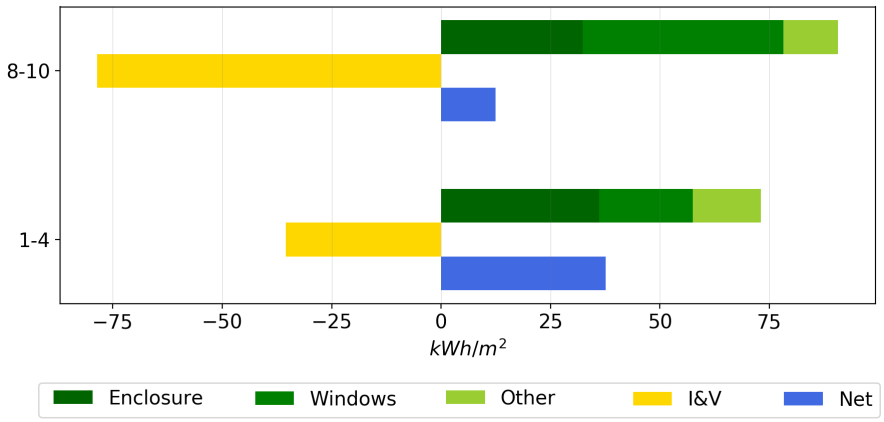

(a) Cooling period.

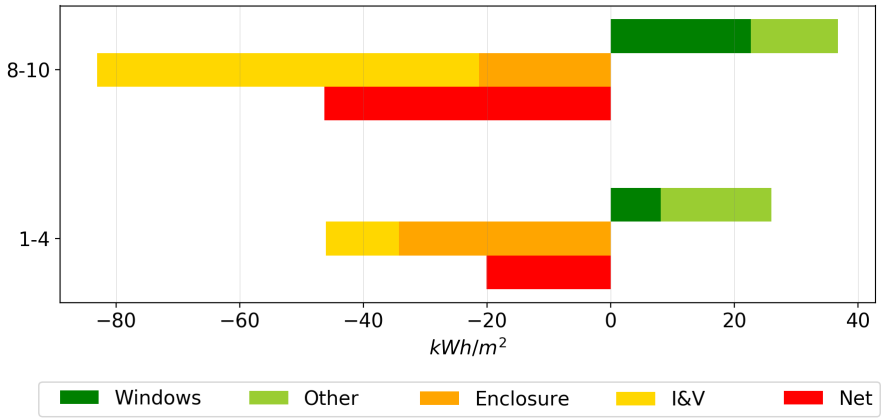

(b) Heating period.

Figure 4.10: Thermal energy gains and losses.

These differences in heat gains also impact in the infiltration and ventilation losses. As happened for the subregions, higher gains in deciles 1-4 households result in higher zone operative temperatures, which in turn lead to less time the occupants take advantage of natural ventilation rather than using the HVAC for achieving comfort. This, combined with the lower glazed areas that are there in deciles 1-4 households, results in lower infiltration and ventilation losses.

During heating period, deciles 8-10 also have higher gains and losses than 1-4 (because of the different percentage of occupied area), but in this case this results in higher net energy losses relative to the occupied area. The main sources of thermal losses in deciles 8-10 are the infiltration and ventilation loads. Once again the differences among the enclosure constructions are clear,

as deciles 1-4 have 60% more losses through the enclosure with less enclosure area.

Differently than for the subregions, when analysing the results disaggregated by deciles, the decision of whether to express them relative to the occupied area, to the total area or per occupant would have a great impact on the obtained values. Up to now, all the study about the deciles energy patterns was done based on the requirements relative to the occupied area. However, if the results were to be expressed as energy per occupant Fig. 4.9 would turn into Figure 4.11.

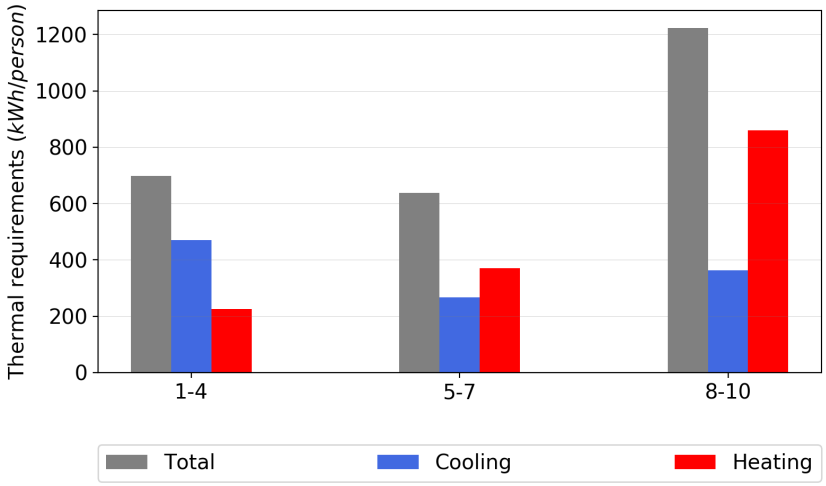

Figure 4.11: Heating and cooling requirements in deciles.

A person in deciles 8-10 thus requires, in average, 1223 kWh each year so as to maintain thermal comfort whereas a person in deciles 1-4 requires 698 kWh; and this is despite the higher deciles living in houses with better quality constructions. Once again, the lowest requirements are for deciles 5-7 with 639 kWh per occupant each year. These results are very different than those from Fig. 4.9b, where deciles 1-4 have the highest requirements. Hence, the basis on which the results are expressed should be conscientiously selected, as the best alternative would depend on the aim of the analysis.

Continuing with the analysis for the requirements relative to the occupied area, the obtained results within each decile rank could also be separated according to the households vintage. By doing this, the segment with the highest improvement potential could be identified. For example, the energy contributions during cooling period in the oldest and the newest houses in deciles 1-4 are those shown in Figure 4.12. The net gains in the houses built

more than 30 year ago are 84% bigger than those in the newest houses during cooling period. The main difference is in the enclosure gains, which are due to the different construction materials, specially in the roof.

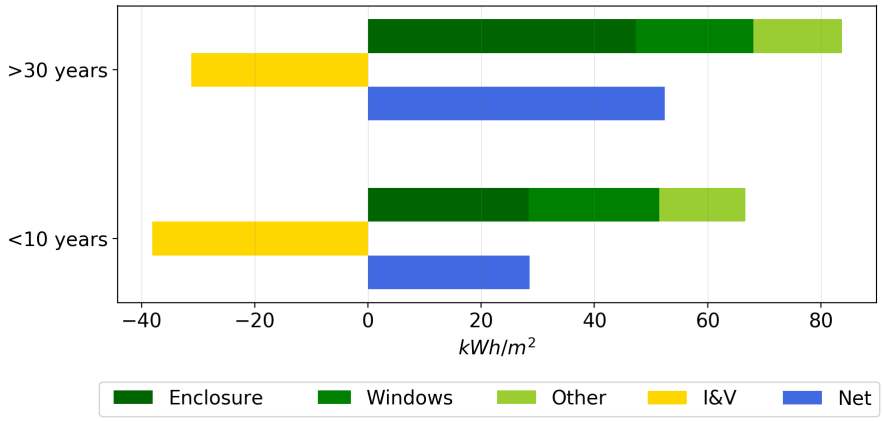

Figure 4.12: Thermal energy gains and losses during cooling period in deciles 1-4.

Disaggregated by sizes

If the analysis is focused on households sizes, the obtained results are those in Figure 4.13. It can be observed that 80% of the households are larger than 40m^2 and concentrate the 85% of energy requirements. The largest households are those with the highest total requirements, but this is not the case if these requirements are analysed relative to the occupied area. The smallest households are the most thermal energy intensive per occupied area (see Fig. 4.13b), and this is due to the high cooling requirements, which double those in the larger households.

When comparing the components contribution to thermal requirements between the smallest and largest houses, the patterns of Figure 4.14 are obtained. During cooling period, the large differences between the thermal requirements are due to the much higher enclosure gains in the smaller households (see Fig. 4.14a); even though there would be less enclosure area per conditioned area. Gains through the windows on the other hand, are higher in the larger houses but are compensated with higher infiltration and ventilation losses. During heating period, larger houses higher infiltration losses compensate the smaller houses higher enclosure losses, and both end up having similar thermal requirements (see Fig. 4.14b).

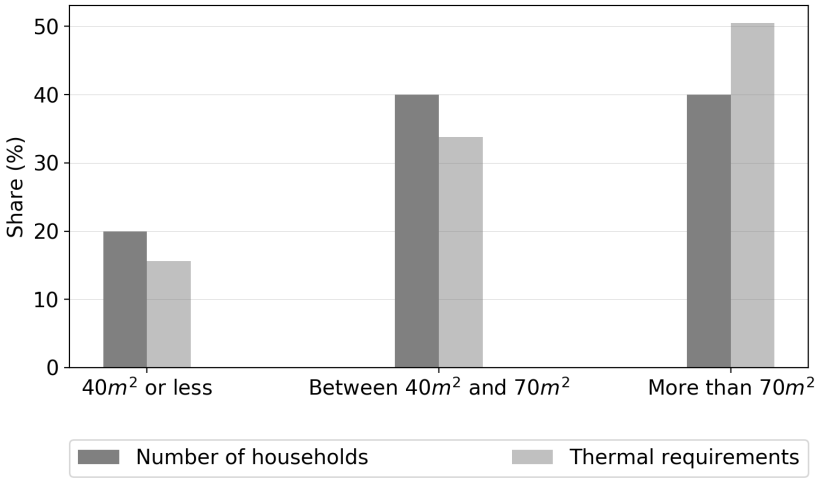

(a) Shares of stock and requirements according to sizes.

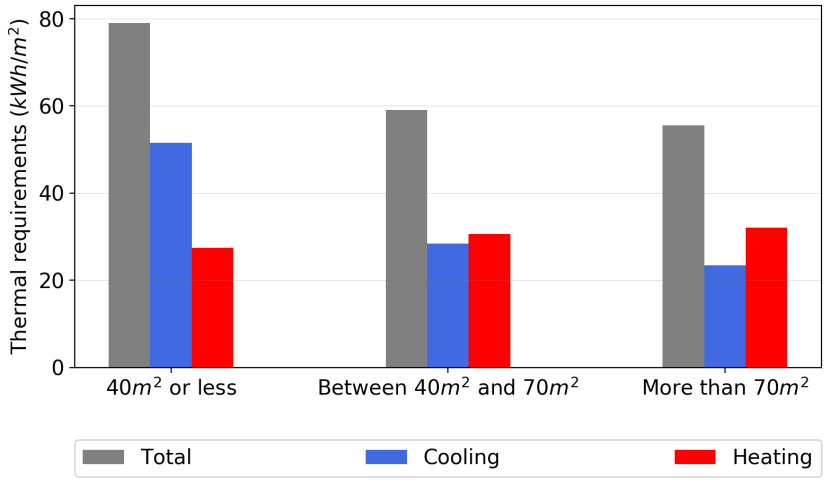

(b) Heating and cooling requirements according to sizes.

Figure 4.13: Requirements disaggregated by sizes.

These results for the components shares in total thermal loads bear some resemblance to those obtained when distinguishing between deciles (Fig. 4.10). In fact, when analysing how deciles categories are distributed among the smallest and largest households groups, it can be observed that household size and decile rank are not independent attributes (see Figure 4.15).

Disaggregated by vintage

The final characteristic which was used to determine a building archetype, and according to which the results can also be disaggregated, is the household vintage. Results distinguishing between the three vintage categories defined

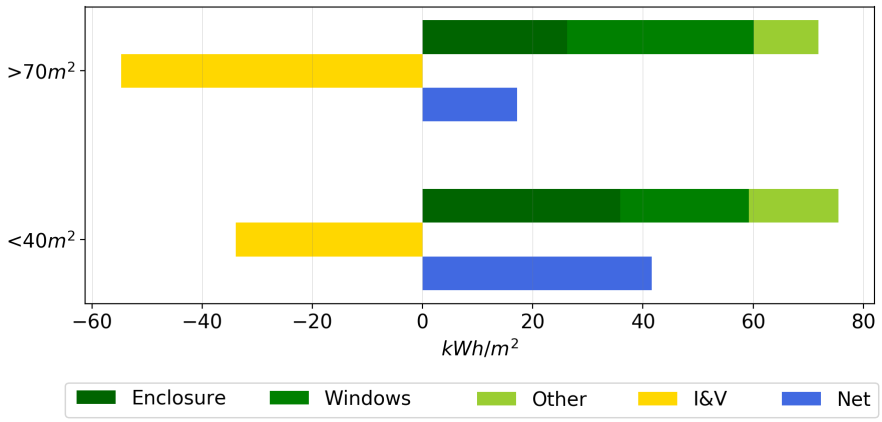

(a) Cooling period.

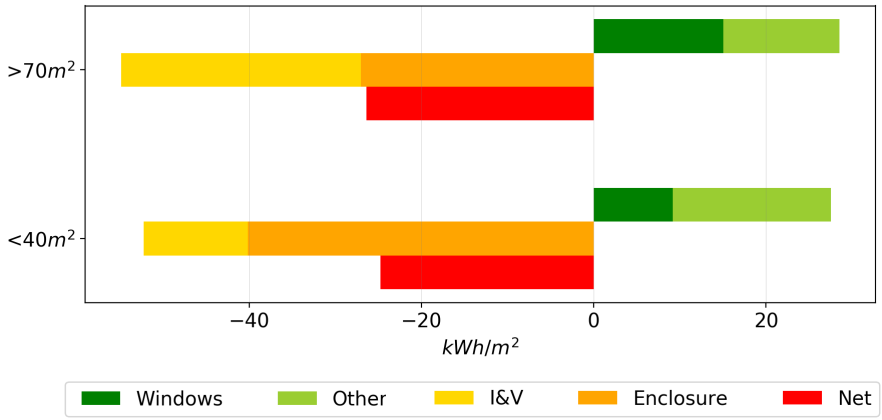

(b) Heating period.

Figure 4.14: Thermal energy gains and losses.

in the housing stock characterisation are shown in Figure 4.16. Almost half of the Uruguayan housing stock corresponds to households built more than 30 years ago, while only 17% corresponds to households with less than 10 years old. Moreover, the older households thermal energy requirements share is of almost 60% against 13% for the newest constructions (see Fig. 4.16a).

This difference between the categories prevalence in the housing stock and their energy requirements share, can be explained by observing the energy requirements relative to the occupied area for each vintage category presented in Fig. 4.16b. The graph shows that the newer the household the less thermal requirements, even though there is the same sizes distribution and a higher share of apartments in the older category (12.9% in the 10 years or less and 17.4% in the 30 years or more categories). This therefore demonstrates the im-

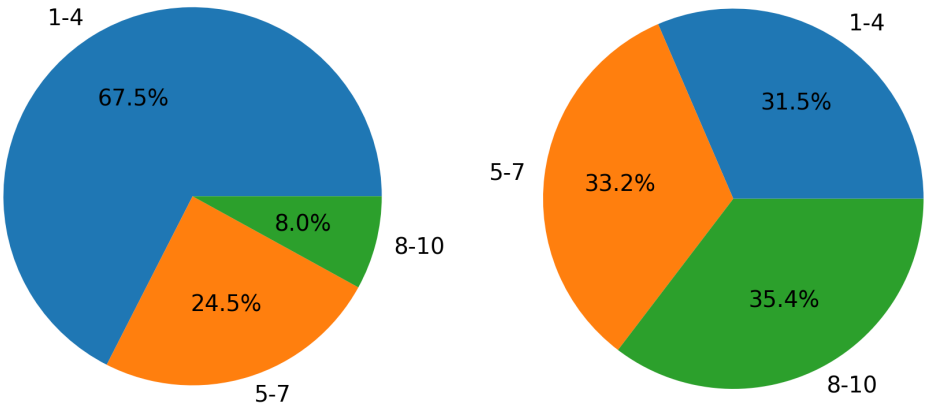

(a) 40m^2 or less. **(b)** 70m^2 or more.

Figure 4.15: Deciles distribution among household sizes.

provements regarding construction material thermal qualities. The households with less than 10 years of built require 43.7kWh/m^2 of which 26.8kWh/m^2 are for cooling and 16.9kWh/m^2 are for heating. Those built between 10 and 30 years ago require 48.4kWh/m^2 of which 21.7kWh/m^2 are for cooling and 26.7kWh/m^2 are for heating. Finally, the households with more than 30 years of built require 76.8kWh/m^2 of which 36.7kWh/m^2 are for cooling and 38.1kWh/m^2 are for heating.

The comparison between the components contributions for the categories in the two extremes, can be observed in Figure 4.17. The major difference between the two categories in both periods is in the gains and losses through the building enclosure. This is also clear when comparing the mean transmittance for the two categories which are (including the film coefficients) 1.66W/m^{2}K and 2.92W/m^{2}K for the average newer and older households, respectively.

4.3.3 Impact of occupants behaviour

As described in Section 4.2.2, two types of occupants behaviours were modelled in this work. The first represents efficient occupants who operate windows and solar protections (in the occupied zones) so as to minimize energy requirements. The results of the previous section are all for this type of occupants. Contrarily, the second type of occupant defined does not use natural ventilation nor solar protections and, thus, relies exclusively on the HVAC systems to achieve thermal comfort. Therefore, in order to continue with the analyses,

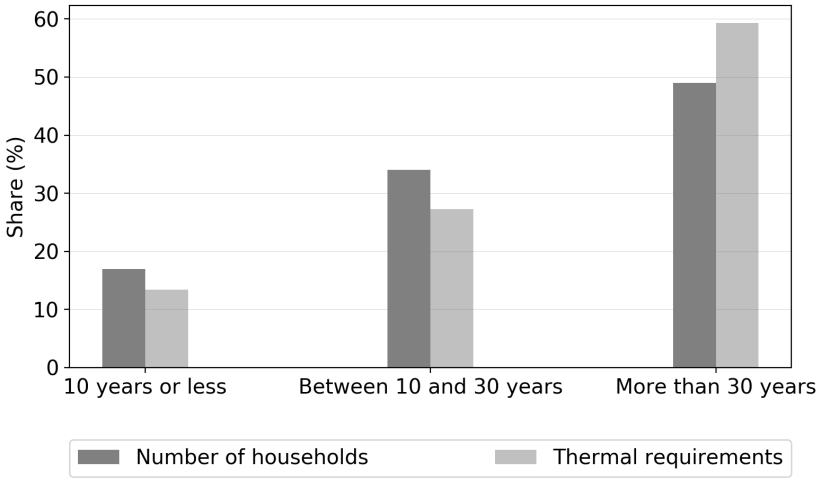

(a) Shares of stock and requirements according to vintage.

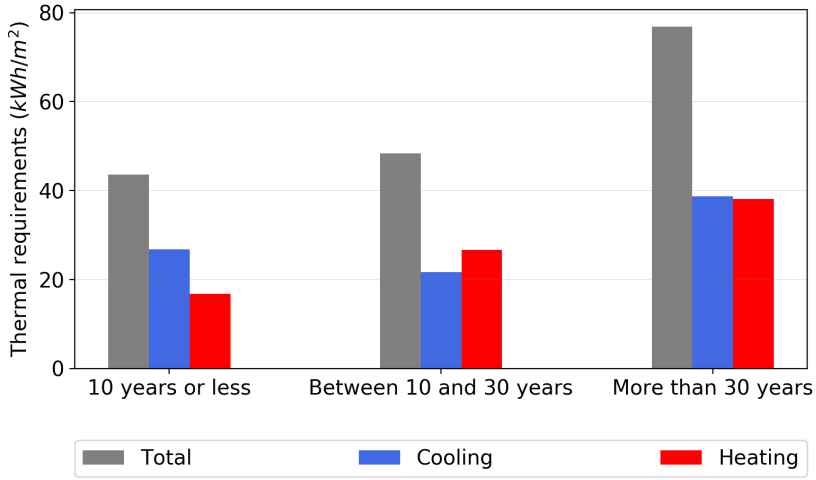

(b) Heating and cooling requirements according to vintage.

Figure 4.16: Requirements disaggregated by vintage.

all the results were also obtained for the inefficient occupant so as to determine to which extent does occupants behaviour affect the households thermal performances.

So as to compare the results for both occupants behaviours, the increase in energy requirements derived from modelling the housing stock with an inefficient occupant was determined and expressed as a percentage of the energy required for the efficient occupant. Total thermal requirements increased 61% when modelling households with the inefficient occupant, this is 4258GWh per year against the 2641GWh of Tab. 4.11. This proves the impact occupants have on the buildings thermal performances, and thus shows the need for mod-

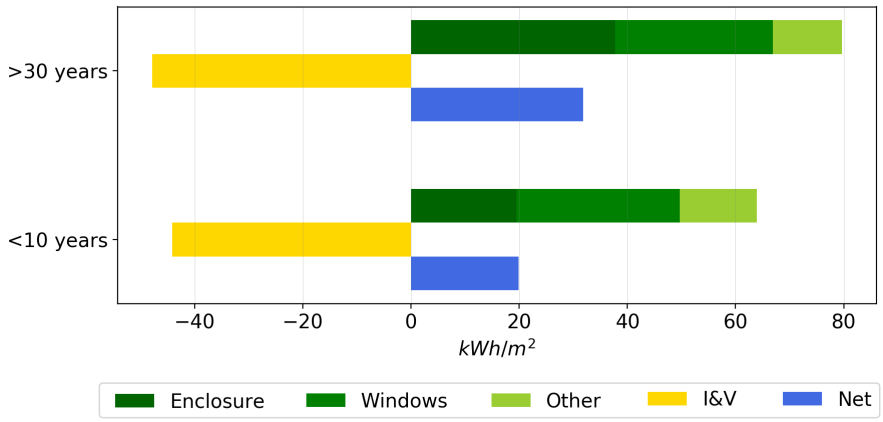

(a) Cooling period.

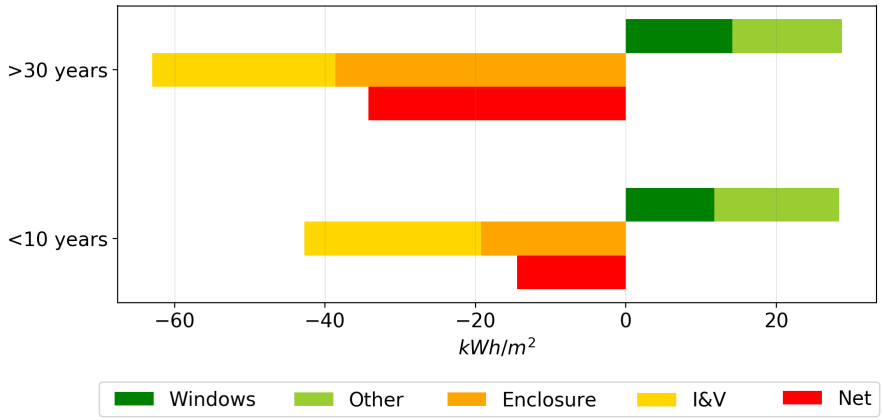

(b) Heating period.

Figure 4.17: Thermal energy gains and losses.

elling occupants as accurately as possible when aiming at characterising the housing stock energy requirements. Based on how the two types of occupants were defined (see Section 4.2.2), it can be accepted that the two behaviours modelled represent the two extremes between which real occupants behaviours would be. Consequently, real Uruguayan housing stock annual requirements should be somewhere in between 2641GWh and 4258GWh.

Besides, the increases obtained are shown in Figure 4.18 for the different categories upon which the housing stock was characterised. First, there is the increase obtained for each type, then for each subregion, decile rank, size and vintage categories. 'Size 1', 'Size 2' and 'Size 3' in Fig. 4.18 correspond to households sizes of 40m^2 or less, between 40m^2 and 70m^2 and more than 70m^2, respectively. Equally, 'Vintage 1', 'Vintage 2' and 'Vintage 3' in Fig. 4.18

correspond to households vintages of 10 years or less, between 10 and 30 years and more than 30 years, respectively.

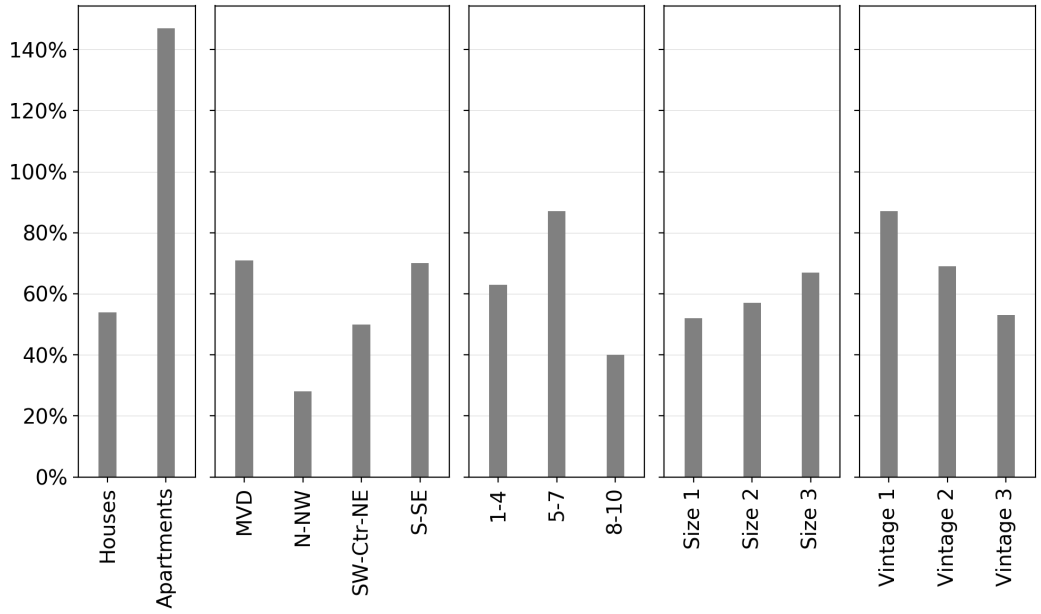

Figure 4.18: Increase in total thermal requirements for inefficient occupant compared to efficient one.

Regarding the buildings type, apartments have proven to be much more sensitive to occupant behaviour than houses (see Fig. 4.18). This might be due to lower percentage of exposed area in apartments, which make them much more dependants on ventilation and solar protections for cooling. The influence of the occupant is more similar among the geographic subregions, however, N-NW is the less affected as in that region even the efficient occupant cannot take great advantage of natural ventilation (see Fig. 4.8a).

Among the decile ranks, 5-7 are the most influenced by the occupant as their requirements increased 87%, whereas 1-4 increased 63% and 8-10 40%. As the differences between the efficient and the inefficient occupant are the use of natural ventilation and solar protections, the main impact would be on cooling loads; which only represent 28% of deciles 8-10 requirements (see Fig.4.9b). Higher deciles being less affected by the occupant is a consequence of the lower share of cooling in these deciles requirements and how the types of occupants were defined. Deciles 1-4 being less affected than deciles 5-7 is due to the less infiltration and ventilation losses during cooling period that lower deciles have (see Fig.4.10a), even for the efficient occupant. Besides,

the lower relevance windows gains have in the lower deciles also contributes to their requirements being less influenced by the occupant not using solar protections.

All sizes categories were similarly affected by the change of occupant as their increase were of 52%, 57% and 67% for the smallest, medium and largest households, respectively. Regarding households vintage, the most affected were the newer ones which increased 87% whereas those built between 10 and 30 years ago increased 69%, and the older ones 53%. The differences in both sizes and vintage are also due to the relevance that infiltration and ventilation losses, as well as solar gains through windows, have in each category during cooling period (see Fig. 4.14a and 4.17a). For the case of vintage, even though infiltration and ventilation losses are higher for the older houses, the importance of windows gains and infiltrations and ventilation losses compared to enclosure gains is quite higher in the newer ones.

All in all, every category analysed was negatively impacted by the occupant substitution. Moreover, in all cases the impact was quite relevant as it varied from 28% for the N-NW housing stock, up to 147% when considering the apartments all along the country. Among each characteristic such as type, subregion, deciles, size and vintage there were some categories which were more sensitive to occupants behaviour, which is something to take into consideration when designing energy policies and/or retrofit measures.

The occupants actions that will have an impact on the buildings thermal performance are, essentially, the windows opening behaviour and the use of solar protections. The HVAC systems set points established by the occupant will also play a major role but, as in this work the analyses are based on thermal requirements for comfort and not energy demand, this aspect was not considered. Therefore, the occupants influence on the households performance is mainly during cooling period, when they should take more action regarding opening windows and solar protections. This is the reason why those categories in which ventilation losses and windows solar gains during cooling period are more relevant, would be more affected by the inefficient occupant.

By comparing the impact in each category shown in Fig. 4.18, with global results of Section 4.3.2, it can be noted that usually the most affected by the occupant -within each characteristic in which the housing stock was divided- were the ones with better performance. For instance, distinguishing between types, apartments performed better than houses for the efficient occupant but

are far more affected by the change of occupant behaviour; and the same happens with the regions, the decile ranks and the vintage categories. In all cases, the category with better performance entailed a higher quality enclosure (and in some cases also less exposed area). Therefore, having a better passive design results in active controls being more relevant in proportion; and thus thermal performance ends up being more susceptible to occupants behaviour. The only exception to this is for the geographic regions where the difference in the occupants impact is due to local climate characteristics.

4.4 Conclusions

In this chapter, the approach followed in this thesis for assessing thermal requirements in Uruguayan residential sector was presented. It entailed the development of a physic-based bottom-up model of the country's housing stock, relying on typical buildings and their prevalence among the whole residential sector. Efforts in making the model as accurate as possible led to automation as the strategy to generate and simulate large amount of models.

A platform was thus developed based on Python scripts and Eppy library, as well as on the outcomes of a housing stock characterisation process. This platform relies on EnergyPlus as the simulation engine and it is capable of carrying out the whole simulation process; including the models characterisation, generation, simulation and results processing.

Then, a simulation was performed consisting of 496 models distributed all along the country and for two different occupants behaviours. This resulted in 992 simulations (496 models for each of the two type of occupants), which ran locally on a PC taking 36 hours and 48 minutes to complete the whole process. The results were analysed in terms of total requirements and also disaggregated according to attributes identified as relevant when characterising the housing stock. Moreover, the different contributions of the buildings components to energy gains and losses were analysed for the cooling and heating periods for the different categories defined. This type of study allows to identify major drivers for thermal requirements and therefore lead to more effective retrofit measures.

The resulting annual thermal requirements were of 2641GWh for efficient occupants, 1296GWh of which correspond to cooling requirements whereas the remaining 1345GWh correspond to heating requirements. Distinguish-

ing between households types, apartments showed a better performance than houses due to less exposed area and better quality constructions. Regarding geographic regions, Montevideo is the one with the highest requirements on the grounds that it concentrates more than 40% of the housing stock. Yet, analysing requirements relative to the households areas, the northern region turned out to be the most energy intensive due to large cooling requirements.

Focusing on decile ranks, the highest requirements relative to the occupied area were in deciles 1-4 followed by deciles 8-10. However, while in deciles 1-4 68% of total requirements were for cooling purposes, in deciles 8-10 72% were destined to heating. Disaggregating by sizes, the smallest households turned out to be the ones with largest requirements per square meter and, when the households vintage was analysed, the older households requirements were almost double than those in the newer ones.

Finally, the impact of the occupants behaviour was analysed by comparing the results obtained for the efficient and the inefficient occupants. An increase of 61% was obtained for the whole housing stock thermal requirements as a consequence of the occupants behaviour substitution. Focusing on the subregions, despite being the most energy intensive, N-NW was the least affected by the occupants behaviour, thus suggesting that passive design strategies could be effective in that region. Distinguishing between types, apartments turned out to be much more sensitive to occupants behaviour than houses, as their requirements increase was more than 140% against around 50% in houses. Regarding occupants socio-economic status, households corresponding to deciles 5-7 were the most affected by the change of occupant behaviour as their requirements increased almost 90%. Contrarily, deciles 8-10 were the least affected with an increase of 40%. All these results provide evidence for the importance of modelling the occupants schedules and behaviours as accurately as possible if aiming at a faithful characterisation of the housing stock thermal performance.

All in all, the main outcome of this work, apart from the results regarding energy requirements, is the tool developed which characterises, generates and simulates the households models and, furthermore, processes the results. As it is, the tool is capable of quantifying energy requirements for thermal comfort and also of evaluating the impact of energy efficiency retrofits in the buildings enclosures or the usage patterns. Moreover, taking this tool as a starting point and incorporating other end-uses and the transformation into final energy, it is

possible to develop a forecasting model which can be used to obtain projections of energy demand or to analyse the impact of the application of certain energy policies. Nevertheless, it is important to acknowledge that the results are highly dependent on how the housing stock was characterised (this is, how the archetypes were defined and distributed along the different regions) and also on the hypotheses considered when generating the models. It would therefore be important to calibrate the tool before using it to make projections.

Chapter 5

Conclusions

Urban Building Energy Models (UBEM) are gaining worldwide interest as tools capable of providing deep understanding of building energy patterns, of the country as a whole and down to the individual building level. Nevertheless, in Uruguay there are no developments that model energy demand in the residential sector in detail, despite it being a relevant sector in terms of energy consumption. In this regard, a first approach towards a Uruguay's UBEM was developed in this thesis.

The methodology entailed, first, the selection of EnergyPlus as the software to perform the simulations and also the determination of the results that would be processed. Secondly, and given that in this work archetypes were used to represent the whole housing stock, an example case was studied to evaluate the impact different orientations and surroundings have on the results. The intention was to determine the relevance of considering variability in these characteristics when using the same model to represent different buildings. Finally, the process of models generation, simulation and results processing was automated by means of Python functions and Eppy library.

The main outcome of this work is the tool developed which characterises, generates and simulates the households' models and, furthermore, processes the results. It has proven to be a suitable and promising tool for modelling the residential sector based on EnergyPlus. As it is, the tool is capable of quantifying annual or seasonal energy requirements for thermal comfort in the Uruguayan housing stock as it was characterised in FSE_1_2017_1_144779 [4]. Also of evaluating the impact of energy efficiency retrofits in the buildings enclosures or the usage patterns. Besides, the effect climate change could pro-

duce in the energy required for heating and cooling could also be determined. All of these studies could be performed either for the whole residential sector, or disaggregated according to certain relevant characteristics of the buildings modelled. Analysing the results distinguishing among different building categories allows to identify major areas of improvement; which might in turn lead to the design of targeted energy policies and of cost-effective retrofit measures.

Simulations performed for a particular building example showed that the presence of an attached facade is the aspect with the highest impact on heat gains and losses. It entailed a reduction of up to 35% in total energy required for thermal comfort, and its benefits where both during heating and cooling periods, but specially in the former. Concerning the building orientation, it was found that the most favourable ones are obtained as a compromise between those which capitalize on more solar gains during heating period and those with the lowest solar gains during cooling period, both determined taking into consideration the zones usage patterns.

In a larger simulation performed with the objective of obtaining results representative of the Uruguayan housing stock, it was found that the northern region is the most energy intensive due to high cooling loads, which are double than in the other regions. Yet, it was the least affected by the occupants behaviour, thus suggesting that passive design strategies could be quite effective in that region. The opposite happened with apartments, they proved to perform better than houses but are much more sensitive to occupants behaviour. Their requirements increased more than 140% when inefficient occupants were modelled, whereas in houses the increase was of around 50%. Distinguishing between the socio-economic status of the occupants, the lower and the higher decile ranks were those with the highest requirements. The former mostly due to cooling loads, while the opposite is true for the latter. Higher deciles turned out to be the least dependant on occupants behaviour. Finally, and regarding households sizes and vintage, the smaller were the ones with the highest requirements relative to the occupied area, and the same happened with the older constructions.

Nevertheless, the tool developed has its limitations and further work should, first of all, be devoted to improving the model. Given the high impact they have on results, housing stock characterisation and the hypotheses considered should be improved so as to be more representative of reality. For instance, more geometries could be considered when characterising the housing stock

and usage patterns could be more accurately defined. Also, considering the EnergyPlus models used, latent heat ought to be accounted for in the energy balance equations and pressure coefficients might be more accurately determined when solving infiltration and ventilation loads. Besides, and even if improved, the tool is limited to modelling energy requirements for thermal conditioning. Taking this as a starting point, future work should incorporate the remaining end-uses and the transformation of energy requirements into final energy demand. By doing so, it would be possible to develop a forecasting model which can be used to obtain projections of energy demand in the residential sector. Moreover, further development could produce results on an hourly scale, hence providing power demand curves. This could result in a promising tool for evaluating the impact of demand management alternatives or for power lines expansion planning.

Bibliography

[1] EIA Energy Atlas. "World energy statistics & World energy balances". In: (2020), page 703. URL: http://data.iea.org/payment/products/103-world-energy-statistics-and-balances-2018-edition-coming-soon.aspx.

[2] *EnergyPlus: Energy Simulation Software*. URL: http://www.energyplus.net.

[3] MIEM. *Balance Energético Nacional*. 2019. URL: https://ben.miem.gub.uy/preliminar.html.

[4] Curto P and Picción A. *FSE_1_2017_1_144779 - EFICIENCIA ENERGÉTICA EN EL SECTOR RESIDENCIAL. Situación actual y evaluación de estrategias de mejoramiento para distintas condiciones climáticas en el Uruguay*. Montevideo-Salto, Uruguay, 2017. DOI: 10.4000/books.cemca.5418.

[5] Spitler JD. "Editorial: Building performance simulation: The now and the not yet". In: *HVAC and R Research* 12.November (2006), pages 711–713. ISSN: 10789669. DOI: 10.1080/10789669.2006.10391194.

[6] Li X and Wen J. "Review of building energy modeling for control and operation". In: *Renewable and Sustainable Energy Reviews* 37 (2014), pages 517–537. ISSN: 13640321. DOI: 10.1016/j.rser.2014.05.056. URL: http://dx.doi.org/10.1016/j.rser.2014.05.056.

[7] *BEMLibrary*. URL: https://www.bemlibrary.com.

[8] *TRNSYS : Transient System Simulation Tool*. URL: http://www.trnsys.com.

[9] *ESP-r*. URL: http://www.esru.strath.ac.uk/applications/esp-r/.

[10] Judkoff R and Neymark J. "International Energy Agency building energy simulation test (BESTEST) and diagnostic method". In: 1.1 (Feb. 1995). DOI: 10.2172/90674.

[11] Lima F and Oliveira RD. “Modelo termoenergético calibrado do restaurante estudantil do CEFETMG campus II”. In: January 2019 (2018).

[12] Psomas T, Fiorentini M, Kokogiannakis G, and Heiselberg P. “Ventilative cooling through automated window opening control systems to address thermal discomfort risk during the summer period: Framework, simulation and parametric analysis”. In: *Energy & Buildings* (2017). ISSN: 0378-7788. DOI: 10.1016/j.enbuild.2017.07.088. URL: http://dx.doi.org/10.1016/j.enbuild.2017.07.088.

[13] Liu Z, Zhang Y, Xu W, Yang X, Liu Y, and Jin G. “Suitability and feasibility study on the application of groundwater source heat pump (GWSHP) system in residential buildings for different climate zones in China”. In: *Energy Reports* 6 (2020), pages 2587–2603. ISSN: 2352-4847. DOI: 10.1016/j.egyr.2020.09.015. URL: https://doi.org/10.1016/j.egyr.2020.09.015.

[14] U.S. Department of Energy. “EnergyPlus - Getting Started”. In: *Bigladder Software* c (2016), pages 1996–2016. URL: http://bigladdersoftware.com/epx/docs/8-7/getting-started/getting-started-with-energyplus.html.

[15] Drury B, Curtis O, Linda K, and Frederick C. “EnergyPlus : Energy simulation program”. In: *ASHRAE Journal* 42.April (2000), pages 49–56.

[16] Walton G. “Thermal Analysis Research Program.” In: (1983), pages 22–23.

[17] EnergyPlus. “Engineering Reference”. In: *US Department of Energy* c (2010), pages 1–847. ISSN: 03787788. URL: www.energyplus.net.

[18] Li XQ, Chen Y, Spitler JD, and Fisher D. “Applicability of calculation methods for conduction transfer function of building constructions”. In: *International Journal of Thermal Sciences* 48.7 (2009), pages 1441–1451. ISSN: 12900729. DOI: 10.1016/j.ijthermalsci.2008.11.006. URL: http://dx.doi.org/10.1016/j.ijthermalsci.2008.11.006.

[19] U.S. Department of Energy. “EnergyPlus - Auxiliary Programs”. In: (2020).

[20] Pinel P and Beausoleil-Morrison I. “Coupling Soil Heat and Mass Transfer Models to Foundations in Whole-Building Simulation Packages”. In: *Proceedings of eSim 2012: The Canadian Conference on Building Simulation* 2002 (2012), pages 557–570.

[21] Kusuda T and Achenbach P. “Earth Temperature and Thermal Diffusivity at Selected Stations in the United States”. In: *National Bureau of Standards Report* (1965).

[22] Neymark J, Judkoff R, and Crowley M. “International Energy Agency BESTEST for Ground Coupled Heat Transfer”. In: (2008).

[23] COMSOL. *COMSOL Multiphysics® Modeling Software*. 2016. URL: https://www.comsol.com/.

[24] U.S. Department of Energy. “EnergyPlus - InputOutputReference”. In: c (2016), pages 1996–2016. URL: https://energyplus.net/documentation.

[25] Gu L. “Airflow network modeling in energyplus”. In: *IBPSA 2007 - International Building Performance Simulation Association 2007* January 2007 (2007), pages 964–971.

[26] Philip S. “eppy Documentation”. In: *Github Repository* Release 0.5.52 (2019). URL: https://github.com/santoshphilip/eppy.

[27] Morrissey J, Moore T, and Horne RE. “Affordable passive solar design in a temperate climate : An experiment in residential building orientation”. In: *Renewable Energy* 36.2 (2011), pages 568–577. ISSN: 0960-1481. DOI: 10.1016/j.renene.2010.08.013. URL: http://dx.doi.org/10.1016/j.renene.2010.08.013.

[28] Andersson B, Place W, Kammerud R, and Scofield MP. “The Impact of Building Orientation on Residential Heating and Cooling”. In: 8 (1985), pages 205–224.

[29] Vasov MS, Stevanović JN, Bogdanović VB, Ignjatović MG, and Randjelović DJ. “Impact of orientation and building envelope characteristics on energy consumption case study of office building in city of nis”. In: *Thermal Science* 22 (2018), S1499–S1509. ISSN: 03549836. DOI: 10.2298/TSCI18S5499V.

[30] Spanos I, Simons M, Holmes KL, Associates KH, and Kingdom U. “Cost savings by application of passive solar heating”. In: 23.2 (2005), pages 111–130. DOI: 10.1108/02630800510593684.

[31] Liu D, Wang W, and Ge H. "Impact of urban densification on building energy consumption". In: 16001 (2020), pages 1–6.

[32] Chagolla MA, Alvarez G, Simá E, Tovar R, and Huelsz G. "Effect of tree shading on the thermal load of a house in a warm climate zone in Mexico". In: *ASME International Mechanical Engineering Congress and Exposition, Proceedings (IMECE)* 7.PARTS A, B, C, D (2012), pages 761–768. DOI: 10.1115/IMECE2012-87918.

[33] Hwang WH, Wiseman PE, and Thomas VA. "Simulation of Shade Tree Effects on Residential Energy Consumption in Four U. S. Cities". In: September (2016).

[34] Lawrie LK and Crawley DB. *Development of Global Typical Meteorological Years (TMYx)*. 2019. URL: http://climate.onebuilding.org.

[35] Alonso-Suárez R, Bidegain M, Abal G, and Modernell P. *Año Meteorológico Típico para Aplicaciones de Energía Solar (AMTUes): series horarias típicas para 5 sitios del Uruguay*. 2016. ISBN: 9789974016477.

[36] *ANSI/ASHRAE Standard 55-2017*. Technical report. 2017. URL: www.ashrae.org/technology..

[37] Civil A/C0CBdC. "NBR 15575". In: *subregión* (), pages 1–16.

[38] Li W, Zhou Y, Cetin K, Eom J, Wang Y, Chen G, and Zhang X. "Modeling urban building energy use: A review of modeling approaches and procedures". In: *Energy* 141 (2017), pages 2445–2457. ISSN: 03605442. DOI: 10.1016/j.energy.2017.11.071. URL: https://doi.org/10.1016/j.energy.2017.11.071.

[39] Swan LG and Ugursal VI. "Modeling of end-use energy consumption in the residential sector: A review of modeling techniques". In: *Renewable and Sustainable Energy Reviews* 13.8 (2009), pages 1819–1835. ISSN: 13640321. DOI: 10.1016/j.rser.2008.09.033.

[40] Kavgic M, Mavrogianni A, Mumovic D, Summerfield A, Stevanovic Z, and Djurovic-Petrovic M. "A review of bottom-up building stock models for energy consumption in the residential sector". In: *Building and Environment* 45.7 (2010), pages 1683–1697. ISSN: 03601323. DOI: 10.1016/j.buildenv.2010.01.021. URL: http://dx.doi.org/10.1016/j.buildenv.2010.01.021.

[41] Pérez-García J and Moral-Carcedo J. "Analysis and long term forecasting of electricity demand trough a decomposition model: A case study for Spain". In: *Energy* 97 (2016), pages 127–143. ISSN: 03605442. DOI: 10.1016/j.energy.2015.11.055.

[42] Zhang Q. "Residential energy consumption in China and its comparison with Japan, Canada, and USA". In: *Energy and Buildings* 36.12 (2004), pages 1217–1225. ISSN: 03787788. DOI: 10.1016/j.enbuild.2003.08.002.

[43] Raffio G, Isambert O, Mertz G, Schreier C, and Kissock K. "Targeting residential energy assistance". In: *Proceedings of the Energy Sustainability Conference 2007* (2007), pages 489–496. DOI: 10.1115/ES2007-36080.

[44] Aydinalp-Koksal M and Ugursal VI. "Comparison of neural network, conditional demand analysis, and engineering approaches for modeling end-use energy consumption in the residential sector". In: *Applied Energy* 85.4 (2008), pages 271–296. ISSN: 03062619. DOI: 10.1016/j.apenergy.2006.09.012.

[45] Aydinalp M, Ismet Ugursal V, and Fung AS. "Modeling of the appliance, lighting, and space-cooling energy consumptions in the residential sector using neural networks". In: *Applied Energy* 71.2 (2002), pages 87–110. ISSN: 03062619. DOI: 10.1016/S0306-2619(01)00049-6.

[46] Davila CC, Reinhart C, and Bemis J. *Modeling Boston: A workflow for the generation of complete urban building energy demand models from existing urban geospatial datasets*. Technical report.

[47] Wilson E et al. "Energy Efficiency Potential in the U. S. Single-Family Housing Stock". In: January (2017). URL: www.nrel.gov/publications..

[48] NREL. *ResStock - NREL*. URL: https://resstock.nrel.gov/.

[49] MIEM - DNE. "Política Energética 2005-2030". In: *Ministerio de Industria, Energía y Minería - Dirección Nacional de Energía* (2005). URL: http://www.dne.gub.uy.

[50] DNE-MIEM. "Prospectiva de la Demanda Energética". In: (2018), page 50. URL: https://www.miem.gub.uy/energia/estudio-de-prospectiva-de-la-demanda-energetica-2018.

[51] DNE-MIEM. "Estudio de medidas de eficiencia energética en el sector residencial y evaluación de costos y beneficios asociados en Uruguay". In: (2015).

[52] Yan D, O'Brien W, Hong T, Feng X, Burak Gunay H, Tahmasebi F, and Mahdavi A. "Occupant behavior modeling for building performance simulation: Current state and future challenges". In: *Energy and Buildings* 107 (2015), pages 264–278. ISSN: 03787788. DOI: 10.1016/j.enbuild.2015.08.032. URL: http://dx.doi.org/10.1016/j.enbuild.2015.08.032.

[53] Bui DK, Nguyen TN, Ghazlan A, Ngo NT, and Ngo TD. "Enhancing building energy efficiency by adaptive façade: A computational optimization approach". In: *Applied Energy* 265 (May 2020). ISSN: 03062619. DOI: 10.1016/j.apenergy.2020.114797.

[54] Glazer J and Gard PE. "Using Python and Eppy for a Large National Simulation Study". In: (2016), pages 230–237. URL: www.ashrae.org.

[55] INE. *Encuesta Continua de Hogares (ECH) - Instituto Nacional de Estadística*. 2019. URL: http://www.ine.gub.uy/encuesta-continua-de-hogares1.

[56] Alonso-Suárez R, Abal G, Siri R, and Musé P. "Satellite-derived solar irradiation map for Uruguay". In: *Energy Procedia* 57 (2014), pages 1237–1246. ISSN: 18766102. DOI: 10.1016/j.egypro.2014.10.072. URL: http://dx.doi.org/10.1016/j.egypro.2014.10.072.

[57] MIEM, IIE, and IMFIA. *Proyecto de Energía Eólica - Mapa eolico de Uruguay*. 2009. URL: http://www.energiaeolica.gub.uy/index.php?page=mapa-eolico-de-uruguay.

APPENDICES

Appendix A

Example case materials and air leakage properties

In Tables A.1 to A.9 there are the materials sequences for each construction in the archetype selected for the analyses in Chapter 2, along with their thermal properties. These constructions were defined in $FSE\_1\_2017\_1\_144779$ [4] as representative of deciles 5-7 households built more than 30 years ago.

Table A.1: Exterior wall material properties from outside to inside layer.

Material	**Thickness** (cm)	**Density** (kg/m^3)	**Conductivity** (W/mK)	**Specific heat** (J/kgK)
Cement plaster finish coat	2.0	1800	1.0	1000
Cement plaster base coat	1.5	2100	1.4	1000
Bricks	5.0	1300	0.65	1000
Mortar material	1.0	999	0.41	1000
Bricks	12	1300	0.65	1000
Cement plaster finish coat	1.5	1800	1.0	1000

Table A.2: Interior wall material properties.

Material	**Thickness** (cm)	**Density** (kg/m^3)	**Conductivity** (W/mK)	**Specific heat** (J/kgK)
Cement plaster finish coat	1.5	1800	1.0	1000
Bricks	12	1300	0.65	1000
Cement plaster finish coat	1.5	1800	1.0	1000

Table A.3: Roof material properties from outside to inside layer

Material	**Thickness** (cm)	**Density** (kg/m^3)	**Conductivity** (W/mK)	**Specific heat** (J/kgK)
Exposed bricks	3.0	1300	0.79	1000
Ballast	5.0	1950	2.0	1045
Asphalt	2.5	2100	1.4	1000
Cement mortar	1.0	1800	1.0	1000
Rubble concrete	8.0	1800	0.95	1000
Concrete	10	2300	2.3	1000
Cement plaster finish coat	1.5	1800	1.0	1000

Table A.4: Floor material properties from outside to inside layer

Material	**Thickness** (cm)	**Density** (kg/m^3)	**Conductivity** (W/mK)	**Specific heat** (J/kgK)
Concrete slab	8.0	2000	1.4	1000
Mortar material	2.0	999	0.41	1000
Ceramic tile	0.5	2000	1.0	800

Table A.5: Bedrooms floor material properties from outside to inside layer

Material	**Thickness** (cm)	**Density** (kg/m^3)	**Conductivity** (W/mK)	**Specific heat** (J/kgK)
Concrete slab	8.0	2000	1.4	1000
Mortar material	2.0	999	0.41	1000
Eucalyptus wood	1.0	500	0.13	1600

Table A.6: Doors material properties

Door	**Material**	**Thickness** (cm)	**Density** (kg/m^3)	**Conductivity** (W/mK)	**Specific heat** (J/kgK)
Exterior	Eucalypt wood	3.8	500	0.13	1600
Interior	MDF	0.50	600	0.14	1700
	Air gap	3.0	-	-	-
	MDF	0.50	600	0.14	1700

Table A.7: Air gap thermal resistance.

Material	**Thermal resistance** (m^2K/W)
Air gap	0.18

Table A.8: Windows glazing properties.

Material	**Thickness** (cm)	**Conductivity** (W/mK)	$\tau_{sol,vis}$	τ_{IR}	$\rho_{sol,vis}$	ε_{IR}
Glazing	0.40	1.4	0.88	0	0.0808	0.84

Table A.9: Windows frame properties.

Material	**Thickness** (cm)	**Width** (cm)	**Conductance** (W/m^2K)
Iron frame	0.80	2.5	4167

Appendix B

"Model 11" data sheet

In Figure B.1 there is the data sheet of the geometry selected for the analyses in Chapter 2. Note that in the data sheet, there are both the tree and the building wall shading the model.

MODEL 11		HOUSE	
Deciles	5-7	Net area	55.1 m^2
Vintage	Less than 10 / Between 10 and 30 / More than 30	Interior volume	132.1 m^3
Reference	Plano Económico - Servicio de tierras y viviendas, Intendencia de Montevideo	Glazed area	6.9 m^2

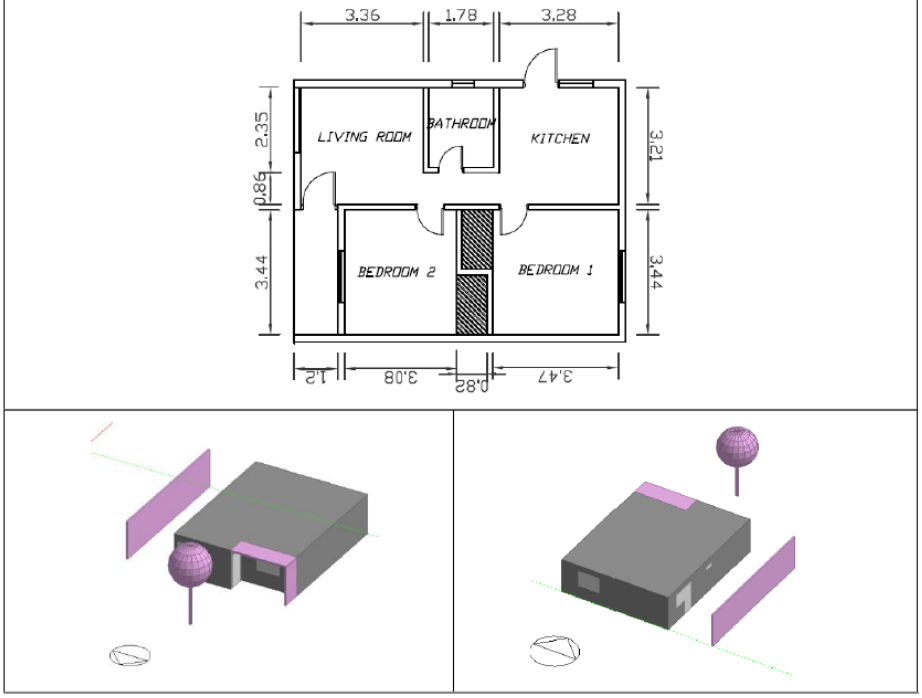

Figure B.1: "Model 11" data sheet.

Appendix C

Error in EnergyPlus weather files

During the analyses performed in Chapter 3, the incident beam solar radiation on a vertical plane in Montevideo was determined. In order to do so, a simulation was performed for a cube of side 1m using Montevideo's EnergyPlus weather file (EPW). All the EPWs used in this thesis were developed by Lawrie and Crawley [34] and are available at their web repository Climate.OneBuilding. The source data for these EPWs are the outcomes of the work by Alonso-Suárez et al. [35].

The obtained incident beam solar radiation on vertical planes according to their orientation are shown in Figure C.1a. Whereas the results for a north and south oriented vertical surface seem reasonable, the systematic difference observed for east and west orientations seems not. Moreover, when observing the pattern obtained for the Direct Normal Irradiance (DNI) variation with the cosine of the zenith angle (see Figure C.1b), it can be concluded that there is an error in the dataset.

This error has to do with a mismatch in the TMY and the EPW timestamps. Whereas in [35] the values are for the hour (the timestamp 7:00hs corresponds to the interval 6:30-7:30hs), in the EPWs the timestamp indicates the end of the interval (timestamp 7:00 corresponds to the interval 6:00-7:00hs). This difference led to a mismatch in which the values for each hour were assigned, in the EPWs, to the hour plus 30 min; explaining the graph patterns of Fig. C.1.

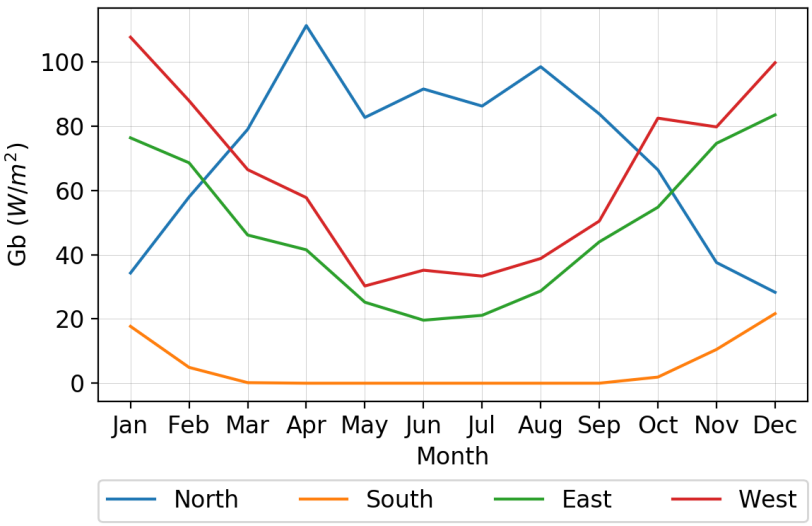

(a) Incident beam solar radiation on a vertical plane in Montevideo.

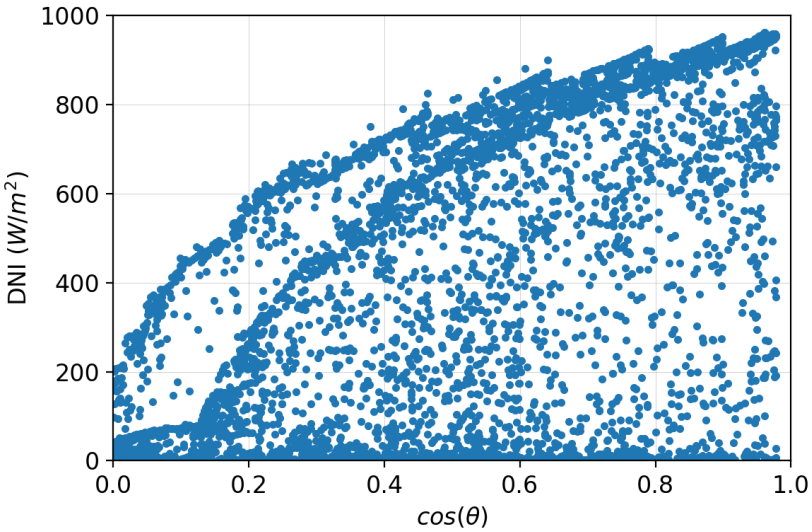

(b) DNI variation with zenith angle's cosine in Montevideo.

Figure C.1: Original EPW file.

Given that for the simulation of the whole housing stock, variability regarding buildings orientation was considered -and averaged- this issue should not have a relevant impact on the results. However, it must certainly affect the analyses of Chapter 3 as it would drive the orientations with higher solar gains to be rotated towards west. So, in order to continue with the simulations, during the course of this thesis new EPWs were generated in which the values for each hour were substituted with the mean between the value for that hour and for the next one. Despite not being the best course of action for

interpolating solar radiation data, this approach was followed as it offered a simple (and not too time consuming) workaround to this issue. The resulting incident beam solar radiation on vertical planes and the DNI variation with the cosine of the zenith angle are shown in Figure C.2. It can be observed that, after the modifications, the graph patterns seem more reliable; and this is the reason why the modified EPWs were the ones used for the simulations in this work. However, for the EPWs to be a more faithful representation of the TMY, a more thorough correction process should be performed.

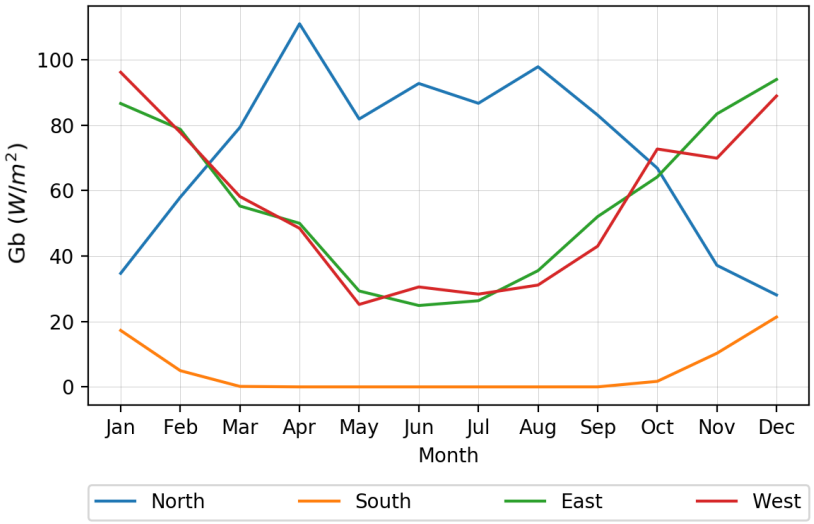

(a) Incident beam solar radiation on a vertical plane in Montevideo.

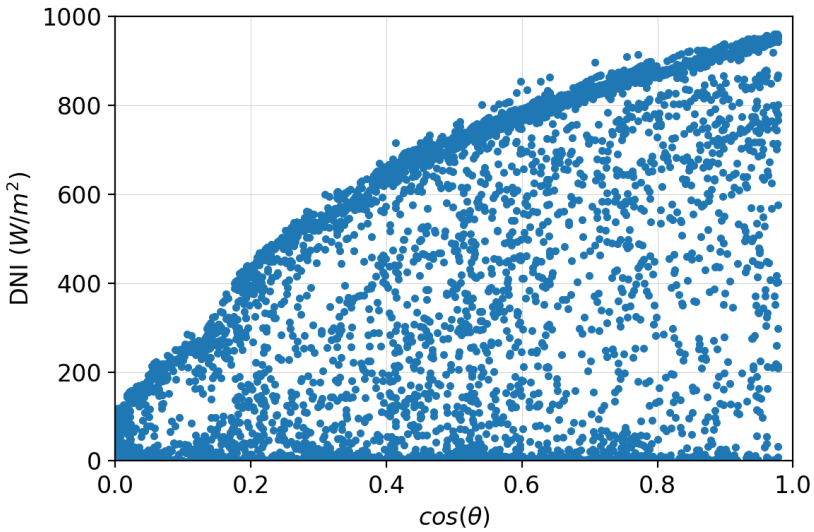

(b) DNI variation with zenith angle's cosine in Montevideo.

Figure C.2: Corrected EPW file.

Appendix D

Simulation platform inputs and source code

The platform developed to automate the models generation, simulation and results processing can be accessed here[1]. It consists of three folders, one containing the simulation inputs, other with the python functions developed and the third with the simulation outcomes. Each time the process is executed this third folder is generated, in which both the households models (in IDF format) and their results would be stored. In the following sections, a deeper understanding of the platform structure is provided, specially concerning the input files structures.

D.1 Inputs folder

The `Inputs` folder contains all the files the platform needs in order to proceed with the model generation and simulation process. Its structure consists of two folders and five files:

- `WeatherFiles`
  - *IrradNorthVertical*
  - EPW Colonia
  - EPW Montevideo
  - EPW Rivera
  - EPW Rocha

[1] Complete URL: https://www.fing.edu.uy/owncloud/index.php/s/hdnhT0a5EloXeUp

  - EPW Salto

- `Models`
  - IDF Model 1
  - ...
  - IDF Model 32
  - *Models.pdf*
- *stockDistribution*
- *geoDistribution*
- *departmentsProp*
- *TotalOccupied*
- *Template.idf*

In the `WeatherFiles` folder, there are the five EnergyPlus weather files (EPWs) used for every simulation. Also, there is the *IrradNorthVertical* file containing the incident irradiance for a vertical surface facing north in each department for which there is an EPW file (Colonia, Montevideo, Rivera, Rocha and Salto). This information is used during the results processing stage. *IrradNorthVertical* is both in csv and xlsx formats, the former is the one the platform reads the information from whereas the latter contains the columns and rows headings for easier readability.

Then, there is the `Models` folder containing 32 IDF files with the geometries selected during the housing stock characterisation process in FSE_1_2017_1_144779 [4] as well as *Models.pdf* file with all the models data sheets. There are also four files (again in csv and xlsx formats) condensing all the information regarding housing stock characterisation and which structures will be described in the following sections. Finally, there is *Template.idf* containing general information such as materials, constructions and components definitions as well as simulation parameters.

D.1.1 *stockDistribution*

This matrix contains the percentages in which the Uruguayan housing stock is divided into the archetypes in each subregion. It also establishes those characteristics determined by the archetypes such as constructions, components air leakage properties, building geometries and number of occupants.

The matrix columns indicate the archetype as a combination of type (house or apartment), size, decile rank and vintage as (see *stockDistribution.xlsx*). The rows on the other hand are divided as follows:

- Rows 1-4: Represent the subregions N-NW, SW-Center-NE, S-SE and MVD. The values in each cell indicate the prevalence of each archetype in each region among the total (expressed as a percentage).
- Rows 5-18: Provide the enclosure construction characteristics. The values in each cell are the names for the enclosure constructions. These constructions and their materials are defined in *Template.idf*, from where the script takes the information when generating the archetypes models.
- Rows 19-24: Provide the components air leakage characteristics. The values in each cell of rows 19, 20 and 24 are the names for the components used to characterized infiltration and ventilation through doors and windows. These components are defined in *Template.idf*, from where the script takes the information when generating the archetypes models. Rows 21-23 are de C''_Q, C'_Q and n used to characterise the cracks in the roof.
- Rows 25-26: Contain the amount of geometries used to model each archetype (row 25) and the geometries names (row 26).
- Row 27: number of occupants in each archetype.
- Rows 28-33: HVACs characteristics. Rows 28-30 indicate the zones in which HVACs systems should be modelled (bedrooms, living room and bathrooms and kitchen). All along this work HVACs were only modelled in the occupied bedrooms and the living room. Row 31 establishes whether the HVAC systems capacity is infinite or limited and, if limited, the next two rows sets the limit for heating and cooling, respectively. In this work all HVACs capacities were set to be infinite.

During the simulation process, after defining the simulation parameters, the platform proceeds to the models characterisation. This stage involves reading from *stockDistribution.csv* the number of models to simulate for each subregion (this is each row from 1 to 4) and for each archetype (each column from 1 to 54), and also extracting all the information in rows 5 to 33 needed to generate those models.

D.1.2 *geoDistribution*

This matrix establishes how the households in each subregion are distributed in the departments. The columns are the subregions in which the country was divided whereas the rows indicate the departments (see *geoDistribution.xlsx*). Thus, the value in each cell establishes the probability for a household in the given subregion (column) to be in the corresponding department (row).

As part of the model characterisation process, and after determining the amount of models to simulate for a given archetype and subregion, the platform determines in which departments those models are located according to the probabilities determined in this file.

D.1.3 *departmentsProp*

This file contains all the department dependant characteristics. In this case, columns represent the coutry's departments while rows indicate the departments characteristics as follows (see *departmentsProp.xlsx*):

- Row 1: Probability of a tree shading the front facade.
- Row 2: Probability of another building shading a given facade.
- Row 3: Probability of the model being attached in 3 of its facades.
- Row 4: Probability of the model being attached in 2 of its facades.
- Row 5: Probability of the model being attached in 1 of its facades.
- Row 6: Probability of the model being detached.
- Row 7: Number of storeys in apartment buildings.
- Row 8: Blocks north. For the cases that there is a number, it indicates the degrees that blocks north are rotated (clockwise) from true north. There can also be the string "random" indicating that the blocks might take any orientation.
- Row 9: Weather file to use for the simulation. Given that there are not EPWs for each department, this table establishes which to use in each case.

As the final stage of the models characterisation process, and after having determined in which department each model is located, the platform reads from *departmentsProp.csv* all these departments dependant characteristics. Then, it completes the models characterisation by assigning the attributes to each

model (such as orientation, surroundings scenario, number of attached facades) based on the read probabilities.

D.1.4 *TotalOccupied.csv*

In this matrix there are the total amount of households in each archetype and each subregion. As can be observed in *TotalOccupied.xlsx* columns are the same as in *stockDistribution* (54 columns one for each combination of type, size, decile and vintage) and rows are rows 1-4 of *stockDistribution* (N-NW, SW-Center-NE, S-SE and MVD). This information is used during the final stage of the simulation process, when extrapolating the obtained results to the whole housing stock.

D.2 Scripts folder

In this folder there are all the python scripts developed. These include the functions described in Section 4.2.3 along with several others. The only function the user needs to execute is *Manager.py* and there is also where he/she should set the simulation parameters such as amount of simulations, type of occupant to model, subregions, archetypes, etc.

D.3 Simulation folder

This folder is generated at the beginning of the platform execution. There, the models developed for each archetype in each subregion are stored and also the results for each case simulated. Therefore, for each simulation performed, the IDF with the household modelled would be added to this folder. Also, a new folder would be generated containing the individual results for that simulation. These individual results include graphs with the monthly requirements, mean temperatures, gains and losses through each component and components relative contributions. There are also some EnergyPlus output files, and two text files containing, the first one, a summary of the model's characteristics (type, size, decile, vintage, type of occupant, number of attached facades, glazed area, etc.) and in the second one there is a log where issues raised during the model generation are described.

Besides, at the end of the simulation *GlobalResults.csv* is generated where there are the obtained annual results, averaged for each archetype in each subregion. Rows in this table identify the archetype, type of occupant and HVAC situation (whether HVAC systems are modelled or not), whereas in the columns there are the obtained results (see *GlobalResults.xlsx*). In the link provided for accessing the platform, the `Simulation` folder contains, as an example, the results for a -rather small- simulation performed. A 'nan' cell value indicates that no model was simulated for the given row. This might be either because the user decided not to simulate that combination of HVAC situation, occupant type, subregion and archetype, or because the number of simulations set was not high enough so as to model the given archetype in the given subregion (according to the values established in *stockDistribution.csv*).